Experimental Study of Neutral Radical’s Effect on Inactivation of Spore-forming Microorganisms by Low Pressure N2/O2 Surface-wave Plasma

静岡大学　博士論文

低圧 N_2/O_2 表面波プラズマによる芽胞形成菌不活化における中性ラジカルの効果に関する実験的研究

楊　小麗

静岡大学
大学院自然科学系教育部
ナノビジョン工学専攻

2015 年 6 月

Doctoral Thesis

Experimental Study of Neutral Radical's Effect on Inactivation of Spore-forming Microorganisms by Low Pressure N_2/O_2 Surface-wave Plasma

Xiaoli Yang

Graduate School of Science and Technology
Educational Division
Department of Nanovision Technology
Shizuoka University

June 2015

Table of Contents

Abstract

Compared with the conventional sterilization methods, plasma sterilization has many advantages in low-temperature, non-toxic, and shorter time treatment. Different types of plasmas with various working gas at low pressure to atmospheric pressure have been extensively demonstrated to be effective in sterilization. But it still has some problems for the commercial application of plasma sterilization. To make clear the plasma inactivation mechanism of spores forming microorganism is important to improve sterilization properties and reliability, but the mechanism is still not completely determined.

In our previous work with the N_2/O_2 gas mixture surface-wave plasmas for the inactivation of spores, the effect of VUV/UV was studied by putting a small metal chamber covered with various optical filters to block the radicals inside the plasma chamber. The result showed that the UV radiation is important lethal factor in N_2/O_2 plasma. In addition to UV effect, the neutral radicals, such as excited oxygen and nitrogen atoms, also play a role in the inactivation of spores. But the specific mechanism of neutral radicals has not completely understood. As a continuation of our previous research, in this work, the effect of oxygen and nitrogen atoms on the inactivation of spore-forming microorganism were studied with atomic density measured with vacuum ultraviolet absorption spectrum (VUVAS) technique and an ultrathin porous ceramic plate which can block UV and only allow radicals penetrate through.

In chapter 1, there is a background introduction about this thesis. Different sterilization methods, the research state about plasma sterilization, important plasma factors related with inactivation of microorganisms was discussed.

In chapter 2, a compact microwave plasma light source for VUVAS technique was developed to measure the absolute oxygen and nitrogen atomic density in N_2/O_2 gas mixture surface-wave plasma. With self-absorption calibrated VUVAS technique based on the theory of resonance escape factor, the absolute oxygen atomic densities were consistently analyzed using two adjacent oxygen atom emissions at 130.22 nm and 130.49 nm for different N_2/O_2 gas mixture ratios in surface-wave plasma (SWP). The oxygen atomic density varied from about 1.32×10^{12} to 3.98×10^{12} cm^{-3} with a changing N_2/O_2 gas mixture ratio, peaking at a N_2/O_2 ratio of 1:9. Results of absolute oxygen atomic densities analogous to previous spore etching results measured under the same discharge conditions,

it indicates that the spore etching effect in N_2/O_2 gas mixture plasmas are strongly correlated to concentration of oxygen atoms. We also found that a minimum oxygen density is needed for effective etching to begin. Synergistically UV radiation emitted by N_2/O_2 gas mixture plasmas can be easily penetrating through the etched spore cortex region into the core region to promote the DNA damages, that is, inactivation of spores.

In chapter 3, the contribution of nitrogen atoms effect on inactivation was discussed. For nitrogen atomic density measured with VUVAS method, the light source can worked at a condition with self-absorption in negligible level, the nitrogen atomic density measured with a traditional VUVAS method decreased gradually from 3.17×10^{11} cm^{-3} at 100% N_2 with the increasing of O_2 percentage. Compared with previous sterilization experiment result, we inferred from these atomic density results that nitrogen atomic density in N_2 and O_2 mixture surface-wave plasma has small contributions on the spore etching and spore inactivation.

In chapter 4, in order to make clear the inactivation effect of neutral radicals in low pressure surface-wave plasma, a new kind of ultra-thin porous ceramic plate was developed. Optical emission spectroscopy results illustrated that more than 99% emission below 400 nm had been blocked by the porous ceramic plate. Spore size measurement results demonstrated clearly that parts of neutral radicals can penetrate through the ceramic plate. Survival curves measurement result indicated that very small amount UV (<1%) which can penetrate through the porous ceramic plate still play a main inactivation effect. A new kind of filter which can perfectly block UV emission from the plasma was needed for the study inactivation effect of neutral radicals in future.

Chapter 5 gives a briefly summary about his thesis and an outlook of further study. Although much work has been done, but the inactivation effect with neutral radicals alone is still unclear now, for a further study, we need to develop a new kind of filter which can perfectly block UV emission and allow most of neutral radicals penetrate through in future.

Chapter 1

Background introduction

In this chapter, a background introduction about this thesis was introduced. First, different sterilization methods will be presented briefly. Second, the basic knowledge of plasma, such as the type of plasms, the way to produce plasma and the applications of plasma and the research status of plasma sterilization, both at low pressure and atmosphere pressure, and the mechanism of plasma sterilization will be introduced. Finally, the scope of this thesis will be given briefly.

1.1 Sterilization and disinfection

Although we have many friendly interactions with microorganisms, but the ongoing battle of human against these invisible cohabitants has a legacy starting from the dawn of humankind and has been heightened by increased knowledge. Emerging infectious diseases have long loomed like a black shadow over the human race, uncontrolled microorganisms had caused huge losses or even disaster to human beings in the history, the appearance of disinfection and sterilization techniques have successfully wiped out portions of it. However, the development of medicine and biology, as well as the new emerging pathogenic microorganisms has presented new challenges to sterilization and disinfection technology.

1.1.1 Some important definitions[1, 2]

1) ***Decontamination*:** is a general term for the destruction or removal of microbial contamination to render an item safe. It can also cover removal of non-microbial matter. This will include methods of cleaning, disinfection and sterilization as appropriate.
2) ***Sterility*:** is the total absence of living organisms, in this context specifically of microbial life (or, in the case of viruses, of the ability to replicate). As sterility cannot be guaranteed by testing; it has to be assured by the application of a suitably validated production process according to protocols defined by control authorities.

3) ***Sterilization*:** is a process used to render an object free from all living organisms with a high degree of quality assurance.

4) ***Disinfection*:** is any process whereby the potential of an item to cause infection is removed by reducing the number of microorganisms present. Such a process may not necessarily eliminate all microorganisms, but can reduce them to a level such that they no longer are able to initiate infection. Numbers of bacterial spores may not necessarily be reduced. The main methods of achieving disinfection are by the use of heat or chemicals.

5) ***Validation*:** In order to validate a sterilization process, standardized preparations of selected microorganisms (called biological indicators) are used. They usually consist of a population of bacterial spores. The recommended species by the European and the US Pharmacopeia are *Geobacillus stearothermophilus* for steam or gas sterilization, *Bacillus subtilis* for dry-heat or gas sterilization, *Bacillus pumilus* for irradiation and *Pseudomonas diminuta* for sterile filtration.

6) ***SAL (Sterility assurance level)*:** SAL is the probability of a non-sterile item in a population. The SAL of a process for a given product is established by appropriate validation studies. A SAL value of 10^6 is generally regarded as acceptable.

7) D-value refers to decimal reduction time and is the time required at a certain sterilization factors to kill 90% of the organisms being studied. Thus after a colony is reduced by 1 D, only 10% of the original organisms remain, i.e., the population number has been reduced by one decimal place in the counting scheme.[3]

1.1.2 Risk categories and levels of decontamination required

The choice of method of disinfection or sterilization depends on many factors, such as the type of material to be treated, the organisms involved, the cost and the time available for decontamination, and the risks to staff and patients. But the infection risk is the basic principle. The infection risks to patients from equipment and the environment can be classified as shown in table 1.1.[2]

1.1.3 The methods of disinfection and sterilization

Disinfection and sterilization are both decontamination processes. While disinfection

is the process of eliminating or reducing harmful microorganisms from inanimate objects and surfaces. Disinfection can be carried out using UV, heat, chemicals. Chemical disinfection is less amenable to quality assurance monitoring than sterilization or thermal disinfection processes. The correct chemical must be used at the right concentration for an adequate exposure period in the absence of factors that may interfere with the process.

Table 1.1 Risk categories and levels of decontamination required [2]

High risk	*Definition*	Items in close contact with a break in the skin or mucous membrane or introduced into a normally sterile body area
	Examples	Surgical instruments, syringes and needles, intrauterine devices and associated equipment, dressings, urinary and other catheters
	Suitable methods	Sterilization is required. High-level disinfection may sometimes be acceptable if sterilization is not possible or practicable
Intermediate risk	*Definition*	Items in contact with intact mucous membranes
	Examples	Respiratory equipment, gastroscopes, or other items contaminated with particularly virulent or readily transmissible organisms, or if the item is to be used on highly susceptible patients
	Suitable methods	Disinfection required
Low risk	*Definition*	Items in contact with normal and intact skin
	Examples	Stethoscopes, washing bowls
	Suitable methods	Cleaning and drying usually adequate
Minimal risk	*Definition*	Items not in close contact with patients or their immediate surroundings
	Examples	Floors, walls, ceilings and sinks
	Suitable methods	Cleaning and drying usually adequate

Sterilization is the process of killing all microorganisms, such “extreme” forms of decontamination are needed during critical times like surgery, or in environments like industrial, laboratory or hospital. Sterilization methods used widely falls into the following three basic categories: 1) High temperature/pressure sterilization (autoclave); 2) Chemical

sterilization; 3) Radiation sterilization. The following is the brief introduction of the three basic categories.

1.1.3.1 Thermal methods of sterilization

Thermal method is the oldest, but also the most effective and accepted method of sterilization. It leads to the destruction of key molecules and structures (enzymes, RNA, DNA, proteins and lipids) of the microorganism. In 1832, William Henry, a Manchester physician, studied the effect of heat on contaminated material that is clothes worn by sufferers from typhus and scarlet fever. He found that garments so treated could be worn with impunity by others, who did not then contract the diseases.[4] There are two common ways to utilize heat for sterilization:

1) ***Steam Sterilization/Autoclave***: The steam autoclave is the oldest, safest, most widely used and most cost-effective method of sterilization in the medical equipment industry. Steam is generated in a pressure chamber so that it reaches a temperature 121-148 ℃ at 15 p.s.i. The time items are kept exposed is dependent on the temperature and size of load and usually ranges from10 to 60 min. Autoclaving is an acceptable method for noncritical applications.
2) ***Dry Heat Sterilization:*** Dry heat is effective at inactivating microorganisms, but in general, the temperatures required are higher than is required for steam sterilization to achieve an equivalent level of germicidal action. Table 1.2 shows the temperature and treatment time needed for Steam and dry heat Sterilization. This method should be used only for materials that might be damaged by moist heat or that are impenetrable to moist heat (e.g. powders, petroleum products, sharp instruments).

Table 1.2 Treatment time and temperatures in thermal sterilization processes[4]

Process	**Temperature (℃)**	**Holding period (min)**
Moist heat (autoclaving)	121	15
	126	10
	134	3
Dry heat	Minimum of 160	Not less than 120
	Minimum of 170	Not less than 60
	Minimum of 180	Not less than 30

The advantages of thermal sterilization are nontoxic, easy to control and monitor, good penetration property, but the disadvantages, deleterious for heat-sensitive or water-sensetive material, limit its application field.

1.1.3.2 Radiation sterilization

Irradiation sterilization effectively kills microorganisms, because ionizing radiation has sufficient energy to cause the release of electrons from target atoms in a given compound, and leads to the loss of essential structure and function, which is vital to cell or viral survival. Radiation sterilization can be accomplished using one of three forms of radiation: gamma sterilization using radioisotopes, electron beam using electron accelerators, or beta radiation using an electron accelerator. Other forms of electromagnetic radiation are mostly used for disinfection purposes, including UV, infrared radiation, and microwaves.

1.1.3.3 Chemical sterilization

Although a wide variety of chemicals, such as alcohols, aldehydes, antimicrobial metals, and halogens, can be used as disinfection, only a limited number have actually been developed for use in sterilization processes. They include the epoxides (particularly ethylene oxide [EO]) formaldehyde hydrogen peroxide-based systems, and other oxidizing-agent-based liquid and gaseous processes.

1) ***EO:*** As a reactive antimicrobial, EO has been widely used for low-temperature equipment (including device) sterilization, as well as decontamination of dried-food and pharmaceutical products. EO is one of the most widely used products for industrial sterilization, particularly for temperature-sensitive medical devices or other materials. But EO is toxic at relatively low concentrations. The typical recommended daily occupational-safety level is 1 ppm. This disadvantage is unfavorable to the application in the medical field.
2) ***Formaldehyde***: Two sterilization methods that use formaldehyde gas can be categorized as low temperature steam-formaldehyde (LTSF) sterilization, and high-temperature formaldehyde alcohol sterilization. LTSF systems are used for medical,

dental, and some industrial sterilization processes. The most widely used application is for sterilization of reusable medical devices in health care facilities. As with EO, there remains a significant concern about the safe use of formaldehyde gas, which is toxic and irritating and is considered mutagenic and carcinogenic.

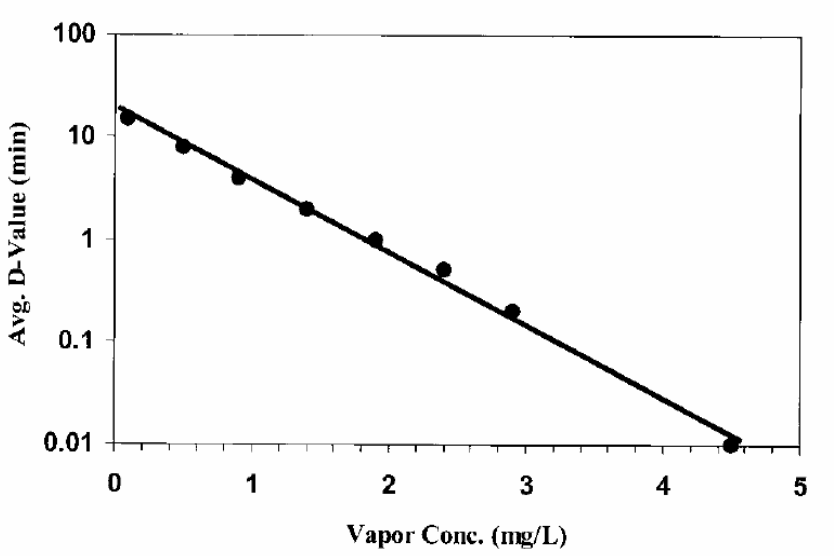

Figure 1.1 average D-value of G. stearothermophilus spores as a function of H_2O_2 concentration

3) ***Hydrogen peroxide (H_2O_2)*** is a powerful oxidizing agent with broad-spectrum activity and a good safety profile. Hydrogen Peroxide at low concentrations solutions, or formulations, and gas based processes are widely used for antisepsis, disinfection, and fumigation. Higher concentrations (generally in the 25 to 60% range) are required for sporicidal activity. These required concentrations have restricted use due to safety and compatibility concerns. In some cases, heated peroxide (30 to 59% solutions in water) has been used for sterilization, and some formulations in combination with other oxidizing agents. Figure 1.1 shows an example of the effect of the hydrogen peroxide gas concentration on sporicidal activity. Various gas concentrations were tested under atmospheric pressure with G. stearothermophilus spores.[5] Certain materials absorb and break down peroxide, which can lead to inefficient sterilization processes and/or longer aeration times. In general, peroxide (particularly the gaseous form) is not

suitable for the sterilization of large amounts of cellulosics or other protein-based materials.

4) ***Other oxidizing agent: s***ome specific applications with hydrogen peroxide, chlorine dioxide, PAA, and mixed oxidants can also be used for sterilization, but their use in sterilization processes is somewhat limited.

1.1.4 Principles of ideal sterilization method

1) Compatible with a wide variety of materials and surfaces, and sterilization factors can penetrate though packaging materials and contact with all the surface of the items (inside outside, deep pipelines, etc.).
2) It can kill most challenging microorganisms, such as bacterial endospores, satisfy the requirements of SAL.
3) Favorable occupational and environmental safety profile.
4) Little damage to items after several sterilization cycles.
5) It should be easy to use, and has suitable physical, chemical or biological monitoring methods for the sterilization process.
6) Cost effectiveness

1.2 Plasma sterilization

Traditional sterilization methods, such as dry heat (oven), moist heat (autoclave), or chemicals, have some major drawbacks. High processing temperature is not available for heat sensitive materials, chemical methods have the toxicant residues problem of, and these conventional methods also have the problem of long treatment time (approximately 12 h in the case of ethylene oxide exposure).[6, 7] With the development of medical and biotechnology, conventional sterilization techniques can not satisfy some special sterilization requirements, such as precision medical instruments and some heat or wet sensitive materials. This situation led to the development of new sterilization methods. Low temperature plasma sterilization has the advantage of fast, high efficiency, less damage to items, and no toxic residues, it had been regarded as one of the most promising alternative solution to conventional sterilization methods.

1.2.1 Introduction about plasma

As well known, the condensed state of mater can change from solid, to liquid and gaseous with different temperature, if enough external energy is introduced to the gaseous state mater, some of the atoms and molecules will be ionized, if the ionization reaches a certain level, mater will go to the fourth state, which had been defined firstly by Crookes in 1987.[8]

But until 1928, the fourth state of mater, which is a mixture of charged particles and neutral radicals, with a roughly zero net electrical charge, was named firstly as plasma by I. Langmuir [9]. Plasm was mixture of 6 kinds of typical particles: ions, electrons, ground stated atoms or molecules and excited atoms or molecules.

1.2.1.1 The properties of plasma

1) ***Conductivity:*** Due to the highly mobile electrons and charged particles, plasmas are generally very good conductors of electricity as well as thermal conductors.
2) ***Quasi-electrically neutral*****:** Plasmas resulting from ionization of neutral gases generally contain equal numbers of positive and negative charge carriers. In the absence of external disturbances, a plasma is macroscopically neutral. The net resulting electric charge is zero. But plasmas are termed quasi-neutral. "Quasi" because the small deviations from exact neutrality have important dynamical consequences for certain types of plasma mode. Strongly non-neutral plasmas occur primarily in laboratory experiments when electric and magnetic fields were applied to the plasma.[10]
3) ***Diffusivity:*** *P*articles in plasma will diffuse from dense regions to regions ordinary of happens when the density gradients is presence. The diffusion is also affected by magnetic and electric fields.
4) ***Wave phenomena:*** Plasmas can sustain a variety of waves: Longitudinal electrostatic plasma waves, high-frequency transverse electromagnetic waves, Alfven and magnetosonic waves in the low-frequency region.[11]
5) ***Emission of radiation:*** Radiation transition of ions, atoms and molecules is important plasma process, the emission spectrum produced from the radiation transition is also an important diagnostic tool for different plasma parameters.

1.2.1.2 The types of plasmas

According to the existence state, plasma can be classified into natural and artificial plasmas. It was realized that most of the matter in the known universe exists as a plasma, the sun, solar wind, ionosphere of the earth, lightning, stars, as well as most interstellar matter are natural plasmas. External energy, such as electric, magnetic fields, radiation and heat, etc., is artificially added to gas, the plasma produced from the ionization gas is called artificial plasma.

According to the thermodynamic states, plasmas can be delineated into two main categories, high temperature (fusion-type) plasmas and low temperature plasmas which are inclusive of gas discharges. Active species of high temperature (electrons, ions, neutrals) are in a state of thermal equilibrium. Low temperature plasmas can be further delineated into thermal plasmas, also known in the literature as quasi-equilibrium plasmas, which are in a state known as a local thermal equilibrium state (LTE), and non-thermal plasmas (NTP), which are also called non-equilibrium plasmas or cold plasmas.[12]

According to the pressure, plasma can be divided to low pressure plasma and atmospheric pressure plasma. Because the atoms or molecules are easy discharge at low pressure, the traditional method to produce plasma was always kept in a vacuum chamber. Plasma generated in a vacuum sealed chamber is defined as low pressure plasma. Large area plasma is easy to be produced in low pressure. The electron temperature is much higher than gas temperature at low pressure, thus, some high energy reaction is easy to happen at low substrate temperature at low temperature, and the reaction purity is also easy to control at low pressure, thus low pressure is always a hot area for industry and research.[13-15] But the cost of low pressure plasma is relatively high for the expensive vacuum system, and the reaction is still limited by the vacuum chamber size. Atmospheric pressure plasma just remedies these shortcomings, atmospheric pressure plasma just remedy these shortcomings. Although it is difficult to obtain a large area uniform discharge, the atmospheric pressure plasma has extended the application field of plasma, and became a hot research field in plasma.[16]

1.2.1.3 Methods of plasma generation

There are various methods to create a plasma, some methods of plasma generation and the types of plasmas resulting from them are given in Table 1.3.

Table 1.3 Methods of plasma generation[17]

Character of action	Matter	Type of plasma
Electric field	Gas	Stationary gas discharge plasma
Electromagnetic wave	Gas	Alternative gas discharge plasma
Resonant radiation	Atomic vapor	Photoresonant plasma
Excitation from chemical reactions	Chemically active mixture	Chemical (flame) plasma
Laser	Surface or particles	Laser plasma
Injection of electrons or ions	Surface or ionized gas	Beam plasma
Injection of nucleating vapor	Ionized gas	Cluster plasma
Injection of dust particles	Ionized gas	Dusty plasma
Ionization by hard radiation	Gas (air) with aerosols	Aerosol plasma

Gas discharge is the most widespread method to produce plasma with a variety of characteristics. Electric discharge, electromagnetic wave, such as radio frequency or microwaves, photoionization using lasers is common way to make gas discharge plasma in the laboratory. [11]

1.2.1.4 The application of plasma

Plasmas have various application in technology because of their unique electrical properties and ability to influence chemical processes. Artificial plasmas had been used in many field, such as energy field (controlled thermonuclear fusion[18]), the synthesis and surface treatment of materials[19, 20], environmental pollution treatment[21, 22], medical field[23], the industrialization of many of these process applications is expanding rapidly. We will focus on the plasma applications to medicine, which represents today probably the most novel and exciting component of plasma science.

1) ***Sterilization and disinfection*** Cold plasmas generated by electrical discharges can be employed for bio-decontamination and sterilization of surfaces, medical instruments,

water, air, food, even of living issues without causing their damage and other side effects, and represents a great potential in medicine and defense against terrorism. Plasmas can efficiently kill bacteria, yeasts and molds and other hazardous microorganisms, including potential bio-terrorism agents, even spores and biofilms that are generally very difficult to inactivate by traditional methods, which are in addition non-friendly for the environment.[24]

2) ***Skin and tissue treatment*** Direct or indirect plasma interaction with living cells of microorganisms or even humans is a new quickly developing field issuing in many bio-medical *in vivo* applications, e.g. for the treatment of skin diseases and foot ulcer. Plasma enables painless treatment of dental caries or root canal disinfection and other dental applications. Koban found that Ar/O_2 plasma improves osteoblast spreading on human dentin, it may allow a new regeneration regimen for periodontitis.[25]

3) ***Blood coagulation*** Fridman et.al reported the promotion of DBD plasma on blood coagulation in 2006[26], then, Kalghatgi, SU et.al found the mechanism is the direct DBD plasma treatment can trigger selective natural mechanisms of blood coagulation. Kuo et.al found the plasma jet accelerated the blood coagulation and wound healing [27, 28]

4) ***Apoptosis*** Plasma induced apoptosis (programmed cell death) of melanoma or other tumor cells in vivo had been successfully tested, which brings forth a great potential for cancer treatment. Lee and Shi, XM investigate the inhibition effect and mechanism of low-temperature plasma (LTP) on melanoma cells. Kumar, N et.al also observed that apoptosis of breast cancer cells was induced by the increased concentration of OH radicals recently [29-31].

5) ***Cosmetic applications*** Plasma tooth whitening[32], skin regeneration[33], removal of wrinkles and scars [34]became a new research field. In 2005 the UF Food and Drug Administration licensed plasma skin regeneration technology (PSR) for skin rejuvenation and for the treatment of wrinkles.[35]

1.2.2 Research status of plasma sterilization

1.2.2.1 Low pressure plasma sterilization

According to Paschen's law, large volume plasma is easier to be produced at low pressure than atmosphere pressure, and diffusion properties of particles is also better at low pressure, thus early experiments on microorganism inactivation by low temperature plasmas were mostly carried out at low gas pressures.[36]

Patents by Ashman and Menashi (1972)[37] as well as by Boucher (Gut) (1980)[38], Bithell (1982) and Jacobs (1988)[39]showed that an electrical discharge in an appropriate gas (or gases) could lead to sterilization. But these initial sterilization methods imply the application of gas mixtures containing components with inactivation properties (such as H_2O_2 and aldehydes). Few years later, two commercial plasma-based sterilizers, the hydrogen peroxide plasma-based (Johnson & Johnson : Sterrad®) sterilizer (1993) and the peracetic acid plasma-based (AbTox Inc.: Plazlyte®) sterilizer (1995), entered into the market.[7]. In the Sterrad® case, the chemical phase is provided by 1.8 ml of hydrogen peroxide at a concentration of 58% vol., while in the Plazlyte® system, it comes from a mixture of peracetic acid (5%), hydrogen peroxide (22%), acetic acid (10%) and water (63%). However, in 1998, because of some medical malpractices, AbTox went out of business. Even Sterrad® commercialized successfully more than twenty years, but it had been reported that the inactivation effect of Sterrad® mainly came from hydrogen peroxide itself, the plasma discharge just removed the residual hydrogen peroxide, there has been controversy over whether Sterrad® was really a plasma sterilization, it also had the problem in killing some spores[40]. Other commercial hydrogen peroxide plasma sterilization device appeared later had the same problems. Subsequently, the research of plasma sterilization technology with different gas compositions and high efficiency became a new development trend.

Lerouge had reported the sterilization effect of O_2, [41, 42] O_2/Ar、O_2/H_2、O_2/Ar /H_2、CO_2 and O_2/CF_4 in low pressure microwave plasma, the result showed that O_2/CF_4 had good etching effect and high inactivation effect, spores in 10^6 order was killed in 15 mins. Bol'shakov et al. studied the effect of a low-pressure radio-frequency oxygen plasma on bacteria with inductively coupled plasma (ICP) mode and capacitively coupled plasma

mode, found ICP mode provided better efficiency in destroying bacterial cells owing to its higher electron and ion densities.[43] Boscariol et al. studied the influence of discharge power of an oxygen ICP discharge on the inactivation kinetics of Bacillus subtilis spores, D-value of 8 min at 300 W decreased to approximately 3 min at 400W.[44]

Liu et.al and Moisan et.al studied the effect of plasma exposure method (direct or remote) can on the inactivation of bacteria, inactivation effect of microorganisms is much faster in direct contact with the plasma than in the remote discharge region, because in the afterglow region, there are fewer electrons and charged particles, some of the neutral particles are chemically reactive radicals and some others are possibly in a metastable state, all these species have a limited lifetime, which extends from a few to some tens of ms. The advantage of remote plasma sterilization is the damage reduction to the sterilized items. [7, 45]

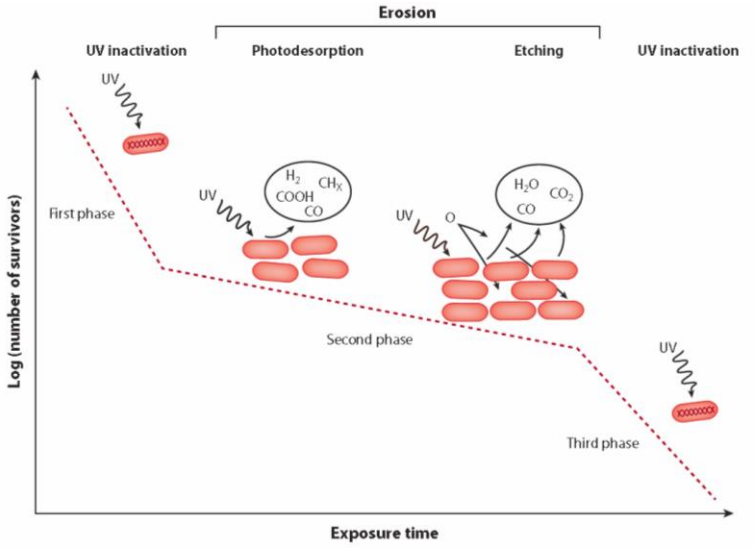

Figure 1.2 Schematic illustration of the three-phase survival curve characterizing plasma sterilization[46]

Moisan and his group have carried out detailed studies on the inactivation effects of low-pressure microwave afterglow plasma from 2000. They found that, Ar, N_2 and O_2 had different sterilization efficiency, the inactivation efficiency of Ar and N_2 was improved when O_2 was introduced to the system, and the UV emission of NO_γ produced by N_2 and O_2 gas mixture enhanced the sterilization. They also focused on the inactivation kinetics

and tried to correlate these results with the physics and chemistry of the afterglow. The survival curves in the experiments with *B. subtilis* spores exhibited three inactivation phases, as schematically shown in Figure 1.2. The first phase provides the highest killing rate (smallest D-value) and is dominated mainly by the action of UV radiation on isolated spores or on the first layers of stacked spores. The second phase, which has the slowest kinetics, is attributed to erosion processes by UV photons (photodesorption) and by other active species such as atomic oxygen (etching). These erosion processes progressively remove matter from the microorganisms or from the material covering them. Finally, the third phase starts when the last living spores have been sufficiently eroded, allowing UV photons to hit their genetic material directly. As a result, the D-value of this last phase is often close to the D-value of the first phase.[46-51] For different For the O_2/N_2 gas mixture plasma, the high inactivation efficacy to *Geobacillus stearothermophilus* spores was obtained when O_2 proportion is set to maximize the UV emission intensity, typically below 2%. Increasing the O_2 proportion increased the etching rate but decreased inactivation efficacy. This result indicates the dominant role of UV radiation in the inactivation process. This dominant role of UV radiation in low-pressure plasma sterilization has also been emphasized by other research groups [52, 53].

In 2006, a project about the low pressure plasma treatment for medical devices：European project BIODECON，was co-sponsored by research groups in Germany, Italy and other countries.[54] This project was supported by European. In order to compare the efficiency and study the sterilization mechanism in detail, similar plasma device was chose for collaborative researchers in different countries. ICP plasma with H_2, Ar, N_2, O_2 and their gas mixture in the pressure 0.1-20 Pa was used to study the inactivation effect to microorganisms and bio-molecules. As for different working gas, the etching rate was $Ar/O_2>Ar/N_2>Ar/H_2>Ar$. The inactivation effect of ternary mixture $Ar/O_2/N_2$ was better than Ar/N_2 and O_2/N_2, sterilization and destruction of biomolecules by etching can be achieved at the same time. For heavy the stacking spores, Rossi et al.[55] claimed that the main mechanism responsible for bacterial inactivation at low pressure is etching instead of UV radiation. The authors performed sterilization tests on the *G. stearothermophilus* spores with different N_2/O_2 mixtures ranging from pure nitrogen to pure oxygen. The best

sterilization results were achieved in mixtures with high amounts of atomic oxygen, whereas mixtures producing the highest UV emission gave a lower sterilization efficacy.

It had been proved that low-pressure plasma had high efficacy in sterilization. Many research groups committed to the development of new sterilizer, but large differences in sterilization kinetics have been observed among different groups. How to kill spores in an elongate pipeline and severely stacked microorganisms are hotspot

1.2.1.2 Atmospheric-pressure plasmas sterilization

Low pressure plasma sterilization need expensive vacuum systems and complex operations, thus many researchers turned to study low temperature plasma sterilization at atmospheric pressure. Atmospheric-pressure plasma is easier to operate and adjust, it can also be extend to the sterilization of liquid and gas. Several methods that allow researchers to easily generate non-thermal plasmas at high pressures, up to 1atm. Mechanisms and kinetics of sterilization processes in atmospheric-pressure non-thermal plasmas are more sophisticated than those in low-pressure plasmas because of the significant contribution of collisional gas-phase reactions at higher pressures and therefore a wide variety of active species involved in the sterilization process [56].

Dielectric barrier discharge (DBD) and atmospheric-pressure plasma jet (APPJ) are the most widely used for bacterial inactivation atmospheric-pressure. The electrode spacing is usually in the order of millimeter for DBD at atmospheric pressure, thus,even direct treatment is more effective than remote exposure, it is more feasible to choose remote DBD treatment. The chemical condition of the cell on a given surface, its physical orientation, and its degree of surface exposure can thus significantly influence the killing efficiency [57-59]. Numerous plasma jets with different features (such as a plasma needle or a plasma pencil, plasma torch, plasma gun) have been developed and described in the literature [29, 30, 60-64]. These jets differ in properties such as design, size, working gas, and frequency of applied voltage, but the principle is the same. The plasma is ignited inside a nozzle equipped with one or two electrodes and expands outside the nozzle via a high gas flow, but nozzle size in millimeter or few centimeters is a disadvantage for a homogeneous treatment of large areas, however, large-scale treatments are possible by applying multiple nozzles next to one another [65-67]. Bacterial inactivation by APPJs is performed mostly

in noble gases, such as Ar, He, the inactivation will be improved when a small amount of oxygen can be added to the working gas [68].

Non-thermal atmospheric plasma showed good properties on the inactivation of microorganisms, it had been widely used in the medical field and had good disinfection efficiency, but further study is needed to use it in the sterilization with SAL level.

1.2.3 Plasma factors responsible for sterilization

Plasma is a complicated process consisting of different plasma factors, such as UV photons, excited species, and neutral radicals. Varying these factors by different operation conditions (such as power, pressure, gas composition and gas flow rate) is a conventional way to find the sterilization mechanism and improve the sterilization efficiency.

1.2.3.1 Heat

Low temperature plasma sterilization is usually carried out below 60℃, Most non-thermal plasmas operate at low temperatures (room temperature to approximately 70°C), thus heat is not a major contributor to the sterilization effect in non-thermal plasmas. But some researchers regarded that temperature may play a synergistic role to other plasma factors in the sterilization process.[69, 70]

1.2.3.2 UV radiation

Plasma process is always accompanied by optical radiation, including ultraviolet and visible light, DNA damage by UV is considered to be important for sterilization. DNA had two absorption peaks near 185 nm and 260 nm.The formation of thymine dimers resulting from UV radiation inhibits the ability of the bacteria to replicate. In addition, intracellular repair system proteins play an important role in UV resistance as well. Recent studies have shown that proteins are the primary cellular targets implicated in the lethal effects of UV-A.[71, 72] The presence of UV radiation in the plasma strongly depends on the operating pressure. Vacuum plasma discharges are able to provide significant UV radiation in the range of wavelengths effective in sterilization.Therefore, UV radiation is considered an important contributor in low pressure plasma sterilization. The inactivation efficiency of UV and VUV photons on a given type of spores depends upon its actual structure and

composition. Munakata et.al reported two domains of high inactivation efficiency on B. atrophaeus spores , namely 100–180 nm and 210–290 nm, it has while photons with wavelengths above 300 nm, according to this plot, should have a much reduced effect on these spores. [73]. Moisan's group had studied the UV emission in N_2/O_2 gas mixture plasam, they pointed out that UV emission coming from NO is important in the sterilization, incouding NO_β (270-380 nm)and NO_γ (220-290 nm), and NO_γ was the main inactivatior facor. The research of Rossi also confirmed this result.[74, 75]. For atmospheric-pressure plasmas, the effect of UV depanding on the discharge type and gas compositions, Guo Jan et.al summarized the inactivation results of at atmospheric-pressure plasmas carried out by different groups and found that, the researchers who proposed that UV radiation plays a major role in inactivation process would have used Ar or N_2/O_2 gas mixture as working gas and the microwave-driven discharge as discharge type, the researchers who concluded that UV radiation does not play a major role in microbial inactivation process would have used pure O_2, He/O_2 gas mixture or air as operating gas and the discharge type is usually not the microwave-driven discharge**.**[76].

1.2.3.3 Charged particles

In low pressure plasma, charged particles and electrons can be accelerated by electric field, because the little colliction at low pressure, the particles can obtain high energy, which can produce etching on the surface of microorganisms. At atmospheric pressure, charged particles and electrons will have low energy for the heavy collisions, the etching effect was small, but such researchers, such as Fridman et.al [57] and Mendis et al.[77] have stated that charged particles play an essential role in sterilization, especially in the case of direct plasma treatment at atmospheric pressure.

Recently, based on the reslut of different groups, Guo Jan postulate a convincing mechanism underlying the interaction of charged particles with microorganism. As shown in figure 1.3 (a) The charged particles randomly absorb on the outside of the cell wall and generate electric field non-uniformly. Transmembrane potential increases with the charge accumulation. When the transmembrane potential reaches to a certain threshold, the protein of ion channel change its form, allow the ion channel to open, and make certain ions such

as Na^+, K^+, Ca^+ and Cl^- to pass through. However, the ions generated in the non-thermal plasma cannot go through the membrane. Therefore, charge accumulation is still

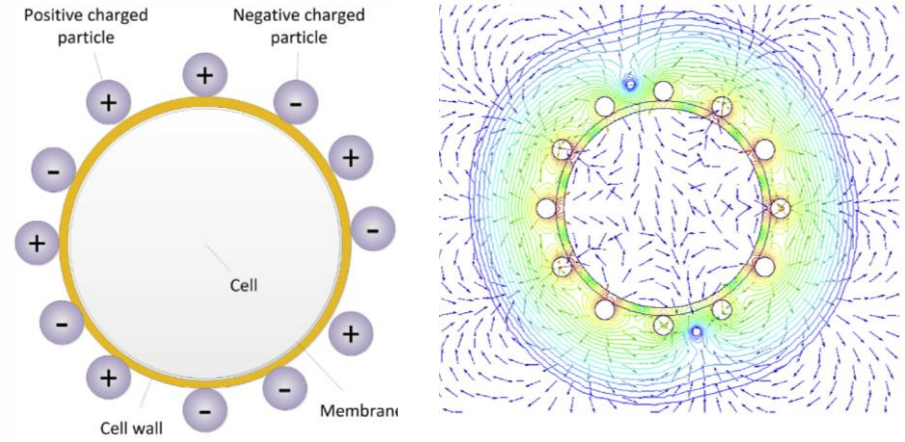

(a) (b)

Figure 1.3 (a)A distribution of the charged particles on the cell and (b)simulation of electric field intensity induced by the charged particles on the cell.[76]

proceeding. When the intensity of the electric field generated by charged particles is high enough, it can change the three dimensional structure of the proteins so much as to separate the proteins from the cell membrane, creates large pores in the cell membrane and weakens it. Hence, the charged particles generated in the non-thermal plasma can peculate into the cell, and disturb the activity of proteins and enzymes. Probably, cytoplasm can leak out of the cell through these holes, which is the reason that causes the cell death.[76] But This mechanism is effective only for gramnegative bacteria, which possess thin outer membranes and a thin murein layer, and for gram-positive bacteria and spores which have a much thicker murein layer, this phenomenon probably does not occur.

1.2.3.4 Reactive species

Non-thermal plasma discharge can produce a lot of reactive species, such as O, O_2*, O_3, OH・, NO, and NO_2, these species react with the biomolecules on the cell surface, or even penetrate the biofilm to destroy biomolecules inside the cell. Thus reactive species can be a significant contributor for the microbial inactivation process. For the O_2 included plasma, reactive oxygen atoms play an important role in sterilization by etching and oxidation of biomolecules.[78-81] Lipids, polysaccharides, proteins, nucleic acids and

other biological macromolecules can be oxidized by oxygen species, and membrane lipid is the most sensitive to plasma oxidation. The cell wall of gram-negative bacteria is thinner than gram-positive bacteria, so it is more sensitive, inclusions leakage is observed after short treatment time. Gram-positive bacteria such as *Staphylococcus aureus* has some resistance to plasma oxidation for their thick polysaccharides in cell wall, but active oxygen particles can still work by penetrating through the cell, thereby killing the cells. According to the results of a scanning electron microscope, the morphology of Staphylococcus aureus changed little after plasma treatment, but E. coli is seriously damaged. Because of the thick cell wall containing polysaccharides, yeast and spores are resistant to plasma oxidation relative.[82-84]

Yusupov et.al used reactive molecular dynamic simulations to investigate the interaction of important plasma species, such as OH, H_2O_2, O, O_3, as well as O_2 and H_2O, with bacterial peptidoglycan. Their results showed that OH, H_2O_2, O, and O_3 can break structurally important bonds of peptidoglycan (i.e. C–O, C–N, or C–C bonds), which consequently leads to the destruction of the bacterial cell wall.[85] Kong et.al presented a plasma inactivation mechanism using E. coli K-12 mutants as biosensors for key plasma species of atmospheric pressure He/O_2 glow discharges, they identified the dominant role of excited oxygen atoms as well as minor roles for UV, OH radicals, O_2 metastables, and excited NO. E. coli mutant missing DNA repair capabilities and wild E. coli had similar survival curves, it indicated that helium plasma has limited DNA damage, UV was not the main factor for sterilization. E. coli mutants that lack of scavenging function to reactive oxygen particles, are very sensitive to the plasma, it indicated that the reactive oxygen species play an important role in the plasma sterilization.[86]

With the results and conclusions proposed by different researchers, it can be understood that the oxygen element probably plays an essential role in inducing the reactive species to take effect on the interaction with microorganisms. But the exact roles played by other reactive species in the microbial inactivation process remain to be investigated in detail.

1.3 Motivation and scope of this work

Although plasma had high inactivation efficiency on microorganisms, but it still had problem in commercial applications for the reliability and cost. For the future application of sterilization require a comprehensive understanding on the role of plasma agents and the mechanism underlying their interaction with microorganism. Several researchers have reported different postulates regarding the role of plasma in microbial inactivation, but the mechanism has not yet been completely determined due to the complexity of both the non-thermal plasma and the microorganisms.

N_2 and O_2 gas mixture plasma had attracted the attention of many researchers because of the abundant reactive oxygen species and effective UV radiations. In our previous work, N_2 and O_2 gas mixture surface-wave plasma (SWP) was used for the low-temperature plasma sterilization of medical instrument. Different possible factors such as oxygen etching, UV radiation and ion bombardment were studied to figure out the sterilization mechanisms. The result showed that the UV radiation is the important lethal factor in low pressure N_2 /O_2 gas mixture surface wave plasma, but UV radiation has the limitation in penetration ability, it can't work well on elongated tube or some device with complete structure. In addition to UV's effect, our previous result also showed that neutral radicals, such as oxygen or nitrogen atoms, also play a role in the inactivation of spores. Neutral radicals have good diffusion properties, it can compensate for the limitations of UV. It is considered to be an important factor to improve the reliability of sterilization. But, their behaviors in the sterilization process have been not studied enough, because only a few reliable measurement techniques for the absolute densities of radicals in reactive plasmas have been developed, and also for the limited technology and methods to study the neutral radical's behavior in plasms sterilization, especially at low pressure.

The motivation of this work is to make clear the inactivation effect of neutral radicals on spores in low pressure N_2 /O_2 gas mixture surface wave plasma, and find the threshold density of neutral radicals for the sterilization of spore forming microorganisms. When the mechanism underlying the interaction of neutral radicals with microorganism is clear, it will benefit to the design of optimal plasma sterilization system for some special applications.

The thesis is summarized as follows:

Chapter 1 is the background introduction of this thesis. It includes the traditional method of sterilization and disinfection, basic knowledge about plasma, research state about plasma sterilization and main plasma factor relation with the microorganism inactivation.

Chapter 2 provides the absolute oxygen atomic density measured with a Self-absorption calibrated VUVAS method and the effect of oxygen atoms on spore etching is discussed.

Chapter 3 presents the nitrogen atoms measured with conventional VUVAS method, and its contribution on sterilization.

Chapter 4 the sterilization effect of pure neutral oxygen atoms was studied with an ultrathin porous ceramic plate.

Chapter 5 is the briefly summary of the work in this thesis.

References

[1] M. Perrut. Sterilization and virus inactivation by supercritical fluids (a review). Journal of Supercritical Fluids, 66, 359 (2012).

[2] P. Hoffman, G. Ayliffe & T. Bradley Disinfection in healthcare. (John Wiley & Sons, 2008).

[3] P. G. Mazzola, T. C. Penna & A. M. Da S Martins. Determination of decimal reduction time (D value) of chemical agents used in hospitals for disinfection purposes. BMC infectious diseases, 3, 24 (2003).

[4] A. P. Fraise, P. A. Lambert & J.-Y. Maillard Russell, Hugo & Ayliffe's Principles and Practice of Disinfection, Preservation & Sterilization. (John Wiley & Sons, 2008).

[5] G. E. Mcdonnell Antisepsis, disinfection, and sterilization: types, action and resistance. (ASM press, 2007).

[6] B. J. Park, D. Lee, J.-C. Park, I.-S. Lee, K.-Y. Lee et al. Sterilization using a microwave-induced argon plasma system at atmospheric pressure. Physics of Plasmas (1994-present), 10, 4539 (2003).

[7] M. Moisan, J. Barbeau, S. Moreau, J. Pelletier, M. Tabrizian et al. Low-temperature sterilization using gas plasmas: a review of the experiments and an analysis of the inactivation mechanisms. International Journal of Pharmaceutics, 226, 1 (2001).

[8] W. Crookes. Contributions to Molecular Physics in High Vacua. Proceedings of the Royal Society of London, 28, 477 (1878).

[9] I. Langmuir. Oscillations in ionized gases. Proceedings of the National Academy of Sciences of the United States of America, 14, 627 (1928).

[10] R. Fitzpatrick. Introduction to Plasma Physics. The University of Texas at Austin: sn, 242 (2008).

[11] S. Bhattacharjee Compact Plasma and Focused Ion Beams. (Taylor & Francis, 2013).

[12] R. A. Wolf Atmospheric pressure plasma for surface modification. (John Wiley & Sons, 2012).

[13] M. Druyvesteyn & F. M. Penning. The mechanism of electrical discharges in gases of low pressure. Reviews of Modern Physics, 12, 87 (1940).

[14] R. D'agostino, P. Favia, Y. Kawai, H. Ikegami, N. Sato et al. Advanced plasma technology. (John Wiley & Sons, 2008).

[15] A. Bogaerts, E. Neyts, R. Gijbels & J. Van Der Mullen. Gas discharge plasmas and their applications. Spectrochimica Acta Part B: Atomic Spectroscopy, 57, 609 (2002).

[16] C.-h. Yi, Y.-h. Lee, D. W. Kim & G.-y. Yeom. Characteristic of a dielectric barrier discharges using capillary dielectric and its application to photoresist etching. Surface and Coatings Technology, 163, 723 (2003).

[17] B. M. Smirnov Fundamentals of ionized gases: basic topics in plasma physics. (John Wiley & Sons, 2012).

[18] G. Federici, C. H. Skinner, J. N. Brooks, J. P. Coad, C. Grisolia et al. Plasma-material interactions in current tokamaks and their implications for next step fusion reactors. Nuclear Fusion, 41, 1967 (2001).

[19] Z. A. Munir, U. Anselmi-Tamburini & M. Ohyanagi. The effect of electric field and pressure on the synthesis and consolidation of materials: A review of the spark plasma sintering method. Journal of Materials Science, 41, 763 (2006).

[20] A. Al Khawwam, C. Jama, P. Goudmand, O. Dessaux, A. El Achari et al. Characterization of carbon nitride layers deposited by IR laser ablation of graphite target in a remote nitrogen plasma atmosphere: nanoparticle evidence. Thin Solid Films, 408, 15 (2002).

[21] S. Li, X. Ma, L. Liu & X. Cao. Degradation of 2,4-dichlorophenol in wastewater by low temperature plasma coupled with TiO2 photocatalysis. Rsc Advances, 5, 1902 (2015).

[22] N. Wang, D. Z. Chen & L. S. Zou. Influence of non-thermal plasma pre-treatment on the scaling characteristics of viscous oil wastewater during evaporation. Applied Thermal Engineering, 75, 779 (2015).

[23] M. Yousfi, N. Merbahi, A. Pathak & O. Eichwald. Low-temperature plasmas at atmospheric pressure: toward new pharmaceutical treatments in medicine. Fundamental & Clinical Pharmacology, 28, 123 (2014).

[24] N. De Geyter & R. Morent. Nonthermal Plasma Sterilization of Living and Nonliving Surfaces. Annual Review of Biomedical Engineering, Vol 14, 14, 255 (2012).

[25] I. Koban, K. Duske, L. Jablonowski, K. Schröder, B. Nebe et al. Atmospheric Plasma Enhances Wettability and Osteoblast Spreading on Dentin In Vitro: Proof-of-Principle. Plasma Process. Polym., 8, 975 (2011).

[26] G. Fridman, M. Peddinghaus, M. Balasubramanian, H. Ayan, A. Fridman et al. Blood coagulation and living tissue sterilization by floating-electrode dielectric barrier discharge in air. Plasma Chemistry and Plasma Processing, 26, 425 (2006).

[27] S. U. Kalghatgi, G. Fridman, M. Cooper, G. Nagaraj, M. Peddinghaus et al. Mechanism of blood coagulation by nonthermal atmospheric pressure dielectric barrier discharge plasma. IEEE Trans. Plasma Sci., 35, 1559 (2007).

[28] S. P. Kuo, O. Tarasenko, J. Chang, S. Popovic, C. Y. Chen et al. Contribution of a portable air plasma torch to rapid blood coagulation as a method of preventing bleeding. New J. Phys., 11 (2009).

[29] N. Kumar, P. Attri, E. H. Choi & H. S. Uhm. Influence of water vapour with non-thermal plasma jet on the apoptosis of SK-BR-3 breast cancer cells. Rsc Advances, 5, 14670 (2015).

[30] X.-M. Shi, G.-J. Zhang, Z.-S. Chang, X.-L. Wu, W.-L. Liao et al. Viability Reduction of Melanoma Cells by Plasma Jet via Inducing G1/S and G2/M Cell Cycle Arrest and Cell Apoptosis. IEEE Trans. Plasma Sci., 42, 1640 (2014).

[31] J. K. Lee, M. S. Kim, J. H. Byun, K. T. Kim, G. C. Kim et al. Biomedical applications of low temperature atmospheric pressure plasmas to cancerous cell treatment and tooth bleaching. Japanese Journal of Applied Physics, 50, 08JF1 (2011).

[32] P. Sun, J. Pan, Y. Tian, N. Bai, H. Wu et al. Tooth whitening with hydrogen peroxide assisted by a direct-current cold atmospheric-pressure air plasma microjet. Plasma Science, IEEE Transactions on, 38, 1892 (2010).

[33] S. Kilmer, N. Semchyshyn, G. Shah & R. Fitzpatrick. A pilot study on the use of a plasma skin regeneration device (Portrait® PSR3) in full facial rejuvenation procedures. Lasers in medical science, 22, 101 (2007).

[34] T. Kono, W. F. Groff, H. Sakurai, T. Yamaki, K. Soejima et al. Treatment of traumatic scars using plasma skin regeneration (PSR) system. Lasers in surgery and medicine, 41, 128 (2009).

[35] J. Heinlin, G. Morfill, M. Landthaler, W. Stolz, G. Isbary et al. Plasma medicine: possible applications in dermatology. JDDG: Journal der Deutschen Dermatologischen Gesellschaft, 8, 968 (2010).

[36] M. Moisan & J. Pelletier Physics of Collisional Plasmas: Introduction to High-Frequency Discharges. (Springer Science & Business Media, 2012).

[37] L. E. Ashman & W. P. Menashi Treatment of surface with low-pressure plasmas,US Patent: 3 701 628 (1972).

[38] R. M. G. Boucher Seeded gas plasma sterilization method,US Patent: 4 207 286 (1980).

[39] P. T. Jacobs & S.-M. Lin Hydrogen peroxide plasma sterilization system,US patent 3,701,628 (1988).

[40] M. Krebs, P. Becasse, D. Verjat & J. Darbord. Gas–plasma sterilization: relative efficacy of the hydrogen peroxide phase compared with that of the plasma phase. International Journal of Pharmaceutics, 160, 75 (1998).

[41] S. Lerouge, A. Fozza, M. Wertheimer, R. Marchand & L. H. Yahia. Sterilization by low-pressure plasma: the role of vacuum-ultraviolet radiation. Plasmas and Polymers, 5, 31 (2000).

[42] S. Lerouge, M. Wertheimer & Y. L'h. Plasma sterilization: a review of parameters, mechanisms, and limitations. Plasmas and Polymers, 6, 175 (2001).

[43] A. Bol'shakov, B. Cruden, R. Mogul, M. Vs Rao, S. Shama et al. Radio-frequency oxygen plasma as a sterilization source. AIAA journal, 42, 823 (2004).

[44] M. Boscariol, A. Moreira, R. Mansano, I. Kikuchi & T. Pinto. Sterilization by pure oxygen plasma and by oxygen–hydrogen peroxide plasma: An efficacy study. International journal of pharmaceutics, 353, 170 (2008).

[45] H. Liu, J. Chen, L. Yang & Y. Zhou. Long-distance oxygen plasma sterilization: Effects and mechanisms. Applied Surface Science, 254, 1815 (2008).

[46] M. Moisan, J. Barbeau, M.-C. Crevier, J. Pelletier, N. Philip et al. Plasma sterilization. Methods and mechanisms. Pure and applied chemistry, 74, 349 (2002).

[47] S. Moreau, M. Moisan, M. Tabrizian, J. Barbeau, J. Pelletier et al. Using the flowing afterglow of a plasma to inactivate Bacillus subtilis spores: Influence of the operating conditions. Journal of Applied Physics, 88, 1166 (2000).

[48] M. Moisan, J. Barbeau, S. Moreau, J. Pelletier, M. Tabrizian et al. Low-temperature sterilization using gas plasmas: a review of the experiments and an analysis of the inactivation mechanisms. International journal of Pharmaceutics, 226, 1 (2001).

[49] K. Kutasi, B. Saoudi, C. D. Pintassilgo, J. Loureiro & M. Moisan. Modelling the Low-Pressure N2 O2 Plasma Afterglow to Determine the Kinetic Mechanisms Controlling the UV Emission Intensity and Its Spatial Distribution for Achieving an Efficient Sterilization Process. Plasma Process. Polym., 5, 840 (2008).

[50] M. Boudam & M. Moisan. Synergy effect of heat and UV photons on bacterial-spore inactivation in an N2–O2 plasma-afterglow sterilizer. Journal of Physics D: Applied Physics, 43, 295202 (2010).

[51] M. Moisan, K. Boudam, D. Carignan, D. Keroack, P. Levif et al. Sterilization/disinfection of medical devices using plasma: the flowing afterglow of the reduced-pressure N-2-O-2 discharge as the inactivating medium. European Physical Journal-Applied Physics, 63 (2013).

[52] J. Feichtinger, A. Schulz, M. Walker & U. Schumacher. Sterilisation with low-pressure microwave plasmas. Surface & Coatings Technology, 174, 564 (2003).

[53] D. Vicoveanu, S. Popescu, Y. Ohtsu & H. Fujita. Competing Inactivation Agents for Bacterial Spores in Radio-Frequency Oxygen Plasmas. Plasma Process. Polym., 5, 350 (2008).

[54] P. Awakowicz & A. Von Keudell. BIODECON: Plasma decontamination in medical technology. Plasma Process. Polym., 3, 75 (2006).

[55] F. Rossi, O. Kylián & M. Hasiwa. Decontamination of surfaces by low pressure plasma discharges. Plasma Process. Polym, 3, 431 (2006).

[56] A. Fridman Plasma chemistry. (Cambridge University Press, 2008).

[57] G. Fridman, A. D. Brooks, M. Balasubramanian, A. Fridman, A. Gutsol et al. Comparison of direct and indirect effects of non-thermal atmospheric-pressure plasma on bacteria. Plasma Process. Polym., 4, 370 (2007).

[58] R. B. Gadri, J. R. Roth, T. C. Montie, K. Kelly-Wintenberg, P. P.-Y. Tsai et al. Sterilization and plasma processing of room temperature surfaces with a one atmosphere uniform glow discharge plasma (OAUGDP). Surface and Coatings Technology, 131, 528 (2000).

[59] M. Hähnel, T. Von Woedtke & K. D. Weltmann. Influence of the air humidity on the reduction of Bacillus spores in a defined environment at atmospheric pressure using a dielectric barrier surface discharge. Plasma Process. Polym., 7, 244 (2010).

[60] J. Goree, B. Liu & D. Drake. Gas flow dependence for plasma-needle disinfection of S. mutans bacteria. Journal of Physics D: Applied Physics, 39, 3479 (2006).

[61] H. S. Uhm, J. P. Lim & S. Z. Li. Sterilization of bacterial endospores by an atmospheric-pressure argon plasma jet. Applied physics letters, 90, 261501 (2007).

[62] T. Shimizu, B. Steffes, R. Pompl, F. Jamitzky, W. Bunk et al. Characterization of microwave plasma torch for decontamination. Plasma Process. Polym., 5, 577 (2008).

[63] E. Robert, E. Barbosa, S. Dozias, M. Vandamme, C. Cachoncinlle et al. Experimental study of a compact nanosecond plasma gun. Plasma Process. Polym., 6, 795 (2009).

[64] K. D. Weltmann, M. Polak, K. Masur, T. Von Woedtke, J. Winter et al. Plasma processes and plasma sources in medicine. Contributions to Plasma Physics, 52, 644 (2012).

[65] K. D. Weltmann, E. Kindel, T. Von Woedtke, M. Hähnel, M. Stieber et al. Atmospheric-pressure plasma sources: Prospective tools for plasma medicine. Pure and Applied Chemistry, 82, 1223 (2010).

[66] G. Konesky in SPIE Defense, Security, and Sensing 76651P (International Society for Optics and Photonics, 2010).

[67] Q.-Y. Nie, Z. Cao, C.-S. Ren, D. Z. Wang & M. G. Kong. A two-dimensional cold atmospheric plasma jet array for uniform treatment of large-area surfaces for plasma medicine. New J. Phys., 11, 115015 (2009).

[68] C. Huang, Q. Yu, F. h. Hsieh & Y. Duan. Bacterial deactivation using a low temperature argon atmospheric plasma brush with oxygen addition. Plasma Process. Polym., 4, 77 (2007).

[69] H. W. Herrmann, I. Henins, J. Park & G. Selwyn. Decontamination of chemical and biological warfare (CBW) agents using an atmospheric pressure plasma jet (APPJ). Physics of Plasmas (1994-present), 6, 2284 (1999).

[70] F.-J. Trompeter, W. J. Neff, O. Franken, M. Heise, M. Neiger et al. Reduction of Bacillus subtilis and Aspergillus niger spores using nonthermal atmospheric gas discharges. Plasma Science, IEEE Transactions on, 30, 1416 (2002).

[71] F. Bosshard, M. Bucheli, Y. Meur & T. Egli. The respiratory chain is the cell's Achilles' heel during UVA inactivation in Escherichia coli. Microbiology, 156, 2006 (2010).

[72] F. Bosshard, K. Riedel, T. Schneider, C. Geiser, M. Bucheli et al. Protein oxidation and aggregation in UVA-irradiated Escherichia coli cells as signs of accelerated cellular senescence. Environmental microbiology, 12, 2931 (2010).

[73] N. Munakata, M. Saito & K. Hieda. Inactivation action spectra of Bacillus subtilis spores in extended ultraviolet wavelengths (50–300nm) obtained with synchrotron radiation. Photochemistry and photobiology, 54, 761 (1991).

[74] N. Philip, B. Saoudi, M.-C. Crevier, M. Moisan, J. Barbeau et al. The respective roles of UV photons and oxygen atoms in plasma sterilization at reduced gas pressure: the case of N 2-O 2 mixtures. Plasma Science, IEEE Transactions on, 30, 1429 (2002).

[75] O. Kylián, T. Sasaki & F. Rossi. Plasma sterilization of Geobacillus Stearothermophilus by O2: N2 RF inductively coupled plasma. The European Physical Journal Applied Physics, 34, 139 (2006).

[76] J. Guo, K. Huang & J. Wang. Bactericidal effect of various non-thermal plasma agents and the influence of experimental conditions in microbial inactivation: A review. Food Control, 50, 482 (2015).

[77] D. Mendis, M. Rosenberg & F. Azam. A note on the possible electrostatic disruption of bacteria. Plasma Science, IEEE Transactions on, 28, 1304 (2000).

[78] Y. Zhao, A. Ogino & M. Nagatsu. Effects of N2–O2 Gas Mixture Ratio on Microorganism Inactivation in Low-Pressure Surface Wave Plasma. Jpn. J. Appl. Phys., 50, 08JF05 (2011).

[79] L. Yang, J. Chen & J. Gao. Low temperature argon plasma sterilization effect on Pseudomonas aeruginosa and its mechanisms. Journal of Electrostatics, 67, 646 (2009).

[80] M. Laroussi, C. Tendero, X. Lu, S. Alla & W. L. Hynes. Inactivation of bacteria by the plasma pencil. Plasma Process. Polym., 3, 470 (2006).

[81] M. Nagatsu, F. Terashita, H. Nonaka, L. Xu, T. Nagata et al. Effects of oxygen radicals in low-pressure surface-wave plasma on sterilization. Applied Physics Letters, 86 (2005).

[82] K. Kelly-Wintenberg, T. Montie, C. Brickman, J. Roth, A. Carr et al. Room temperature sterilization of surfaces and fabrics with a one atmosphere uniform glow discharge plasma. Journal of Industrial Microbiology and Biotechnology, 20, 69 (1998).

[83] K. Kelly-Wintenberg, A. Hodge, T. Montie, L. Deleanu, D. Sherman et al. Use of a one atmosphere uniform glow discharge plasma to kill a broad spectrum of microorganisms. J. Vac. Sci. Technol. A, 17, 1539 (1999).

[84] T. C. Montie, K. Kelly-Wintenberg & J. Reece Roth. An overview of research using the one atmosphere uniform glow discharge plasma (OAUGDP) for sterilization of surfaces and materials. Plasma Science, IEEE Transactions on, 28, 41 (2000).

[85] M. Yusupov, A. Bogaerts, S. Huygh, R. Snoeckx, A. C. Van Duin et al. Plasma-induced destruction of bacterial cell wall components: a reactive molecular dynamics simulation. The Journal of Physical Chemistry C, 117, 5993 (2013).

[86] S. Perni, G. Shama, J. Hobman, P. Lund, C. Kershaw et al. Probing bactericidal mechanisms induced by cold atmospheric plasmas with Escherichia coli mutants. Applied Physics Letters, 90, 073902 (2007).

Chapter 2

Absolute oxygen atomic density measured with a self-absorption calibrated VUVAS method and its effect on spore etching

In this chapter, in order to understand the etching effect happened in N_2/O_2 gas mixture surface-wave plasma, with a new kind of compact microwave plasma light source, oxygen atomic density was measured with self-absorption calibrated vacuum ultraviolet absorption spectroscopy (VUVAS) technique based on the theory of resonance escape factor, the absolute oxygen atomic densities were consistently analyzed using two adjacent oxygen atom emissions at 130.22 nm and 130.49 nm for different N_2/O_2 gas mixture ratios in surface-wave plasma (SWP). Results of the absolute oxygen atomic densities and its effect on spore etching will be discussed.

2.1 Introduction.

Previous results in our group showed that UV radiation are the import lethal factors in the inactivation of *Geobacillus stearothermophilus* spores in N_2/O_2 gas mixture SWP.[1-3] However, the behaviors of neutral active species in the inactivation process have not been studied enough, because only a few reliable measurement techniques for the absolute densities of radicals in reactive plasmas have been developed. Hashizume, et al. reported the inactivation effect of ground-state atomic oxygen (O (^3P_j)) and excited molecular oxygen ($O_2(^1\Delta_g)$) species measured by the VUVAS technique on *Penicillium digitatum* spores using atmospheric pressure oxygen radical source.[4, 5] They concluded that atomic oxygen was the crucial species responsible for inactivation of *Penicillium digitatum* spores, which are classified as fungi. But in this work, we used *Geobacillus stearothermophilus* spores as bio-indicators, *which was* classified as bacterial spores. Fungi spore (*Eukaryotes*) is common propagule, which will be easily inactivated by heat. On the other hand, bacteria spore (*Prokaryotes*) is the dormancy body with very low moisture content and very strong resistance, so it's very difficult to kill them. Thus, it has been widely used as a biological indicator to evaluate reliability of sterilization methods in the

medical field. Therefore, the study of the neutral radicals effect on the inactivation of spores in plasma was necessary and valuable.

Various methods, such as laser induced fluorescence spectroscopy,[6-8] electron spin resonance spectroscopy,[9] cavity enhanced absorption techniques,[10-12] actinometry techniques,[13] and NO titration,[14] have been developed to measure the absolute densities of oxygen or nitrogen radicals, however, these methods have different limitations and deficiencies.

Laser induced fluorescence spectroscopy is clearly a versatile and powerful technique, although there are some important limitations, such quantum efficiency of detector and background light stemmed from plasma emission and stray laser light, it gives us a precise absolute atomic density, but needs very expensive optical instruments and a sophisticated skill to perform reliable measurement. And laser probably has disturbance on plasma for its high power.

Electron spin resonance (ESR) spectroscopy is a useful technique for measuring various radicals produced in plasmas, it had also been used to measure hydroxyl or oxygen radicals in non-thermal atmospheric pressure plasma jet-water system or dielectric barrier discharge, but it is difficult to introduce the radicals into the ESR observation region, especially in a low pressure plasma device.

Cavity enhanced absorption techniques need to install reflection mirror inside the discharge chamber, so it has special requirements on the plasma discharge device, and the plasma etching on the reflection mirror will also decrease the accuracy of the measurement result.

For actinometry techniques, the actinometry relation $I_O/I_{Ar}=K[O]/[Ar]$ is valid, when the following conditions are fulfilled: first, emitting excited state atoms are solely produced by electron impact on the ground-state atoms; second, excited states decay primarily radidtively; third, the electron-impact cross sections for O and Ar have similar thresholds and shapes. Thus, the validity of actinometry method depends on the plasma parameters, mainly the pressure, the atom dissociation rate, and the electron energy distribution function (EEDF), it has been proved by some group that actinometry method was invalid in low pressure (mtorr) distributed electron cyclotron resonance microwave plasmas.

NO titration introduce new gas to the plasma system, it will has disturbance on the plasma discharge, and it can only measure the neutral radical density in the afterglow of plasmas, not an in situ measurement method.

Compared with these methods, vacuum ultraviolet absorption spectroscopy (VUVAS) technique was a simple in situ method to determine the absolute atomic density with low cost and minimal influence on the processing plasma, thus it has been widely used for the absolute radical density determination in processing plasma.[4, 15, 16]

For VUVAS measurement, it's important to estimate the emission line profile. Accurate determination of emission line profiles need very high resolution monochromator. Gerard Gousset had measured the line shape of oxygen atoms near 130 nm with a very large resolution monochromator(resolution 5×10^{-4} nm)[17], however, this kind of ultrahigh resolution monochromator is rare in common laboratory. When you can't get the emission line profile with a high resolution monochromator, a widely used compromise solution in VUVAS measurement is to use a light source which has a negligible level self-absorption of the emission line probes, but it's a tough work to find this kind of light source for the limit of the experimental conditions. Although tunable laser systems have been used as light sources in VUVAS measurements, they are usually expensive and their tunable range is limited to a narrow wavelength region, especially with tunable diode lasers. With a plasma light source, it usually requires considerable effort to satisfy the light source requirements, so this issue often limits the applicability of the VUVAS method to the precise measurement of absolute radical densities in processing plasmas.

This study presents an alternative method; that is, a self-absorption calibration method for a plasma light source used in VUVAS measurements. With a low resolution monochromator, the self-absorption calibration was performed by spectral analysis of the emission line profile, taking into account the optical escape factor. Using this self-absorption-calibrated VUVAS method, we demonstrated oxygen atomic density measurements in a mixed nitrogen and oxygen surface-wave plasma, with analysis of two different emission lines at 130.22 nm and 130.49 nm. The etching effect of excited oxygen atoms on spore-forming microorganisms was discussed by comparing with the measured absolute atomic densities in SWPs operated with different N_2/O_2 gas mixture ratios. We found that these two probes consistently gave almost identical oxygen atomic densities.

The etching effect of excited oxygen atoms on spore-forming microorganisms was discussed by comparing with the measured absolute atomic densities in SWPs operated with different N_2/O_2 gas mixture ratios.

2.2 Experimental condition

The total experimental setup is schematically shown in figure 2.1. The target plasma is produced in a planar surface-wave sustained plasma generator driven by a 2.45 GHz microwave, which has been used for the low pressure plasma sterilization previously[18]. The cylindrical processing chamber is made of stainless steel with an inner diameter of 30 cm and height of 30 cm, respectively. Slot antenna is cut on the bottom side of the rectangle waveguide and next to the waveguide there is a quartz plate for the surface-wave excitation and propagation. The plasma is produced at a pressure of 13.3 Pa and a total gas flow of

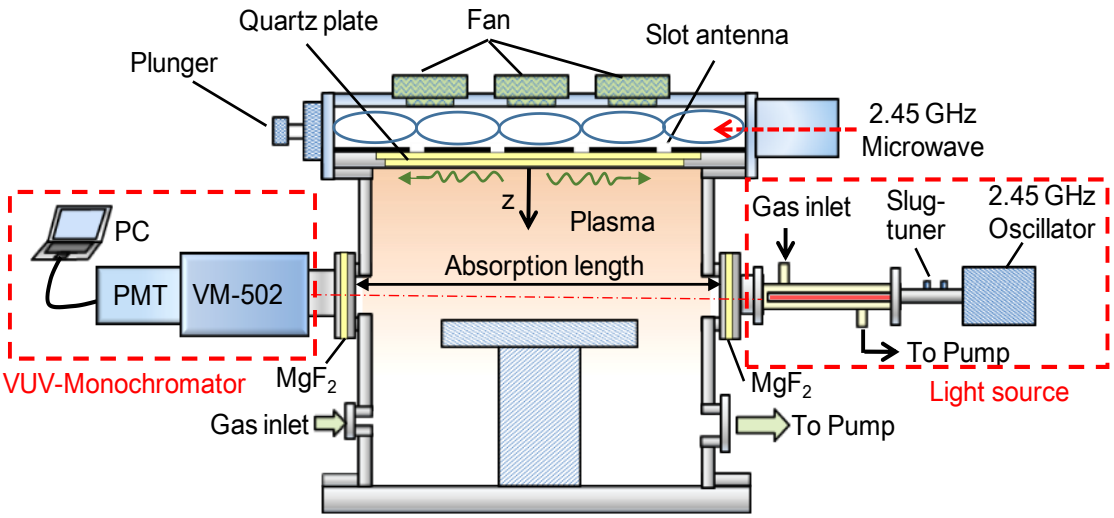

Figure 2.1 Schematic drawing of the experimental set-up.

100sccm.The plasma can be produced under the quartz plate and diffuse downward to the chamber. As shown in figure 1, the absorption length L for VUV absorption measurement was taken as approximately 30 cm, that is, an inner diameter of cylindrical chamber. In our previous sterilization experiments, the sample was placed 10 cm away from the quartz plate in the center of the chamber, so we just set the light path at the same height. The light source is installed on one side (10 cm below the quartz plate) of the chamber and the VUV

monochromator (Acton Research Corporation, VM–502) is fixed at the opposite position. Two MgF_2 glass windows are inserted at both sides to separate it into three different pressure regions. Both pressures in the monochromator and processing chamber can be pumped down to 10^{-3} Pa by separated two-stage differential pumping systems. As previous study on the surface-wave plasma characteristics, in a diffusion region (z=10 cm) plasma can keep certain uniformity [19, 20]. So we can assume a uniform distribution for the O atomic density through the light path in the surface-wave plasma in the absorption measurement.

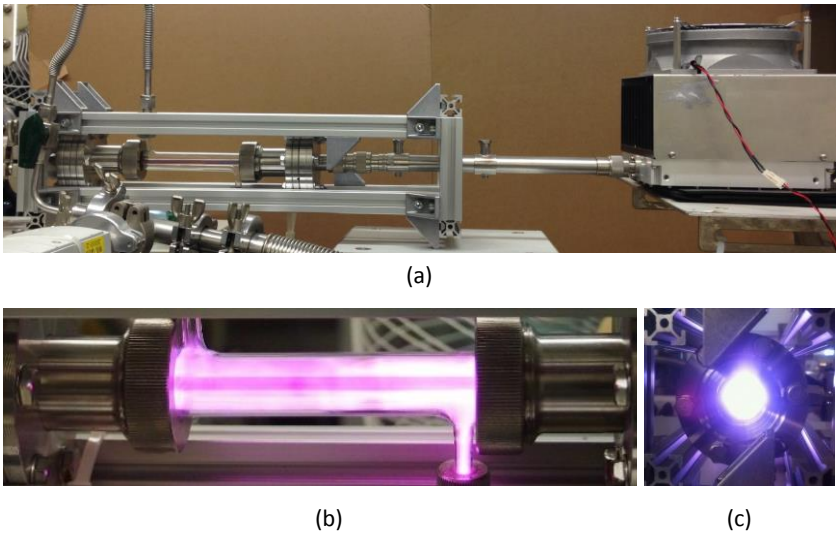

Figure 2.2 (a) photograph of light source in side view; (b) discharge picture of light source in side view; (c) discharge picture of light source in front view. (Discharge condition of the light source: microwave power 85 W, Ar flow rate 10 sccm; N_2 flow rate 0.1 sccm)

A compact microwave plasma generator was prepared as the light source for VUVAS method. The photos of the light source is shown in Fig.2.2. This light source is built on the coaxial type surface-wave plasma. A copper rod electrode with a diameter of 3 mm and length of 16 cm is connected to the coaxial cable on the flange. A capped cylindrical quartz tube with a thickness of 1.5 mm is covered over the copper rod electrode and sealed with ceramics at the bottom part, which offers the boundary for the surface-wave excitation and transmitting. A 2.45 GHz microwave oscillator with a maximum output of 100 W is used as the power source. The coaxial cable can transmit a microwave to the light source

electrode. Double slug tuner is used on the cable to adjust the impedance matching between the microwave source and plasma load. The electrode is packaging in a quartz tube (*I.D.* =18 mm, *L*=18 cm) with two gas taps for vacuum pumping and gas inlet, respectively. A small turbo molecular-rotary pump system is employed for the vacuum in the tube with a basic pressure of 10^{-3} Pa. In suitable working gas condition, the discharge can occur at the bottom part of the electrode firstly, after matching the incident microwave power, surface-wave can be excited and transmitting at the interface between plasma and quartz tube. A typical discharge is shown in figure 2.2(b), and (c). In this work, we have selected Ar and a little amount of O_2 mixture as the working gas for producing 130 nm oxygen transition lines.

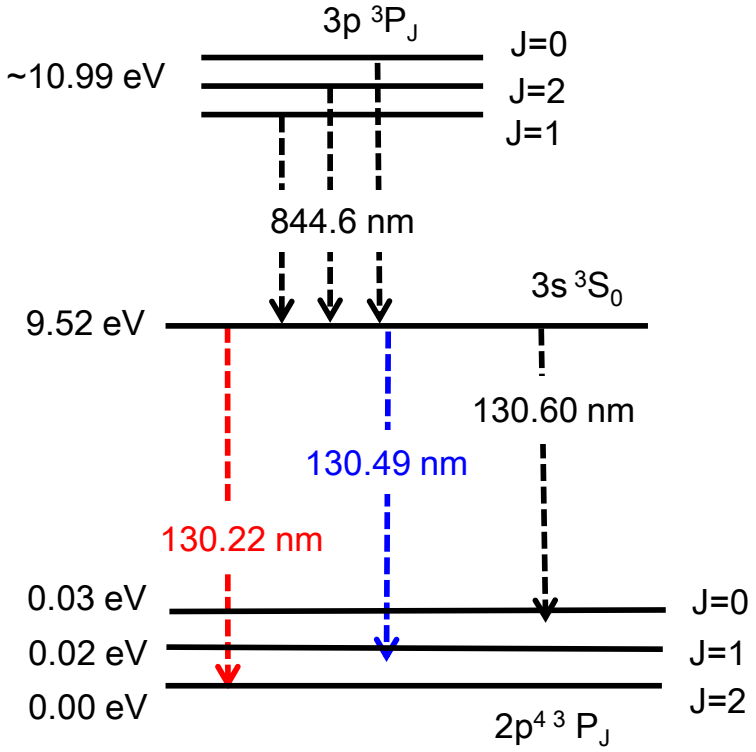

Figure 2.3 The partial energy level diagram of oxygen atoms

As illustrated in figure 2.3, in this work, the resonance line chose for the VUVAS measurement of O atom density was near 130 nm. The ground state ($2p^4$ ^3P_J) of the resonance lines has three sub-levels (J=0, 1, 2) with the intervals of 0.02 and 0.01 eV, and other atomic parameters are listed in table 2.1.

In order to verify the reliability of the calibration method, two emission probes were chosen for the measurement. As the intensity of 130.60 nm is too weak for the measurement, so we adopted 130.22 nm line and 130.49 nm as the probe emissions. Under local thermodynamic equilibrium conditions, the total density of oxygen atoms in the ground state is evaluated by assuming the Boltzmann distribution at a temperature of 500 K among the three sublevels:[21].

$$\frac{N_1}{N_2} = \frac{g_1}{g_2} \exp(-\frac{\Delta E}{kT}) \tag{2.1}$$

Where N_1 and N_2 refer to the atomic density at different energy level; g_1 and g_2 are the statistical weights of the different energy levels; ΔE is the energy difference between the two energy levels; k is Boltzmann's constant (k=8.614×10^{-5} eV/K); T is thermodynamic temperature of the system.

Table 2.1 Transition probability and statistical weights for oxygen resonance lines[22]

λ_0 (nm)	Transition	E_1(cm^{-1})	E_2(cm^{-1})	g_1	g_2	A_{21} (10^8 s^{-1})
130.22	$3s^3\,S^0$-$2p^4\,{}^3P_2$	0	7679.978	5	3	3.41
130.49	$3s^3\,S^0$-$2p^4\,{}^3P_1$	158.265	7679.978	3	3	2.03
130.60	$3s^3\,S^0$-$2p^4\,{}^3P_0$	226.977	7679.978	1	3	0.676

As shown in figure 2.4, a representative absorption ratio measurement process of VUVAS can be divided into four steps. First, the target surface-wave plasma was turned on and the emission intensity was measured as background emission level, intensity I_1. Then the plasma light source was operated, both emissions from the surface-wave plasma and plasma light source were measured as intensity I_2. Finally, surface-wave plasma was turned off, and only the emission from plasma light source was measured as intensity I_3. The dark current was subtracted from the recorded intensities in the above steps. By taking an ensemble average over 30 measurements of the respective emission intensities, we calculated the absorption ratio with the following formula: A=1-(I_2-I_1)/I_3. Finally, we obtained the averaged absorption ratio by repeating the above calculation steps four times.

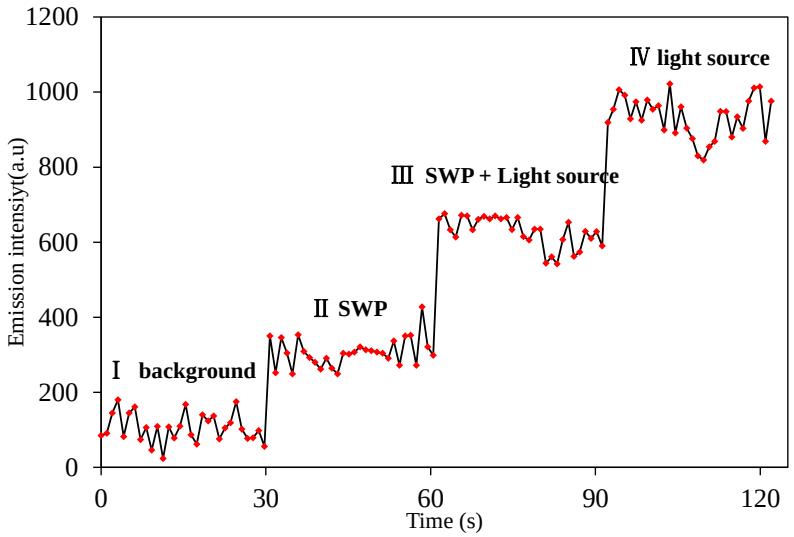

Figure 2.4 A representative absorption ratio measurement process of VUVAS (Light source: Ar 5 sccm, O_2 0.1 sccm, pressure 8.2 Pa, power 70 W; surface-wave plasma: N_2 60 sccm, O_2 40 sccm, incident power 600 W)

2.3 Principles of VUVAS method

According to the theoretical studies of Mitchell and Zemansky[23], the principle of VUVAS will be introduced briefly based on our low pressure plasma condition. When parallel light beam from the light source goes through an absorption cell containing plasma with thickness of L, there is the relationship between the incident intensity I_0 and transmitted intensity I_t:

$$I_t = I_0 \exp(-k_\nu L) \tag{2.2}$$

Where k_ν is absorption coefficient as a function of the absorption line frequency ν. When the pressure of the absorbing gas and the thickness of the absorbing layer are chosen small enough, only the heat motions of the atoms are taken into account, the absorption depends on Doppler broadening. The absorption coefficient of a gas is given by:

$$k_\nu = k_0 \exp(-\omega^2) \tag{2.3}$$

Here ω is normalized frequency chose to simplify the calculation：

$$\omega=2\sqrt{\ln 2}(\nu-\nu_0)/\Delta\nu_D \tag{2.4}$$

Where ν_0 is the central frequency, $\Delta\nu_D$ is the Doppler width, depending only on the absolute temperature T and the molecular weight M of the absorption line:

$$\Delta\nu_D = 7.16\times10^7 \nu_0\sqrt{\mathrm{T/M}} \tag{2.5}$$

k_0 is the maximum absorption coefficient at the central frequency ν_0 of the absorption line when Doppler broadening alone is present. And it is related to the atomic density at the lower energy level:

$$k_0 = \frac{2}{\Delta\nu_D}\sqrt{\frac{\ln 2}{\pi}}\frac{\lambda_0^2 g_2}{8\pi g_1}A_{21}N \tag{2.6}$$

Where λ_0 is the line center wavelength, g_1 and g_2 are the statistical weights of the lower and upper energy levels, respectively, N is the ground state oxygen atomic density in target surface-wave plasma, and A_{21} is the transition probability for the related spectral lines.

The absorption of the incident light due to the plasma is presented by the following formula：

$$A=1-\frac{I_t}{I_0}=\frac{\int E_\nu\left[1-\exp(-k_0 L\exp(-\omega^2))\right]d\omega}{\int E_\nu d\omega} \tag{2.7}$$

where E_ν is the light source emission line profile which depends on the light source characteristic[24]. From equation (2.6), when the light source emission probe was selected, absorption ratio A is dependent only on k_0L, k_0 is a function of atomic density at ground level, it means with a given absorption length L, A only depends on the atom density in the light source.

In this work, the light source worked at low pressure condition, an ideal empirical expression of the emission line profile, which represents roughly the broadening effect coming from the pressure and temperature within the light source, can be given:

$$E_\nu = C\exp(-\omega^2) \tag{2.8},$$

Where C is a constant. Equation (2.8) gives a theoretical profile without self-absorption, it is a typical Gaussian distribution, but in actual experiment, it will be changed by the self-absorption phenomenon happened in the light source. When the self-absorption in light source was small enough to ignore it, equation (2.7) can be used directly in the

VUVAS calculation process, but few light source can fulfill this requirement. When the self-absorption in light source was not in a negligible level, a calibration is necessary to get accurate measurement results. Next part will give a calibration method base on the spectral line escape factor theory.

2.4 Procedure of proposed self-absorption calibration method for the light source

2.4.1 Self-absorption checking method

Self-absorption is a resonance process that a photon emitted by an excited atom at one point in a light source, it may be absorbed by another atom in the transmission path in the same source, it will change spectral line shapes, and produce larger width and incorrect measurement results.[25, 26] Appropriate calibration was necessary for the quantitative analysis with spectral line intensity. Therefore, some techniques can be used to determine the self-absorption effect in the light source[25].

First way to check self-absorption is to double the optical path length by putting a concave mirror at two focal lengths behind the plasma. Then if the emission intensity increase doubles, except for reflection and transmission losses, that means the self-absorption was negligible. But this method is difficult to implement in many setups when the plasma is enclosed inside a chamber with a limited number of viewports, and the transmission losses will also increase when the mirror is etched by the plasma.

Second technique for checking the self-absorption in homogeneous pulsed sources is to put a movable obstacle which can change plasma observation length but keep plasma parameters remain constant. It is possible to determine the self-absorption by measuring the line shapes with different plasma length.

For pulse plasma sources, self-absorption could be checked by measuring the full width at half maximum of the emission spectral line during plasma decay [27].

In the previous VUVAS experiment, a widely used method to self-absorption was to measure the absorption ratios in the same target plasma condition with different light source discharge conditions. In this method, a light source discharge conditions, where observed absorption ratios kept unchanged, are regarded as the operating conditions of

negligible self-absorption[24, 28, 29].

But the most straightforward way to check the self-absorption is measuring the line intensity ratios within multiplets, which was based on the LS-coupling rules: the reduction in the observed intensity of the strongest or metastable line within the multiplet, in respect to the weakest spectral line in the same multiplet shows that self-absorption is present[30]. The degree of the self-absorption can be quantitatively examined by comparing experimentally determined intensity ratios with the ideal intensity ratios which can be got from the theoretical calculations with atomic transition probabilities data[25]. The theoretical ratio of oxygen atoms resonance lines at 130.22, 130.49, and 130.60 nm calculated by using *Specair* [31], was 1:0.59:0.20, however we observed the different intensity ratio of line emission, which clearly shows that the effect of self-absorption of the present light source is not negligible.

2.4.2 Self-absorption calibration method

Drawin and Emard [32], have shown that the relation between the real emission intensity and the intensity at optically thin case can be written as:

$$I_\lambda = I_\lambda^{thin} \Lambda \tag{2.9}$$

Escape factor Λ, which described firstly by is defined as the ratio between the real radiation flux escaping from the plasma and the radiation flux in the ideal optically thin case. It had been used in the calculation of the self-absorption of the spectral lines [33-36], it can be given by the following formula:

$$\Lambda = \int P(\nu) \exp\left[-\tau_0 \frac{P(\nu)}{P(\nu_0)} \right] d\nu \tag{2.10}$$

where τ_0 is the optical thickness at emission line center ν_0, for the emission length of the light source l (16cm), $\tau_0 = k_0' l$ [37], and k_0' is the maximum absorption coefficient at emission line center, it can be obtained from equation (2.6). And $P(\nu)$ is the normalized Gaussian line profile:

$$P(\nu) = \frac{\sqrt{\ln 2}}{\Delta\nu_D} \exp\left[-4 \ln 2 \frac{(\nu - \nu_0)^2}{\Delta\nu_D^2} \right] \tag{2.11}$$

With equation (2.4) and (2.11), equation (2.10) can be rewritten by:

$$A=\int \frac{\sqrt{\ln 2}}{\Delta\nu_D}\exp(-\omega^2)\exp(-k_0' l\exp(-\omega^2))\mathrm{d}\omega \qquad (2.12)$$

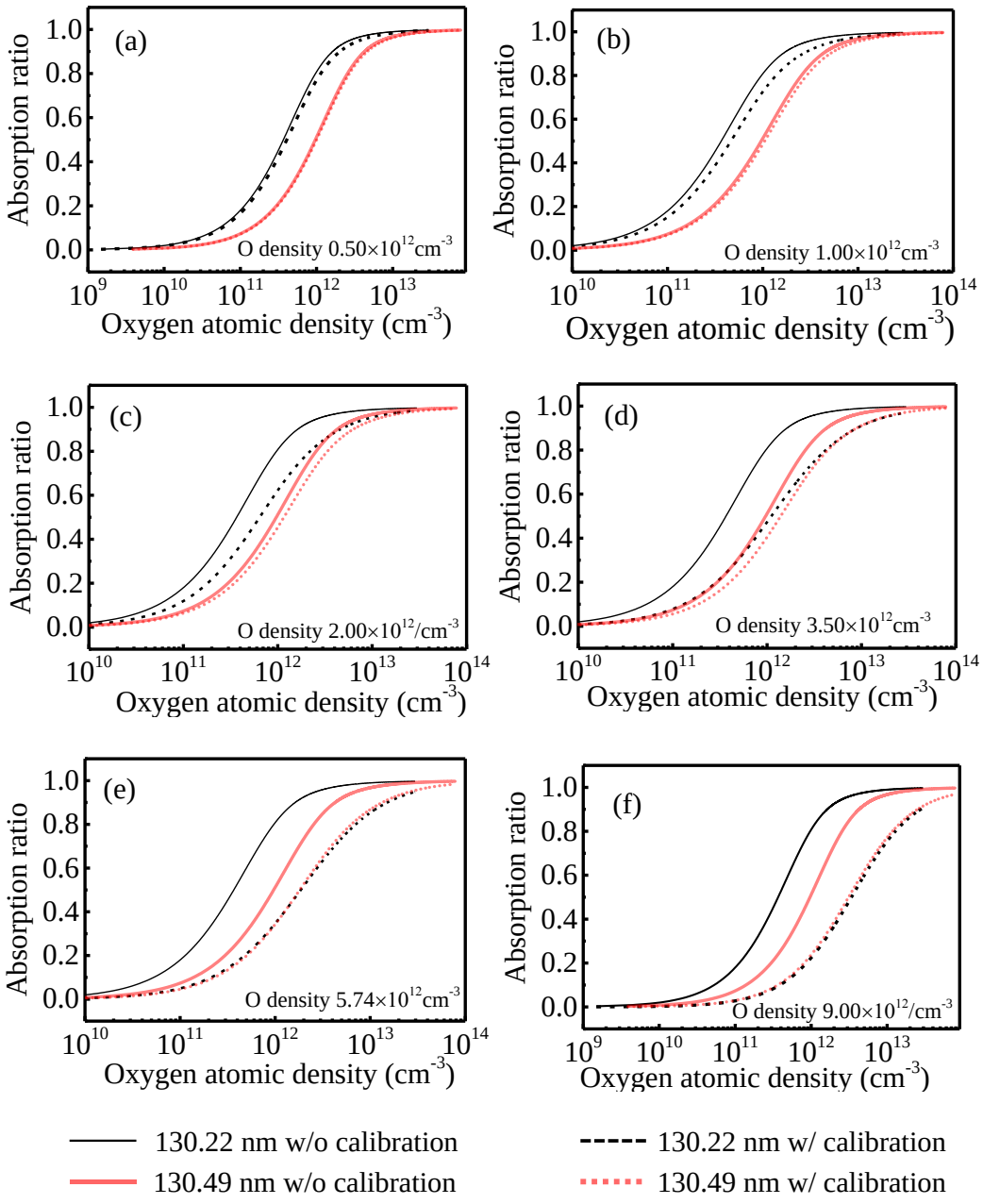

Figure 2.5 Absorption curves of surface-wave plasma calculated at 130.22 nm and 130.49 nm for different O densities in light source, assuming absorption length of 30 cm and gas temperature of 500 K.

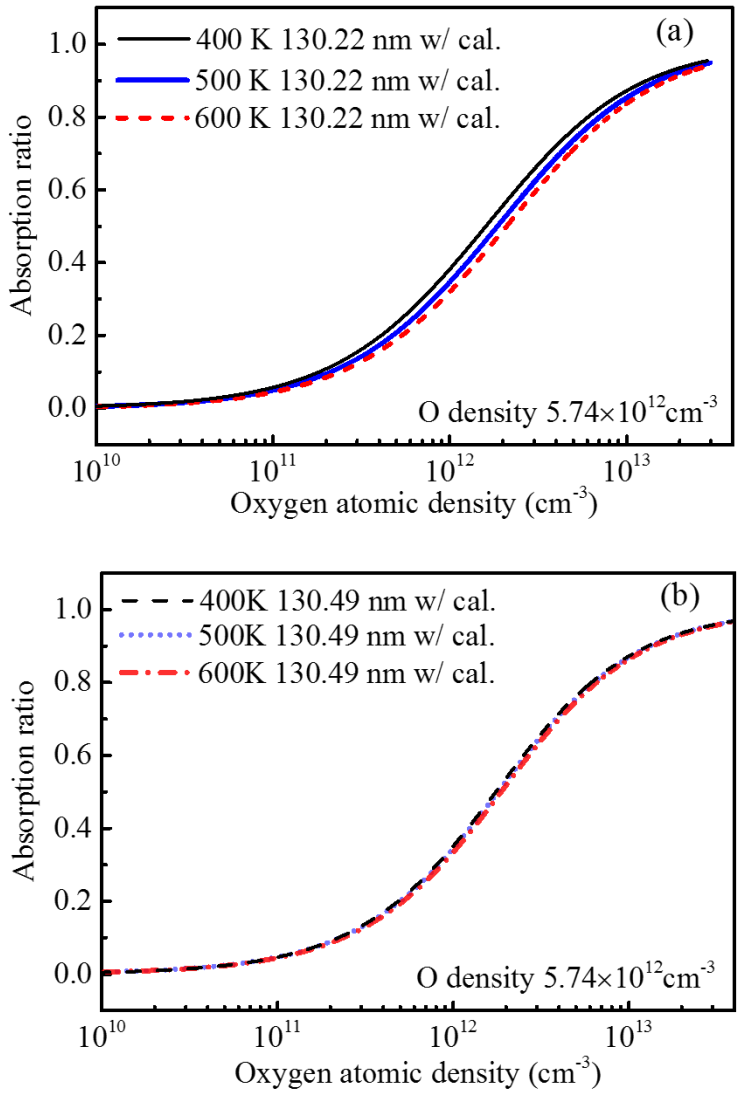

Figure 2.6 Absorption curves of surface-wave plasma calculated at 130.22 nm (a) and 130.49 nm (b) for the gas temperature in SWP was 400 K, 500 K and 600 K respectively, assuming an absorption length of 30 cm.

The value of escape factor lies between 0 and 1, it was the total ratio of the radiation escaped from plasma spread freely without being caught by other atoms in the plasma, and the integrand of the escape factor give a real emission profile:

$$E_v = C\exp(-\omega^2)\exp(-k_0' l \exp(-\omega^2)) \tag{2.13}$$

According our light source discharge condition, assuming the absorption was uniform in the emission direction of the light source, the gas temperature was constant at 600 K, and emission length of the light source was stable at 16 cm, we can deduce from equation

2.13 that the emission line profile with self-absorption calibration only has a strong relationship with the oxygen atomic density in the light source.

With the atomic parameters showed in table 2.1, we calculated the absorption curve with and without self-absorption calibration from equation 2.7 with equation 2.13. According our previous gas temperature measurement result at similar discharge condition, the gas temperature of target surface-wave plasma was assumed to be stable at 500 K.

The absorption curve was calculated for different self-absorption level according different oxygen atomic density in light source. As shown in figure 2.5, the absorption curve with self-absorption calibrated moved to the high atomic density region. From figure 2.5 (a, b), it was found when oxygen atomic density in the light source was 0.5×10^{12} cm^{-3} and 1.0×10^{12} cm^{-3}, the absorption curves with and without self-absorption had very small difference, that means in this condition, the self-absorption was weak enough to ignore it, Gauss profile could be used as E_v directly for the VUVAS calculation. But when the oxygen atomic density increased from 2.0×10^{12} to 9×10^{12} cm^{-3}, it was found from figure 2.5 (c, d, e, f) that the absorption curves with and without self-absorption calibration were quite different. The ideal absorption curves without self-absorption at 130.22 and 130.49 nm were far apart. Therefore, for the same atomic density in the target plasma, the absorption ratio with self-absorption calibration will be lower than the ideal profile without self-absorption. As the atomic density in the light source increased, the calibrated absorption curves at the two emission probes became closer to each other. This was result from the different oxygen atomic densities in the three ground-state sub-levels of the Boltzmann distribution in the light source, in which the percentages of oxygen atomic density at each sub-level were evaluated to be 65.5% at J=2 (130.22 nm) and 26.9% at J=1 (130.49 nm) at 600K. For the same discharge conditions of the light source, the self-absorption effect at 130.22 nm is stronger than at 130.49 nm, so the calibrated absorption curve for 130.22 nm changed faster than for 130.49 nm.

Considering that the gas temperature was changeable for different discharge condition in target surface-wave plasma, absorption curves were calculated with different gas temperature in surface-wave plasma at a constant light source condition (same to figure 2.5 e). As shown in figure 2.6 (a), the absorption curves of 130. 22 nm calculated at 400 K, 500 K and 600 K has small difference, compared with the assumed gas temperature 500 K,

the oxygen atomic densities decreased up to10% at 400 K and increased up to14 % at 600K. From figure 2.6 (b), the oxygen atomic density result calculated from 400 K and 600 K had a maximum 5 % difference with the result of 500 K, thus the difference of absorption curve at 130.49 nm for temperature 400 K, 500 K and 600 K was almost negligible, These errors is allowable in the present experiments. [38, 39]

2.5. Results and discussion

2.5.1 Self-absorption effect of the light source

In this study, self-absorption was checked by measuring the line intensity ratios within multiplets. Peaks ratios of oxygen atoms resonance lines at 130.22, 130.49, and 130.60 nm, which intuitively demonstrated the level of self-absorption, were measured with different light source discharge condition. The optimal light source condition and light probe would be chose based on both of the emission line intensity and self-absorption.

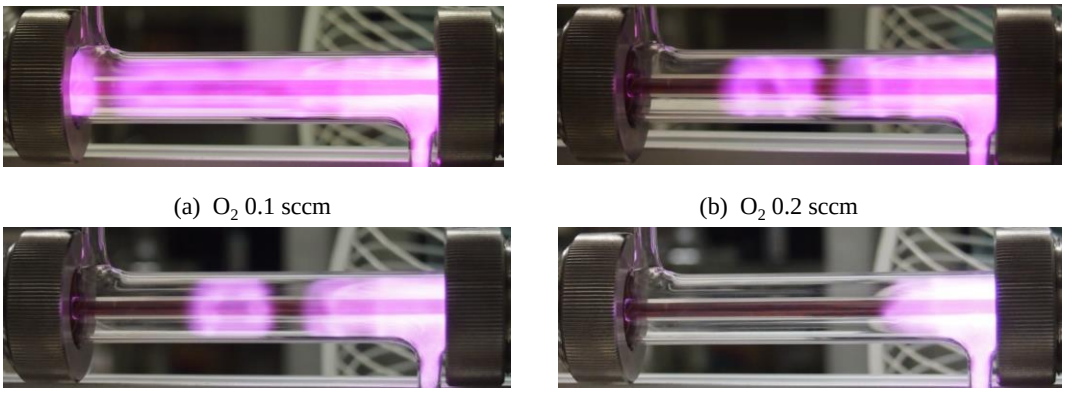

(a) O_2 0.1 sccm (b) O_2 0.2 sccm

(c) O_2 0.3 sccm (d) O_2 0.4 sccm

Figure 2.7 Discharge condition of plasma light source under different O_2 gas flow rates from 0.1 to 0.4 sccm at fixed Ar flow rate of 10 sccm, pressure of 12 Pa and incident power of 60 W.

First, we kept Ar flow rate at 10 sccm, pressure at 12 Pa, and incident power at 70W, as the discharge picture shown in figure 2.7, O_2 gas flow rate was varied from 0.1 sccm to 0.4 sccm. The discharge became a little weak when the oxygen flow rate increased, and the

discharge length almost keep stable when the oxygen flow rate was increase from 0.1 sccm to 0.3 sccm, but when the oxygen flow increased to 0.4 sccm, the discharge length suddenly decrease to very short.

The most import thing is to check the emission intensity and peaks ratio of the three emission lines. As shown in figure 2.8, with the monochromator resolution of 0.1 nm, the three transition lines near 130 nm was separated clearly, but the second and third peaks still had a smaller overlap. From the result shown in figure 2.8, the emission intensity increased slightly when the oxygen flow rate increased from 0.1 sccm to 0.3 sccm, that coming from the increase of the oxygen atomic density when more oxygen was introduced to the system, but the intensity decreased significantly when the oxygen flow rate increased to 0.4 sccm,

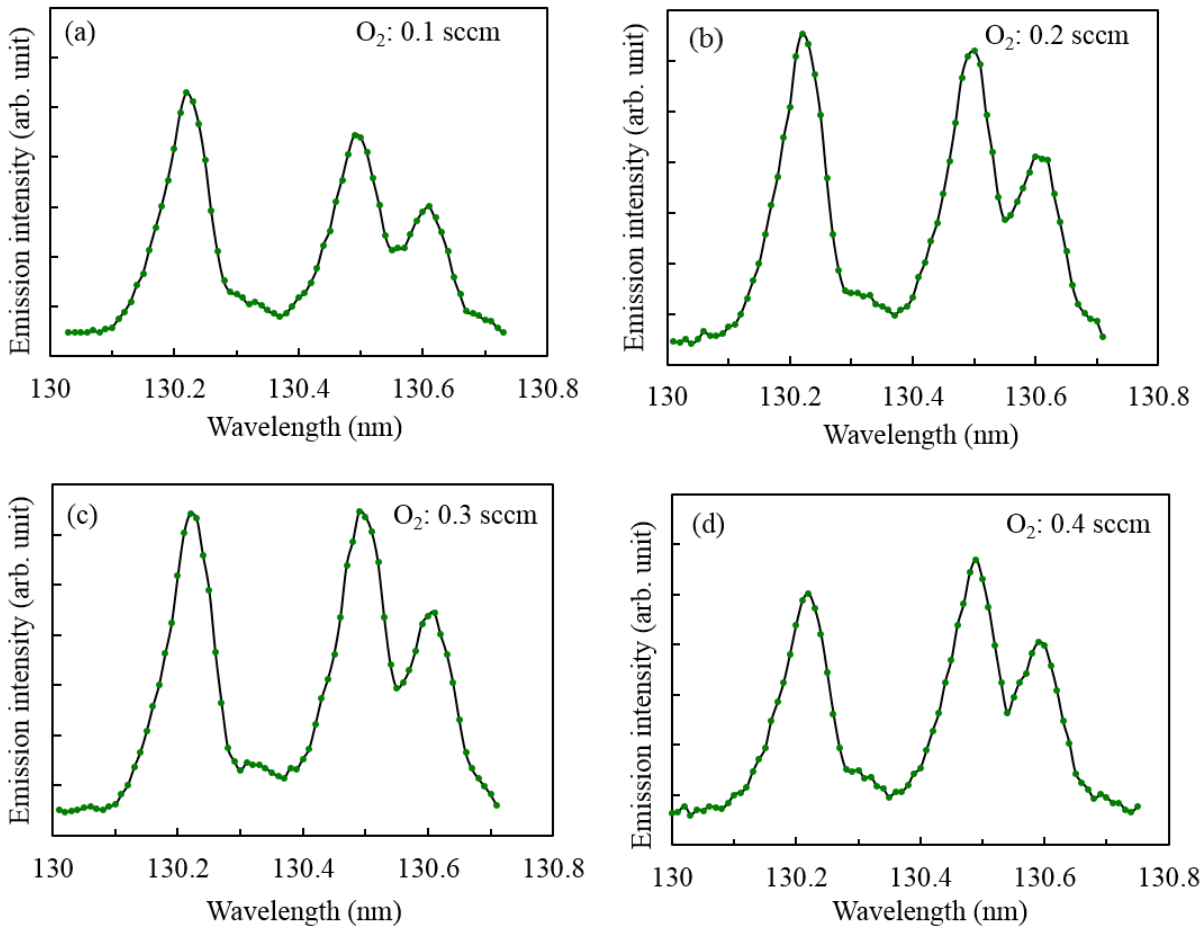

Figure 2.8 Emission spectrum near 130 nm from a plasma light source under different O_2 gas flow rates from 0.1 to 0.4 sccm at fixed Ar flow rate of 10 sccm, pressure of 12 Pa and incident power of 60 W.

it could be easily understood from the discharge picture shown in figure 2.6, the plasma discharge length decreased suddenly at 0.4 sccm oxygen flow rate.

The peak ratios at three emission lines measured from figure 2.8 varied from (a) 1:0.86:0.52 at 0.1 sccm, (b) 1:0.94:0.59 at 0.2 sccm, (c) 1:1.01:0.67 at 0.3 sccm and (d) 1:1.15:0.78 at 0.4 sccm, respectively. According to LS-coupling rules, the short wavelength has biggest self-absorption, thus with the peaks ratios changing trend, we could deduce that the self-absorption increased obviously when the oxygen flow rate increased. Therefore we should chose the small oxygen flow rate for the VUVAS measurement.

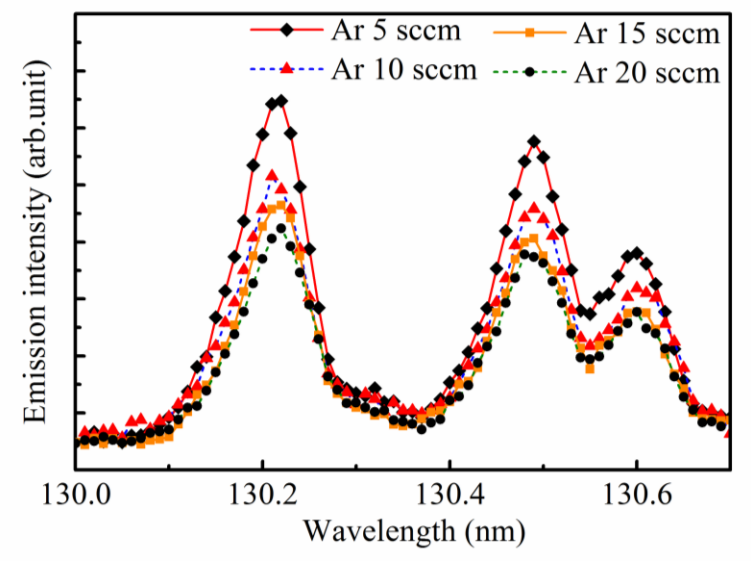

Figure 2.9 Emission line profiles with different Ar gas flow rates (pressure varied from 8.2 to 19 Pa) at fixed O_2 gas flow rate of 0.1sccm and incident power of 70W.

Next, we kept the oxygen gas flow rate at the 0.1 sccm which was the minimum flow rate of the mass flow controller, the incident power was kept at 70 W, and only the Ar flow rate and pressure were changed. As shown in figure 2.9, as the argon flow rate increased from 5 sccm to 20 sccm, the emission intensity decreased gradually, but the peak ratio almost kept constant. It means if the partial pressure of O_2 kept constant, the degree of self-absorption was almost at same level. However, it is better to use a higher emission intensity to improve the signal-to–noise ratio in the VUVAS measurement. Therefore, we selected 5 sccm of Ar gas flow rate and 0.1 sccm of O_2 gas flow rate for the measurement.

We also tried different microwave power, but sometimes the discharge could not be

ignited when the microwave power was below 65 W. Even if the emission intensity increased a little when the power increased to 80 W or 90 W, but the temperature of discharge tube easily increased to 40-50℃ after discharging, so we chose a moderate power of 70 W for the present measurements. Considering both the emission intensity and peak ratio, the optimal discharge condition we got for the light source system was: Ar flow rate at 5 sccm, O_2 flow rate at 0.1 sccm, pressure at 8.2 Pa, and incident microwave

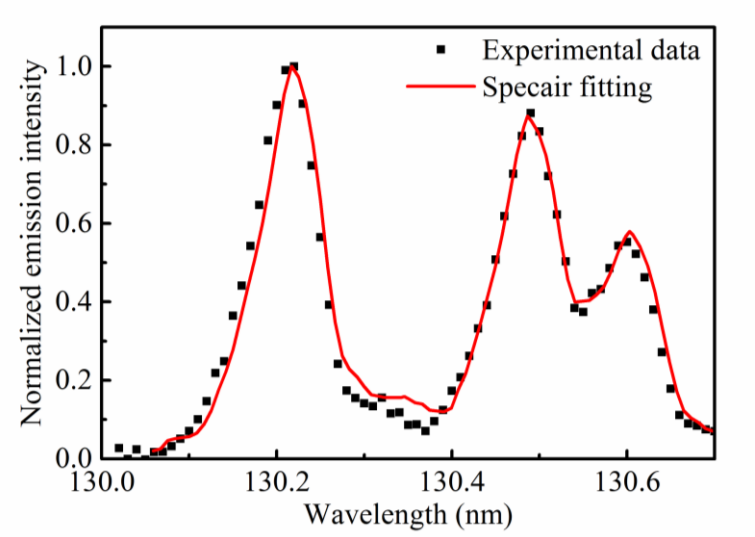

Figure 2.10. Fitting spectra of oxygen emission by *Specair* under the conditions of oxygen atom temperature at 600 K, electron temperature 16000K, pressure at 8.2 Pa, emission path length of 16 cm, and oxygen atomic density of 5.74×10^{12} cm^{-3}.

power at 70 W. The peak ratio in this condition was 1: 0.88: 0.55, even if this ratio still had small overlap, it was far from the ideal peak ratio of 1:0.59:0.20. Usually this kind of light source with such significantly self-absorption can't be used in VUVAS measurement. But in this study, based on spectral analysis and self-absorption calibration based escape factor theory, this light source worked well in VUVAS measurement.

First, we used *Specair* to fit the measured emission profile of optimal conditions. The measured spectral profile in the rage of 130.05-130.35 nm was taken as the slit function for *Specair*[31], where from our light source discharge condition, we assumed oxygen atom temperature at 300 K, pressure at 8.2 Pa, and emission path length 16 cm. After trying different oxygen atomic densities in light source, we found 3.45×10^{12} cm^{-3} is plausible to

fit well with the observed emission profile, which we obtained under our optimal light source discharge condition, as shown in figure 2.10.

Next, we tried to calculate the ideal emission spectrum without self-absorption using *Specair*. The emission profiles calculated with *Specair* with and without self-absorption were shown in figure 2.11. It shows directly that the optimal light source condition had a very big self-absorption. But the profile shown in figure 2.11 still had a small overlap because of the instrument broadening.

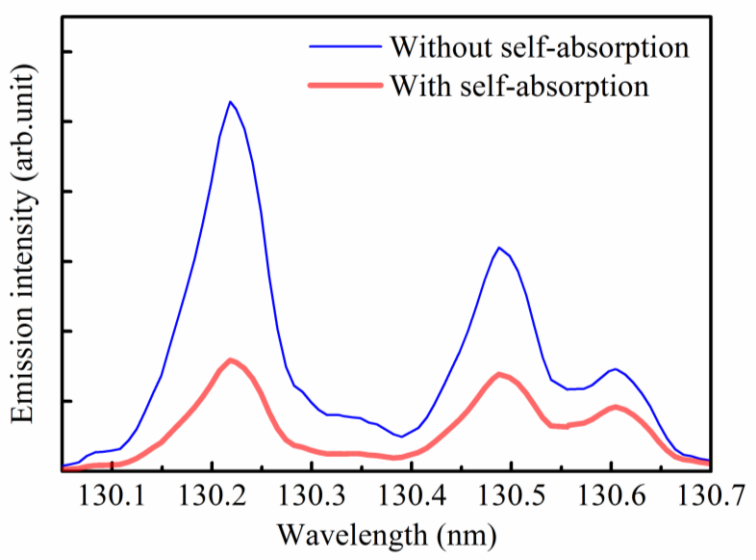

Figure 2.11. Emission spectra without self-absorption calculated by *Specair* in consideration of instrumental broadening.

Thus we removed the effect of instrumental broadening from the spectral emission profiles by *Specair* to get a theoretical line profile, and the result was shown in figure 2.12. As shown in figure 2.12, the ideal line spectrum without self-absorption is a pure Gaussian distribution which can be expressed from equation (2.8), while the real profile with self-absorption can be obtained from equation (2.13).

When removed the instrumental broadening effect, the peak ratio of ideal line spectrum without self-absorption was 1: 0.59: 0.20, because of the self-absorption of short wavelength is stronger than long wavelength, the peaks ratio of experimentally determined profile without overlap at our optimal light source condition was 1: 0.96: 0.68, the big

difference between them showed us the self-absorption of our optimal light source condition was significant.

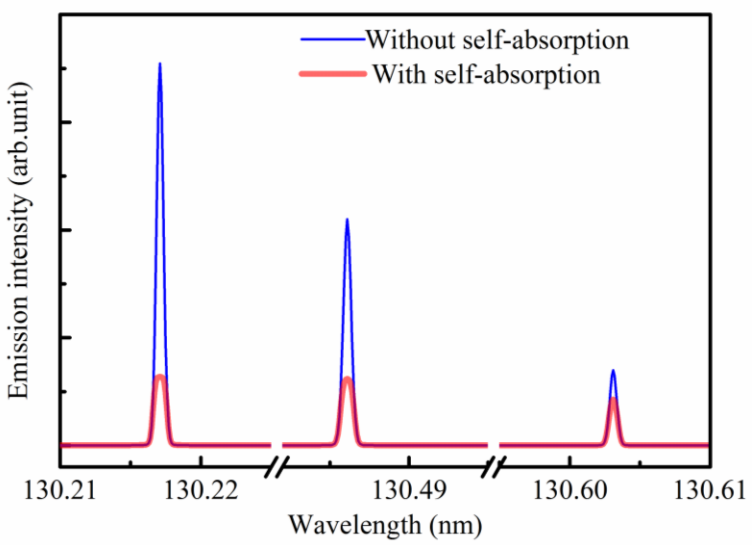

Figure 2.12. The emission profile calculated from Specair without instrument broadening.

Quantitative analysis of self-absorption at three transition lines can be calculated by the peak area integration of the profile without instrument broadening. Here the self-absorption ratio is defined as the proportion between the absorbed part by self-absorption and theoretical peak intensity. With the profile shown in figure 2.12, the ratios between the intensity of self-absorption parts and the ideal intensity without self-absorption calculated at 130.22nm, 130.49nm, 130.60 nm were calculated to be 0.70, 0.57, and 0.29, respectively. It's obvious that self-absorption of short wavelength is stronger than long wavelength. Although 130.60nm had smaller self-absorption, but it has a lower intensity, it will increase the measurement error, therefore, 130.22nm and 130.49nm were chosen as the light probe for VUVAS measurement in this study.

Finally, under the optimum discharge conditions in the light source obtained by *Specair* analysis, we calculated the absorption curves at 130.22 nm and 130.49 nm as a function of oxygen atomic density in the target surface-wave plasma. The corresponding absorption curves with and without self-absorption were already given in figure 2.5 (e).

2.5.2. The absolute oxygen atom densities with different N_2 and O_2 gas mixture ratio in surface-wave plasma.

In order to examine the role of oxygen atoms in the inactivation of the spore forming microorganisms in the N_2/O_2 gas mixture plasma, both of the absorption ratios at 130.22 nm and 130.49 nm were measured for different gas ratio of N_2 and O_2 in surface-wave plasma. The incident power of the surface-wave plasma was kept at 600 W, pressure was fixed at 13.3 Pa with a total flow rate of 100 sccm. As the result shown in figure 2.13, we obtained very similar results of absorption ratios at two light probes for different gas mixture of N_2 and O_2 in surface-wave plasma, and these results are fairly consistent with the calibrated absorption curves shown in figure 2.5(e).

Figure 2.14 shows the oxygen atomic densities with and without self-absorption calibration, which were evaluated from the calculated absorption curves in figure 2.4(d) with the measured absorption ratio in figure 2.13. It is clearly seen from figure 2.14 that oxygen atomic densities with and without self-absorption calibration are quite different. With self-absorption calibrated absorption curves, we obtained very similar atomic densities with different light probes. This result indicates that our calibration method is reasonable and feasible. From figure 2.14, we can also find that the oxygen atomic density without self-absorption calibration was significantly lower than the result with calibration, especially at 130.22 nm. These results indicated that one might be misled to the wrong value of oxygen atomic density by the VUVAS measurement without self-absorption calibration.

It is found from figure 2.14 that the oxygen atomic density with self-absorption calibration varied from about 1.32×10^{12} to 3.98×10^{12} cm^{-3} for different N_2 and O_2 gas mixture ratios, and the highest oxygen density was obtained when the gas mixture ratio of N_2 to O_2 was 1: 9. The present results are very similar to the previous results of optical emission measurement**,** where oxygen atom densities increased by adding a small amount of N_2 into O_2.[40, 41] Similar phenomenon had also been observed that the oxygen atomic density increased clearly when impurity gases, such as SF_6[42], Kr [41]were added to oxygen discharge system. Such increase of dissociation degree for small amount impurity gas can be explained by the a change of electric field E/N reduction[43], various homogeneous reactions, or by a decrease in the wall recombination coefficient[44] .

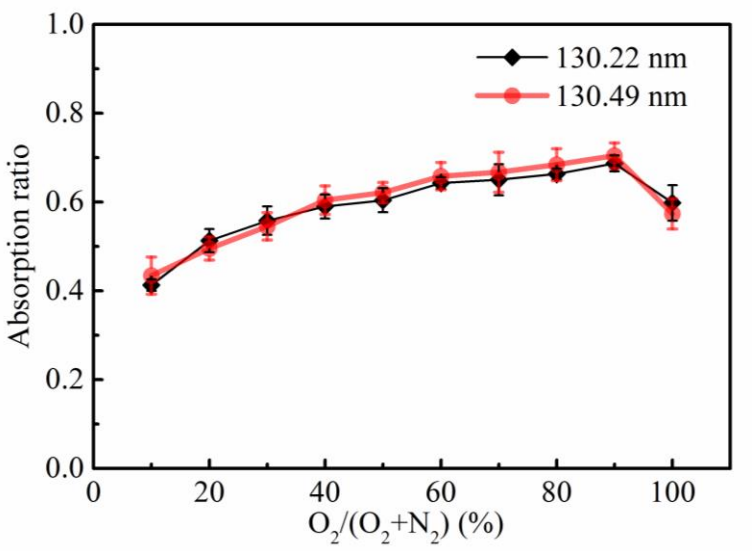

Figure 2.13. Absorption ratios measured at 130.22 nm and 130.49 nm as a function of oxygen gas mixture ratios in surface-wave plasma.

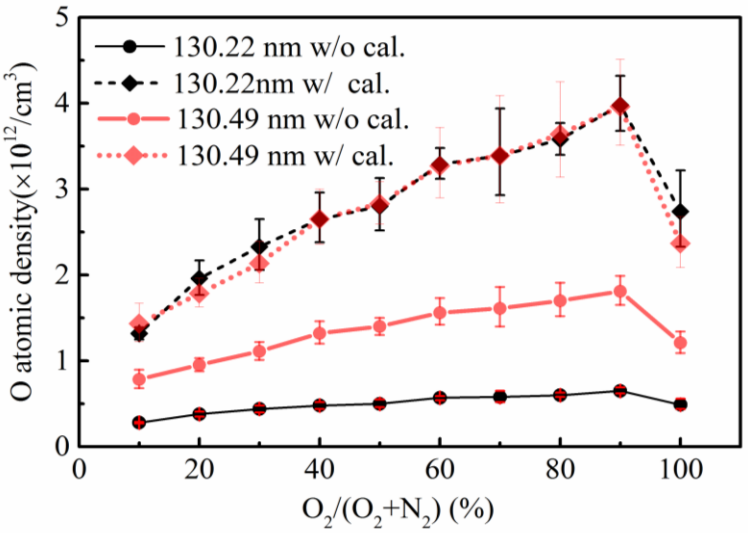

Figure 2.14. Absolute oxygen atomic densities as a function of oxygen mixture ratio in surface-wave plasma evaluated from absorption curves with and without self-absorption calibration at two different probes.

According our previous sterilization measurement results, another possible reason might be the oxygen photodissociation increased when N_2 was introduced. As shown in table 2.2, the threshold wavelengths for different oxygen photodissociation reactions were 242 nm, 175 nm and 133 nm, respectively. When small amount nitrogen was added to the

discharge system, the photos energy of the UV emission coming from NO λ system between 200 nm and 250 nm, and nitrogen atoms below 200 nm can Fully meet the requirements of oxygen photodissociation.

Table 2.2 Threshold wavelengths for oxygen photodissociation

Reaction type	Threshold wavelengths
$O_2+h\nu \rightarrow O(3P)+O(3P)$	242 nm
$O_2+h\nu \rightarrow O(3P)+O(1D)$	175 nm
$O_2+h\nu \rightarrow O(3P)+O(3S)$	133 nm

In our previous work, SWP produced with air-simulated gas was used for the sterilization of Geobacillus stearothermophilus spores, as shown in figure 2.15 (a) the effect of VUV/UV was studied by putting a small metal chamber covered with quartz filter (transmission wavelength >160 nm) at the top to block the radicals inside the plasma chamber. The experimental results shown in figure 2.15(b) indicate that the inactivation efficiency with similar working gas (same pressure with the surface-wave plasma chamber) in small chamber was higher than the condition which the small chamber was kept in vacuum. That means some photochemical reactions happened to produce some radicals which can enhance the inactivation. Considering that the emission wavelength for the

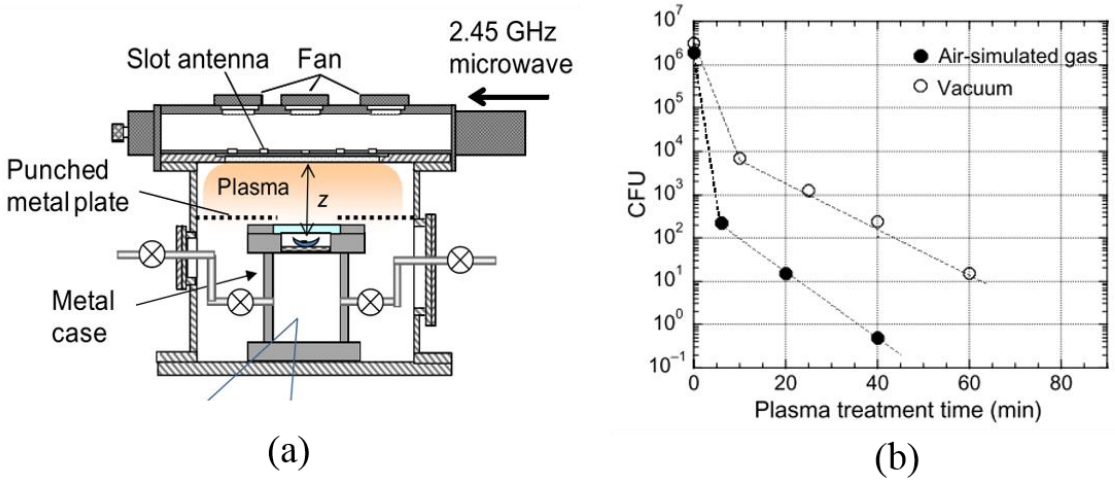

Figure 2.15 (a) Experimental set-up used in previous sterilization experiment. (b) Survival curves of spores treated with air-simulated plasma, with air-simulated gas in small chamber and keeping the small chamber in vacuum.[2]

ionization and dissociation of nitrogen is much lower than transmission wavelength of quartz filter (λ >160 nm), this effect most likely come from the oxygen atoms produced by oxygen photodissociation, the etching effect of oxygen atoms can synergistically improve the inactivation efficiency on spores.

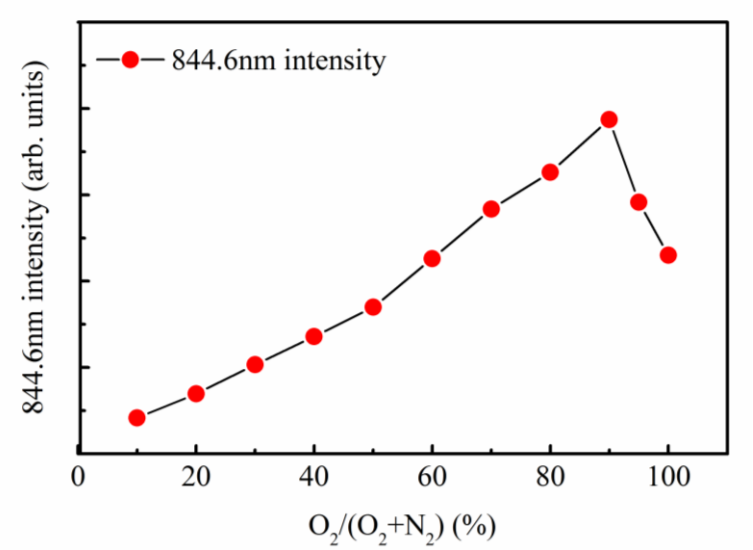

Figure.2.16. Intensity of oxygen atoms observed by OES at 844.6 nm as functions of oxygen mixture ratio.

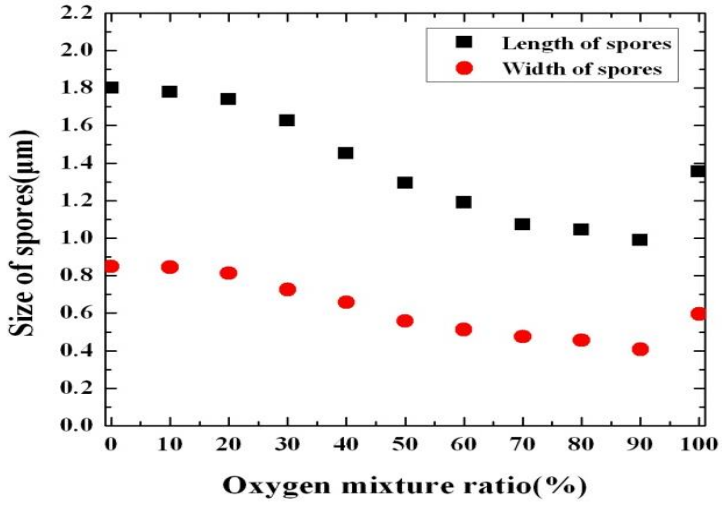

Figure. 2.17 The changes of spore size as a function of oxygen mixture ratio for 1 min plasma treatment.[18]

Oxygen atoms emission line intensity at 844.6 nm which can show the relative density the oxygen atoms, was also measured to confirm our measurement result. As the result

shown in figure 2.16, the variation of absolute oxygen atomic density with respect to N_2/O_2 gas mixture ratio is very analogous to that of the 844 nm emission intensity. As the spore etching result shown in figure 2.17, the changing of oxygen atomic density also agree well with the etching depth in spore length and width which were measured previously after 1 minute plasma treatment under the corresponding conditions.[18] This result illustrated the strong correlation between the oxygen atomic density and the spore etching.

For a deeper understanding of the relation between the oxygen atomic density and the etching effect of spores, spore size changes in length and width were plotted in figure 2.18 as a function of the oxygen atomic densities result at 130.22 nm.

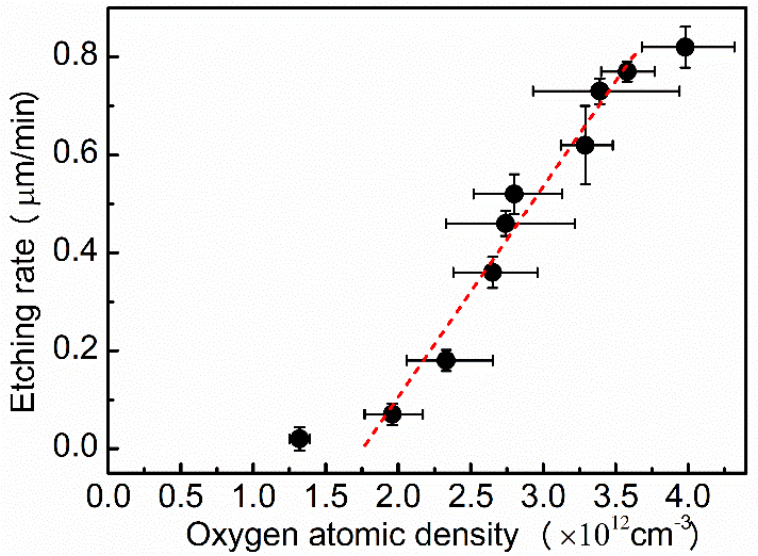

Figure 2.18. Relation between oxygen atomic density and spore length reduction.

At lower oxygen atomic density, the spore size change is negligibly small. However, when the oxygen atomic density becomes greater than 2.0×10^{12} cm^{-3}, the spore length reduction increases quickly. This means that an oxygen density threshold exists for the effective etching of spores. When the oxygen density becomes greater than 3.5×10^{12} cm^{-3}, the etching rate decreases again. These behaviors might come from the multilayer structure of spores.[45] The outermost layer of the spores, mainly consisting of protein, is hard so that a higher concentration of oxygen atoms may be required to etch the outermost surface. After etching the outer coat of spores, the cortex which consists of peptidoglycan, i.e., a polymer consisting of sugars and amino acids, is relatively easily etched by oxygen radicals. When etching reaches the core, the etching rate slowly decreases. This might be due to the

existence of hard inner membrane which holds DNA, protein and amino acids inside the core. From these results, it is considered that the spore etching effect in N_2/O_2 gas mixture plasmas are strongly correlated to concentration of oxygen atoms. But in our previous result, the most efficient inactivation was observed in the range of O_2 gas mixture ratio of 30–80%, rather than at 90%. Therefore, it is considered that the UV emission also play an important role in inactivation process.[18] Synergistically UV radiation emitted by N_2/O_2 gas mixture plasmas can be easily penetrating through the etched spore cortex region into the core region to promote the DNA damages, that is, inactivation of spores.

2.6 Summary

In order to make clear the neutral oxygen atoms effect on spore forming microorganism, we proposed a self-absorption-calibrated VUVAS method, based upon the resonance escape factor theory and numerical analysis of the emission profiles with *Specair*. With a compact microwave plasma light source, absolute oxygen atomic densities were simultaneously and consistently determined by a self-absorption-calibrated VUVAS method with probes at 130.22 and 130.49 nm. After evaluating the self-absorption by examining the peak ratios between three emission lines at 130.22, 130.49, and 130.60 nm, we determined the optimal discharge conditions for the present light source, which has significant self-absorption. Then, the self-absorption effect of the light source was calibrated according to escape factor theory and emission line profile analysis by *Specair*.

With the self-absorption-calibrated absorption curves, we obtained very similar oxygen atomic densities at two different light probes. The oxygen atomic density varied from about 1.32×10^{12} to 3.98×10^{12} cm^{-3} with a changing N_2/O_2 gas mixture ratio, peaking at an N_2/O_2 ratio of 1:9. The variation of absolute oxygen atomic density with respect to N_2/O_2 gas mixture ratio is analogous to previous spore etching results measured under the same discharge conditions, and also to the variation of the emission intensity of oxygen atoms at 844.6 nm. These results strongly support the rationality of the proposed self-absorption-calibrated VUVAS method. The self-absorption calibration method presented here can significantly decrease the light source performance required for VUVAS measurements, and will be useful for the VUVAS measurement in other plasma sources as a plasma diagnostic tool.

The absolute oxygen atom density results correspond to our previous spore etching results of *Geobacillus stearothermophilus* spores. It can be inferred that the spore etching effect in N_2/O_2 gas mixture SWP primarily comes from the oxygen atoms. We also found that a minimum oxygen density is needed for effective etching to begin. As etching plays an important role in plasma inactivation, these results will be helpful to improve plasma sterilization properties in the future.

Reference

[1] L. Xu, H. Nonaka, H. Y. Zhou, A. Ogino, T. Nagata et al. Characteristics of surface-wave plasma with air-simulated N_2–O_2 gas mixture for low-temperature sterilization. J. Phys. D: Appl. Phys., 40, 803 (2007).

[2] M. K. Singh, A. Ogino & M. Nagatsu. Inactivation factors of spore-forming bacteria using low-pressure microwave plasmas in an N_2 and O_2 gas mixture. New J. Phys., 11, 15 (2009).

[3] Y. Zhao, M. K.Singh, A.Ogino & M.Nagatsu. Effects of VUV/UV radiation and oxygen radicals on low-temperature sterilization in surface-wave excited O_2 plasma. Thin Solid Films, 518, 3590 (2010).

[4] H. Hashizume, T. Ohta, F. D. Jia, K. Takeda, K. Ishikawa et al. Inactivation effects of neutral reactive-oxygen species on Penicillium digitatum spores using non-equilibrium atmospheric-pressure oxygen radical source. Appl Phys Lett, 103, 153708 (2013).

[5] S. Iseki, T. Ohta, A. Aomatsu, M. Ito, H. Kano et al. Rapid inactivation of Penicillium digitatum spores using high-density nonequilibrium atmospheric pressure plasma. Appl Phys Lett, 96, 3 (2010).

[6] H. F. Döbele, T. Mosbach, K. Niemi & V. S.-V. D. Gathen. Laser-induced fluorescence measurements of absolute atomic densities: concepts and limitations. Plasma Sources Sci. Technol., 14, S31 (2005).

[7] N. Knake, S. Reuter, K. Niemi, V. Schulz-Von Der Gathen & J. Winter. Absolute atomic oxygen density distributions in the effluent of a microscale atmospheric pressure plasma jet. J. Phys. D: Appl. Phys., 41, 194006 (2008).

[8] E. Wagenaars, T. Gans, D. O'connell & K. Niemi. Two-photon absorption laser-induced fluorescence measurements of atomic nitrogen in a radio-frequency atmospheric-pressure plasma jet. Plasma Sources Sci. Technol., 21, 042002 (2012).

[9] H. Y. Wu, P. Sun, H. Q. Feng, H. X. Zhou, R. X. Wang et al. Reactive Oxygen Species in a Non-thermal Plasma Microjet and Water System: Generation, Conversion, and Contributions to Bacteria Inactivation-An Analysis by Electron Spin Resonance Spectroscopy. Plasma Process. Polym, 9, 417 (2012).

[10] G. Hancock, R. Peverall, G. A. D. Ritchie & T. L. J. The number density of ground state atomic oxygen (O(P-3(2))) measured in an inductively coupled plasma chamber by cavity enhanced absorption. J. Phys. D: Appl. Phys., 40, 4515 (2007).

[11] A. Walsh, D. F. Zhao & H. Linnartz. Cavity enhanced plasma self-absorption spectroscopy. Applied Physics Letters, 101, 4 (2012).

[12] A. J. Walsh, D. F. Zhao & H. Linnartz. Note: Cavity enhanced self-absorption spectroscopy: A new diagnostic tool for light emitting matter. Review of Scientific Instruments, 84, 3 (2013).

[13] A. Granier, D. Chereau, K. Henda, R. Safari & P. Leprince. Validity of actinometry to monitor oxygen atom concentration in microwave discharges created by surface wave in O_2 - N_2 mixtures. J. Appl. Phys., 75, 104 (1994).

[14] P. Va Ina, V. Kudrle, A. Tálský, P. Boto, M. Mrázková et al. Simultaneous measurement of N and O densities in plasma afterglow by means of NO titration. Plasma Sources Science and Technology, 13, 668 (2004).

[15] K. Sasaki, Y. Kawai & K. Kadota. Vacuum ultraviolet absorption spectroscopy for absolute density measurements of fluorine atoms in fluorocarbon plasmas. Appl Phys Lett, 70, 1375 (1997).

[16] A. Kuwahara, M. Matsui & Y. Yamagiwa. Development of vacuum ultraviolet absorption spectroscopy system for wide measurement range of number density using a dual-tube inductively coupled plasma light source. Rev. Sci. Instrum., 83, 123105 (2012).

[17] G. Gousset, P. Panafieu, M. Touzeau & M. Vialle. Experimental study of a d.c. oxygen glow discharge by V.U.V. absorption spectroscopy. Plasma Chem. Plasma Process., 7, 409 (1987).

[18] Y. Zhao, A. Ogino & M. Nagatsu. Effects of N_2–O_2 Gas Mixture Ratio on Microorganism Inactivation in Low-Pressure Surface Wave Plasma. Jpn. J. Appl. Phys., 50, 08JF05 (2011).

[19] M. Nagatsu, A. Ito, N. Toyoda & H. Sugai. Characteristics of ultrahigh-frequency surface-wave plasmas excited at 915 MHz. J. Phys. D: Appl. Phys., 38, L679 (1999).

[20] M. Nagatsu, K. Naito, A. Ogino & S. Nanko. Production of large-area surface-wave plasmas with an internally mounted planar cylindrical launcher. Plasma Sources Sci. Technol., 15, 37 (2006).

[21] J. Zheng, Z. Ji & X. Yu Atomic emission spectroscopy technique and its application. (Chemical industry press, Beijing; 2010).

[22] W. L. Wiese, J. R. Fuhr & T. M. Deters. Atomic transition probabilities of carbon, nitrogen, and oxygen: A critical data compilation. J. Phys. Chem. Ref.Data, Monograph 7. , 1, 340 (1996).

[23] A. C. Q. Mithell & M. W. Zemansky Resonance radiation and excited atoms. (Cambridge University Press, Cambridge; 1961).

[24] H. Nagai, M. Hiramatsu, M. Hori & T. Goto. Measurement of oxygen atom density employing vacuum ultraviolet absorption spectroscopy with microdischarge hollow cathode lamp. Rev. Sci. Instrum., 74, 3453 (2003).

[25] N. Konjević. Plasma broadening and shifting of non-hydrogenic spectral lines: present status and applications. Physics Reports, 316, 339 (1999).

[26] E. Gudimenko, V. Milosavljevic & S. Daniels. Influence of self-absorption on plasma diagnostics by emission spectral lines. Opt. Express, 20, 12699 (2012).

[27] A. M. El Sherbini, T. M. El Sherbini, H. Hegazy, G. Cristoforetti, S. Legnaioli et al. Evaluation of self-absorption coefficients of aluminum emission lines in laser-induced breakdown spectroscopy measurements. Spectrochimica Acta Part B-Atomic Spectroscopy, 60, 1573 (2005).

[28] S. Takashima, M. Hori, T. Goto, A. Kono, M. Ito et al. Vacuum ultraviolet absorption spectroscopy employing a microdiacharge hollow-cathode lamp for absolute density measurements of hydrogen atoms in reactive plasmas. Appl Phys Lett, 75, 3929 (1999).

[29] C. M. E & M. M. Absorption spectroscopy measurements of resonant and metastable atom densities in atmospheric-pressure discharges using a low-pressure lamp as a spectral-line source and comparison with a collisional-radiative model. Spectrochim. Acta, Part B, 65, 199 (2010).

[30] C. R. D The Theory of Atomic Spectra. (1981).

[31] ttp://www.Specair-Radiation.Net/Specair%20manual.Pdf.

[32] H. W. Drawin & F. Emard. Optical Escape Factors for Bound-bound and Free-bound Radiation from Plasmas. I. Constant Source Function. Beiträge aus der Plasmaphysik, 13, 143 (1973).

[33] R. Hannachi, Y. Cressault, P. Teulet, A. Gleizes & Z. B. Lakhdar. Calculation of self-absorption coefficients of calcium resonance lines in the case of a CaCl(2)-water plasma. Spectrochim. Acta, Part B, 63, 1054 (2008).

[34] L. M. Liao & J. He. Calculation of the self-absorption of laser induced Mg I 285.2127 nm spectral line. Optik, 125, 1602 (2014).

[35] A. H. Bassyouni. The escape factor in atomic absorption spectroscopy. J. Quant. Spectrosc. Radiat. Transfer, 28, 161 (1982).

[36] F. E. Irons. The escape factor in plasma spectroscopy—I. The escape factor defined and evaluated. J. Quant. Spectrosc. Radiat. Transfer, 22, 1 (1979).

[37] E.-G. Z & H. A. A. M. The influence of the background interference on the escape of photons in atomic absorption measurements. J. Quant. Spectrosc. Radiat. Transfer, 78, 211 (2003).

[38] K. Sasaki, Y. Kawai & K. Kadota. Determination of fluorine atom density in reactive plasmas by vacuum ultraviolet absorption spectroscopy at 95.85 nm. Rev. Sci. Instrum., 70, 76 (1999).

[39] T. Kitajima, K. Noro, T. Nakano & T. Makabe. Influence of driving frequency on oxygen atom density in O_2 radio frequency capacitively coupled plasma. Journal of Physics D: Applied Physics, 37, 2670 (2004).

[40] A. Granier, D. ChéReau, K. Henda, R. Safari & P. Leprince. Validity of actinometry to monitor oxygen atom concentration in microwave discharges created by surface wave in O_2-N_2 mixtures. J. Appl. Phys., 75, 104 (1994).

[41] J. P. Booth, O. Joubert, J. Pelletier & N. Sadeghi. Oxygen atom actinometry reinvestigated: Comparison with absolute measurements by resonance absorption at 130 nm. J. Appl. Phys., 69, 618 (1991).

[42] S. Kechkar, P. Swift, J. Conway, M. Turner & S. Daniels. Investigation of atomic oxygen density in a capacitively coupled O_2/SF_6 discharge using two-photon absorption laser-induced fluorescence spectroscopy and a Langmuir probe. Plasma Sources Science & Technology, 22 (2013).

[43] J. Nahomy, C. Ferreira, B. Gordiets, D. Pagnon, M. Touzeau et al. Experimental and theoretical investigation of a N_2-O_2 DC flowing glow discharge. Journal of Physics D: Applied Physics, 28, 738 (1995).

[44] V. Kudrle, P. Botos & A. Talsky. Role of admixtures on dissociation of molecular gases. Czechoslovak Journal of Physics, 54, C580 (2004).

[45] L. M. Prescott, J. P. Harley & D. A. Klein Microbiology, Edn. 5. (McGraw-Hill, 2002).

Chapter 3

Absolute nitrogen atomic density measured with VUVAS method and its effect on spore inactivation

In this chapter, with the same light source system used in chapter 2, the nitrogen atomic density will be measured with VUVAS method. Helium and small amount of nitrogen was chose as working gas. The self-absorption checking method used in this chapter was measuring the absorption ratios for different light source discharge conditions when the target surface-wave plasma was kept at a stable condition, the inactivation effect of nitrogen atoms will be discussed based on the atomic density measurement result.

3.1 Introduction.

Many factors that may cause inactivation had been studied for various plasma inactivation processes, such as VUV/UV, neutral and charged species, electric fields, reactive oxygen species (ROS) oxygen including ground-state atomic oxygen $O(^3P_j)$, hydroxyl radicals (OH), metastable oxygen molecules ($^1O_2$), and superoxide anions (O_2^-),[1]. However, few studies have investigated the inactivation effect of nitrogen atoms by the quantitative analysis of the gas phase. But the role of nitrogen atoms is also important to understand the inactivation mechanisms of plasma treatments. Absolute nitrogen atomic density had been measured by Synchrotron vacuum ultra-violet high-resolution Fourier-transform absorption technology[2], two-photon laser-induced fluorescence spectroscopy (TALIF)[3], optical actinometry[4, 5], VUVAS method [6, 7], NO titration[8], modulated-beam line-of-sight threshold ionization mass spectrometry (LOS-TIMS)[9]. During these methods, we chose VUVAS method, because VUVAS had influence on the plasma, and it was also a simple, low cost method.

In order to clarify the effect of nitrogen atoms on the inactivation of spores, the nitrogen atomic densities were measured with different N_2 and O_2 gas mixture ratios in surface-wave plasma. The emission intensity at 337 nm was also measured to verify the VUVAS measurement result.

3.2 Experimental condition

The VUVAS system used for nitrogen atom density measurement was same to the oxygen atomic density measurement system, the detail of the experimental setup and the absorption ratio measurement process were described in chapter 2.

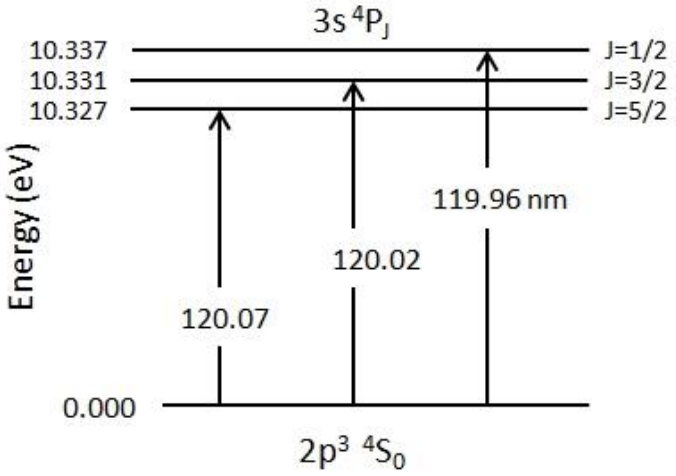

Figure. 3.1 The partial energy level diagram of oxygen atoms

Table 3.1 Transition probability and statistical weights for oxygen resonance lines[10]

λ_0 (nm)	Transition	$E_1(cm^{-1})$	$E_2(cm^{-1})$	g_1	g_2	A_{21} (10^8 s^{-1})
119.96	$3p^3\,{}^4S^0$-$3s\,{}^4P_{1/2}$	83364.620	0.000	4	6	4.01
120.02	$3p^3\,{}^4S^0$-$3s\,{}^4P_{3/2}$	83317.830	0.000	4	4	3.99
120.07	$3p^3\,{}^4S^0$-$3s\,{}^4P_{5/2}$	83284.070	0.000	4	2	3.98

As shown in figure 3.1, the upper level $3s^4P_J$ of the resonance lines of nitrogen atoms is composed of three sub-levels (J=1/2, 3/2, 5/2), the transition lines of nitrogen atom used for absorption measurements were $2p^23s\ {}^4P_{5/2}$–$2p^3\ {}^4S^\circ_{3/2}$ at 119.96 nm, $2p^23s\ {}^4P_{3/2}$–$2p^3\ {}^4S^\circ_{3/2}$ at 120.02 nm and $2p^23s\ {}^4P_{1/2}$–$2p^3\ {}^4S^\circ_{3/2}$ at 120.07 nm of N atom. Atomic parameters of nitrogen atom used for VUVAS calculation are listed in table 3.1.

For the low pressure condition of our light source, only the broadening effect coming from the temperature was took in to consideration, we can get the theoretical emission line profile with a Gaussian distribution from software Speicair[11], the calculated emission line profile was shown in figure 3.2. The intensity ratio of 119.96 nm, 120.02 nm and 120.07 nm calculated from figure 3.2 was 1:0.67:0.33, respectively.

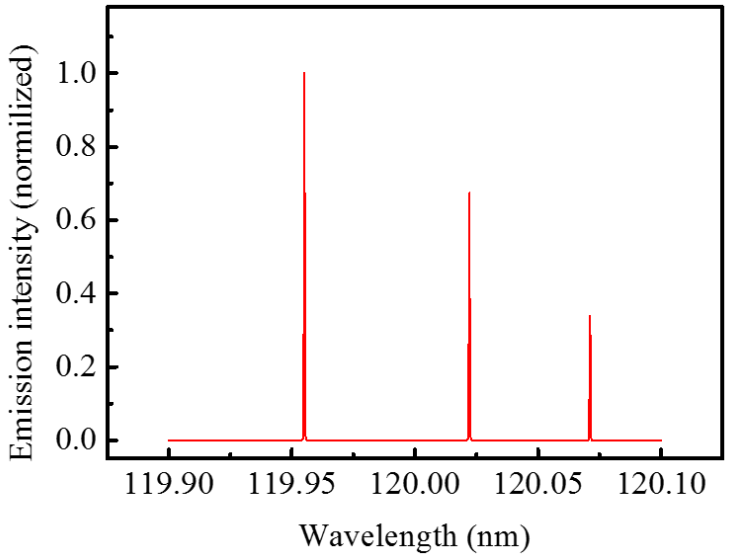

Figure 3.2 The normalized emission lines profile of nitrogen atoms near 130 nm calculated by *Specair*

Because the monochromator used in this study has a maximum resolution 0.1nm with a silt 10 μm, therefore, the resonance lines of nitrogen atomic near 120 nm will be seriously overlapping. As the result shown in figure 3.3, the experimental determined emission profile near 120 nm only showed one peak. The total absorption ratio measured from this peak will represent all the absorption of the three transition lines. Therefore, the method for self-absorption checking and absorption curve calculation will be different from the oxygen atoms measurement for this serious overlap of emission lines.

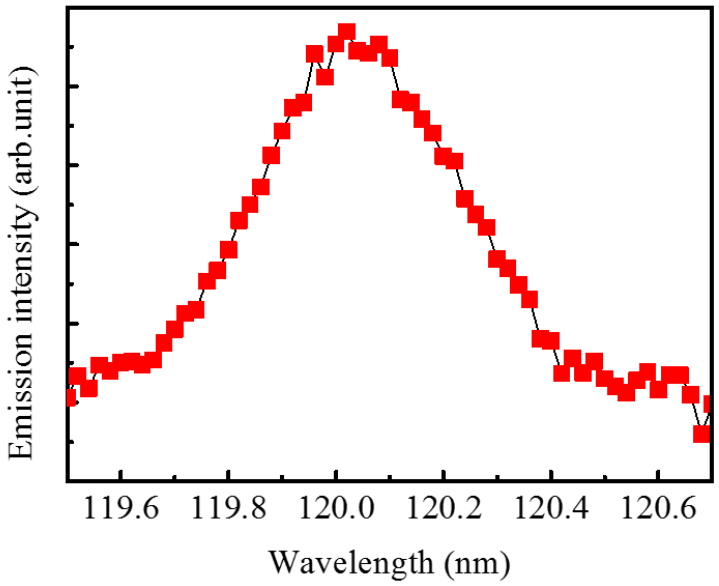

Figure 3.3 Light source emission profile of nitrogen atoms near 120 nm.(Light source condition: incident power 80 W, He 50 sccm, N_2 1 sccm, pressure 4.5 Pa)

3.3 Principles of VUVAS method for overlapped emission line

According the theory described by Mitchell and Zemansky[12], and the study of Nagai in Nagoya University, the absorption ratio of overlapped emission lines can be given as follow:

$$A = \frac{\sum_{x=1}^{3} \int a_x f_1(v)\left(1 - \mathrm{e}^{-k_{01} L a_x f_2(v)}\right)\mathrm{d}v}{\sum_{x=1}^{3} \int a_x f_1(v)\mathrm{d}v} \tag{3.1}$$

Where v is the emission line frequency, a_x (x=1, 2, 3) are the ratio of relative intensities of the three emission lines, according the emission line intensity calculated by Specair, a_1, a_2, a_3 was 1, 0.67, 0.33, respectively. $f_1(v)$ is the emission line profile of light source, in this study, which the light source worked at low pressure and low temperature, $f_1(v)$ was a typical Gaussian distribution, it can be given by equation 2.8. $f_2(v)$ is the absorption line profile of the target surface-wave plasma. For the low pressure condition chose in this study, only the heat motions of the atoms are taken into account, $f_2(v)$ was also a Gaussian distribution. k_0 is the maximum absorption coefficient at the central frequency v_0 of the

absorption line when Doppler broadening alone is present, it can be obtained from equation 2.6.

Then equation 3.1 can be rewritten as follow:

$$A = \frac{\sum_{x=1}^{3} \int a_x \mathrm{e}^{-\omega^2} \left(1 - \mathrm{e}^{-k_{0_1} L a_x \mathrm{e}^{-\omega^2}}\right) \mathrm{d}\omega}{\sum_{x=1}^{3} \int a_x \mathrm{e}^{-\omega^2} \mathrm{d}\omega} \tag{3.2}$$

3.4 Result and discussions

3.4.1 Self-absorption effect of the light source

We had checked the emission lines intensity with different discharge conditions with various Ar and N_2 gas mixture ratio, but the emission intensity is too low for the VUVAS measurement. He mixed with small amount of N_2 was chosen to make the resonance line of nitrogen atoms near 120 nm. A typical discharge condition was shown in figure 3.4, He discharge with this light source system was different from Ar discharge, instead of diffusion along the quartz tube, the plasma concentrated at the bottom of the light source, even this phenomenon is not good to improve the emission line intensity, but it was good to reduce the self-absorption, because the emission layer was reduced for the short discharge region.

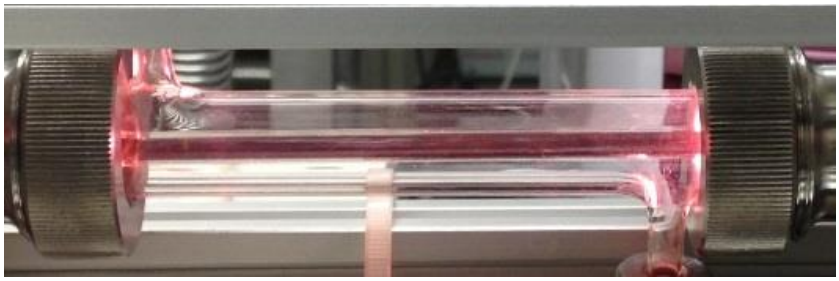

Figure 3.4 Photograph of light source discharge in side view; (Light source condition: incident power 80 W, He 50 sccm, N_2 0.1 sccm, pressure 4.5 Pa)

As the self-absorption theory introduced in chapter 2, for VUVAS method used for nitrogen atomic density measurement, the light source property and self-absorption of resonance lines have a big effect on the measurement. Although the most directly way to

check the self-absorption is measuring the line intensity ratios within multiplets, but for our condition, the resonance lines of nitrogen atom measured from our low resolution Monochromator had serious overlap, the widely method which had been used in other group's VUVAS measurements was adopted, [13-15] the light source self-absorption checking is done by measuring the same target plasma condition with different light source conditions.

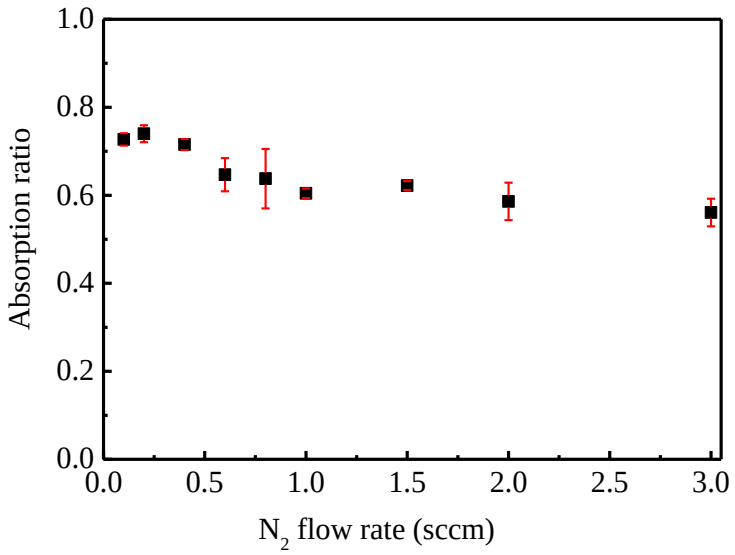

Figure 3.5 Absorption ratio measured near 120 nm to the same target plasma condition with different nitrogen flow rate (SWP： Power 600 W, N_2 100 sccm, pressure 0.1Torr; Light source: power 80 W, He 50 sccm, N_2:0.1-3sccm, pressure: 4.5 Pa)

we operated the 30 cm surface-wave plasma device at a constant condition (incident power= 600 W, working gas is pure N_2 and pressure is 13.3 Pa) , and other discharge parameters, such as incident power, He gas flow rate and pressure were kept stable, only the N_2 flow rate was increased from 0.1 sccm to 3 sccm. As the result shown in figure 3.5, absorption ratios decreased when the N_2 flow rate increased, that means the light source self-absorption was increased with the increasing of N_2 flow rate. The self-absorption can preferentially weaken the middle part of the emission line profile where absorption is strongest. The increasing of N_2 partial pressure increased the nitrogen atomic density in light source, thereby, the self-absorption increased. But the self-absorption almost keep

stable when the N_2 is lower than 0.4 sccm, it means the self-absorption ratio was almost negligible in this range. We also found that when the N_2 flow rate was increased from 1.0 sccm to 3 sccm, the absorption ratios also keep stable, the reason might be the increasing of N_2 flow rate has quench effect on the plasma, for the same incident power, the dissociation rate decreased with the increasing of N_2 flow rate, therefore the nitrogen atomic density kept almost stable in this range, in other words, it means the self-absorption was almost in same level.

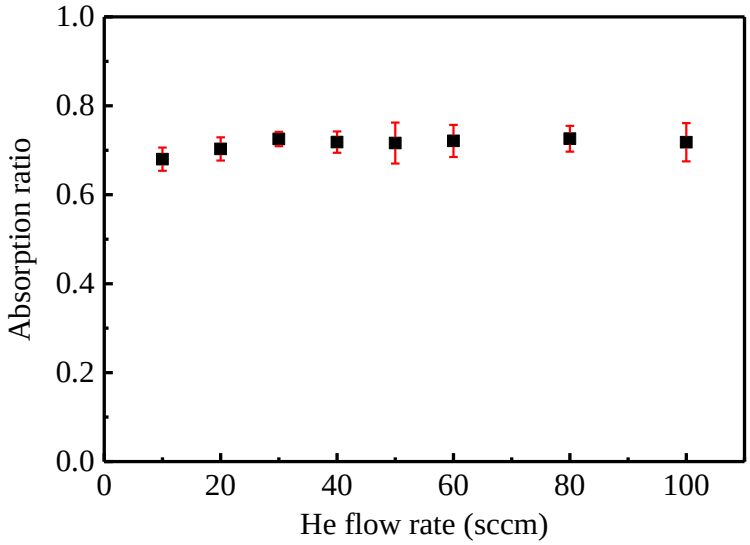

Figure 3.6 Absorption ratio measured near 120 nm to the same target plasma contidon with different He flow rate (SWP： Power 600 W, N_2 100 sccm, pressure 0.1Torr; Light source: power 80 W, He 10-100 sccm, N_2:0.2 sccm, pressure: 4.5 Pa)

For a further study of the effect of N_2 partial pressure on the light source self-absorption, the N_2 flow rate was kept at 0.2 sccm, incident power was stable at 80 W, pressure was constant at 4.5 Pa, we increase He flow rate from 10 sccm to 100 sccm. As the result shown in figure 3.6, for a constant target surface-wave plasma, absorption ratios kept almost stable when the He is 30-100sccm, this result indicated that the self-absorption in the light source was negligible in this He gas flow rate range.

Finally, the discharge condition of light source for nitrogen atomic density measured with VUVAS technology was: incident power 80 W, N_2 flow rate 0.2 sccm, He flow rate

50 sccm, pressure was kept at 4.5 Pa, the light source self-absorption of the nitrogen atom resonance lines near 120 nm can be ignored in this condition.

3.4.2 Absorption curve calculation of the nitrogen atomic density near 120 nm

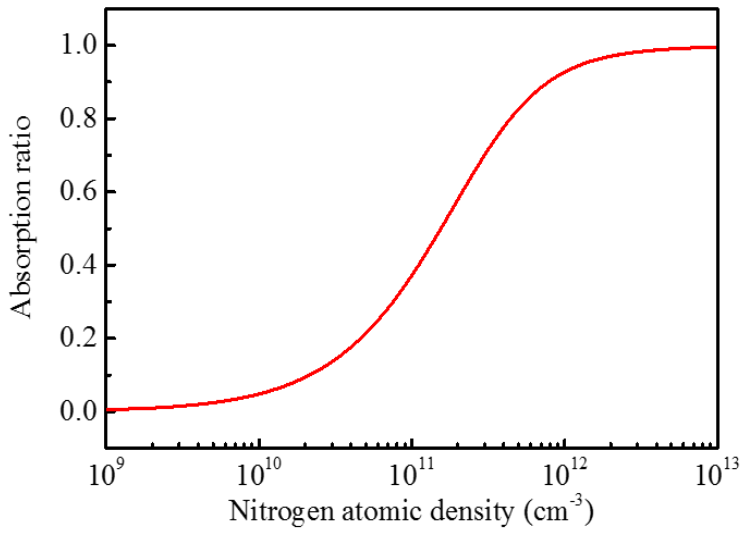

Figure 3.7 Relation between the absorption around 120 nm and the total nitrogen atomic density for the absorption length of L = 30 cm in surface-wave plasma. (Gas temperature of surface-wave was assumed to be 500 K)

According to our previous gas temperature measurement result of similar discharge condition, the gas temperature of target surface-wave plasma was assumed to be stable at 500 K. The light source gas temperature was assumed to be 600K. Because the light source self-absorption of the transmission lines was negligible, we assumed a Gaussian line shapes at 500 K for absorbing nitrogen atoms in the target surface-wave plasma and Gaussian line shapes at 600 K for the emitting nitrogen atom in light source, respectively. With the atomic parameters showed in table 3.1, we calculated the relation between the total absorption of the three transmission lines near 120 nm of nitrogen atoms and the total nitrogen atom density for the absorption length of L=30 cm from equation 3.2 and equation 2.6. From the absorption curve shown in figure 3.7, the sensitive measurement is possible for nitrogen atomic density in the range of $10^{10} \sim 10^{12}$ cm^{-3}.

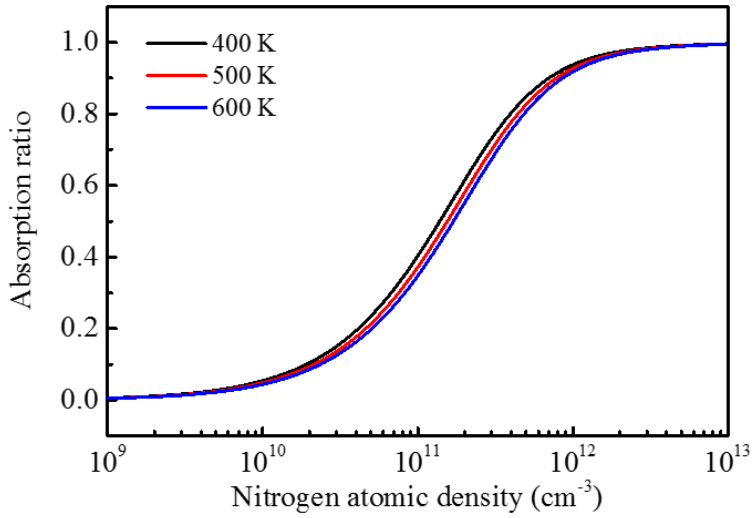

Figure 3.8 Relation between the absorption around 120 nm and the total nitrogen atomic density for the absorption length of L = 30 cm in surface-wave plasma. (Gas temperature of surface-wave was assumed to be 400 K, 500 K, and 600K)

In order to check the temperature instability of target surface-wave plasma to the atomic density measurement results, the absorption curves of the gas temperature 400 K and 600 K in surface wave plasma were also calculated. As the result shown in figure 3.8, for the same absorption ratio, the nitrogen atomic density had about a decreasing up to 10% at 400 K and an increasing up to 9% at 600 k, respectively. This is an allowable error in the VUVAS measurements. [16, 17]

3.4.3. The absolute oxygen atom densities with different N_2 and O_2 gas mixture ratio in surface-wave plasma.

In order to make clear the effect of nitrogen atoms on the inactivation of the spore forming microorganisms in the N_2/O_2 gas mixture plasma, the absolute nitrogen atomic density will be measured with different N_2 and O_2 gas mixture ratio in surface-wave. the incident power of the surface wave plasma was kept at 600 W, pressure was fixed at 13.3 Pa with a total flow rate of 100 sccm, which was same to the previous sterilization experiment and the oxygen atomic density measurements in chapter 3.

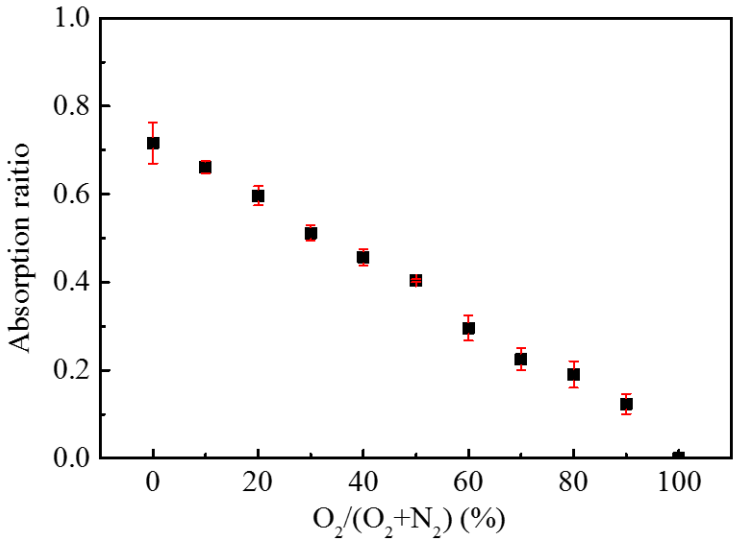

Figure 3.9 Absorption ratios measured near 120 nm as a function of oxygen gas mixture ratios in surface-wave plasma.

As shown in figure 3.9, the total absorption ration of the three resonance lines of nitrogen atoms near 120 nm decreased gradually with the increasing of O_2 proportion in surface-wave plasma. The emission intensity of N_2 molecules(C-B, 0-0) at 337.1 nm were also measured as indicating the UV changing, from figure 3.10, it was clearly shown that the changing of absorption ratio agreed well with the UV emission intensity of N_2 molecules at 337 nm.

The nitrogen atomic density can be obtained from the absorption ratios shown in figure 3.9 and the absorption curve shown in figure 3.7. Figure 3.11 indicates the nitrogen atomic densities with different O_2 and N_2 gas mixture in surface-wave plasma. The highest nitrogen atomic density 3.17×10^{11} cm^{-3} appeared at 100% N_2, then decreased gradually with the increasing of O_2 percentage. According to the study of Yosuke Ichikawa et.al, the electron temperature and density ranges in low pressure N_2 and O_2 gas mixture microwave plasma are almost independent of the gas mixture ratio, [18] thus the increased O_2 proportion couldn't increase the dissociation rate of N_2. In contrast, O_2 molecules and oxygen atoms had quenching effect on nitrogen atoms, and another channel for the reduction of nitrogen atoms was the reaction between nitrogen atoms and atomic oxygen appears to produce NO via a chemical ionization mechanism. [19, 20] therefore, the

decreased N_2 proportion and the queening effect caused the continuous decreasing of nitrogen atomic density.

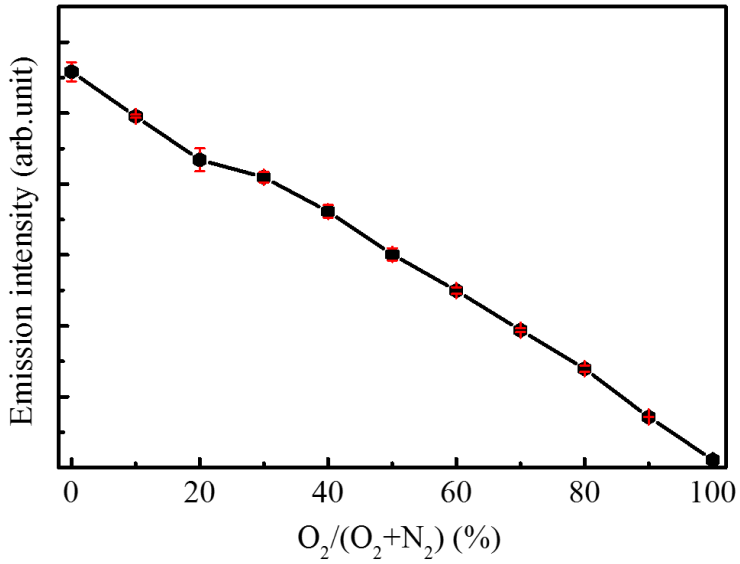

Figure 3.10 Emission line intensity at 337 nm as a function of oxygen mixture ratio in surface-wave plasma

The measurement results of nitrogen atomic density was one order of magnitude lower than the oxygen atomic density, this came from the different ionization energy of N_2 and O_2, the ionization energy of N_2 and O_2 were 15.5 eV, 12.5 eV, respectively, thus the dissociation rate of N_2 was lower than O_2. With the similar low pressure microwave plasma discharge in N_2 and O_2, both of the simulation results and calculation results of Yosuke Ichikawa et.al [21] had illustrated that the dissociation degree of N_2 was one order of magnitude much lower than the O_2.

In our previous sterilization experiments of *Geobacillus stearothermophilus* spores in N_2 and O_2 gas mixture surface-wave plasma with the same discharge conditions, the efficiency inactivation happened when the O_2 proportions was in the 30% 80 %, and the strongest etching happened when O_2 proportions was 90%, which had been explained by the oxygen atomic density measurement result in chapter 2. Therefore, with the result shown in figure 3.11, the highest nitrogen atomic density has the minimum inactivation effect, it can be inferred that nitrogen atomic density in N_2 and O_2 mixture surface-wave

plasma has small contributions on the spore etching and spore inactivation. But the UV emission coming from the transition of nitrogen atom at excited state to the ground state might be important to the inactivation process and the photodissociation of oxygen molecules.

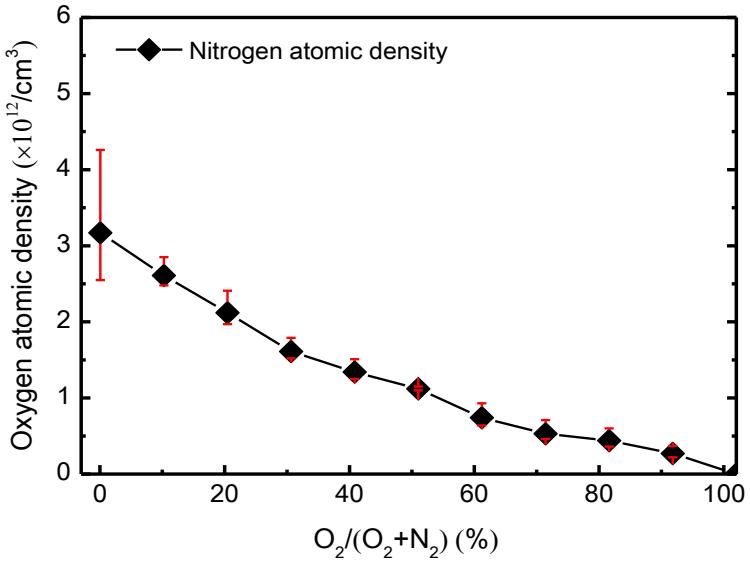

Figure 3.11 Absolute nitrogen atomic densities as a function of oxygen mixture ratio in surface-wave plasma

3.5 Summary

The light source self-absorption of the light probe chose for the nitrogen atomic density measurement was checked by measuring the absorption ratio of same target surface-wave plasma with different light source conditions. Then we chose a light source discharge condition with the self-absorption in negligible levels: incident power 80 W, N_2 flow rate 0.2 sccm, He flow rate 50 sccm, pressure was kept at 4.5 Pa. Because of the serious overlapped resonance lines near 120 nm of nitrogen atoms, we calculated a theoretical absorption curve with overlapped emission lines by assuming the Gaussian distribution for both emission lines in light source and absorption lines in target plasma.

The nitrogen atomic densities were measured with different N_2 and O_2 gas mixtures in surface-wave plasma. Because the ionization energy of N_2 was higher than O_2, the measurement results of nitrogen atomic densities were one order of magnitude lower than the oxygen atomic densities, this agree well with the simulation results and calculation results of other groups. The nitrogen atomic density decreased gradually from 3.17×10^{11} cm^{-3} of 100% N_2 with the increasing of O_2 percentage. Compared with previous sterilization experiment result, we inferred from these atomic density results that nitrogen atomic density in N_2 and O_2 mixture surface-wave plasma has small contributions on the spore etching and spore inactivation.

References

[1] S. Iseki, H. Hashizume, F. Jia, K. Takeda, K. Ishikawa et al. Inactivation of Penicillium digitatum Spores by a High-Density Ground-State Atomic Oxygen-Radical Source Employing an Atmospheric-Pressure Plasma. Appl. Phys. Express, 4, 116201 (2011).

[2] K. Niemi, D. O'connell, N. De Oliveira, D. Joyeux, L. Nahon et al. Absolute atomic oxygen and nitrogen densities in radio-frequency driven atmospheric pressure cold plasmas: Synchrotron vacuum ultra-violet high-resolution Fourier-transform absorption measurements. Applied Physics Letters, 103, 4 (2013).

[3] E. Es-Sebbar, Y. Benilan, A. Jolly & M. C. Gazeau. Characterization of an N-2 flowing microwave post-discharge by OES spectroscopy and determination of absolute ground-state nitrogen atom densities by TALIF. Journal of Physics D-Applied Physics, 42, 11 (2009).

[4] M. Mavadat, S. Turgeon, A. Ricard & G. Laroche. Infrared optical actinometry to determine N- and H-atom density in a N2-H2 microwave discharge. Journal of Physics D-Applied Physics, 45, 9 (2012).

[5] J. Levaton, A. Ricard, J. Henriques, H. R. T. Silva & J. Amorim. Measurements of N((4)S) absolute density in a 2.45 GHz surface wave discharge by optical emission spectroscopy. Journal of Physics D-Applied Physics, 39, 3285 (2006).

[6] Y. Horikawa, K. Kurihara & K. Sasaki. Absolute Densities of N_2(A(3)Sigma(+)(u)), N(S-4(o)), and N(D-2(o)) in an Inductively Coupled Nitrogen Plasma Source. Japanese Journal of Applied Physics, 49, 6 (2010).

[7] S. Tada, S. Takashima, M. Ito, M. Hamagaki, M. Hori et al. Investigation of Nitrogen Atoms in Low-Pressure Nitrogen Plasmas Using a Compact Electron-Beam-Excited Plasma Source. Japanese Journal of Applied Physics, 41, 4691 (2002).

[8] P. Va Ina, V. Kudrle, A. Tálský, P. Boto, M. Mrázková et al. Simultaneous measurement of N and O densities in plasma afterglow by means of NO titration. Plasma Sources Science and Technology, 13, 668 (2004).

[9] S. Agarwal, B. Hoex, M. C. M. Van De Sanden, D. Maroudas & E. S. Aydil. Absolute densities of N and excited N_2 in a N_2 plasma. Applied Physics Letters, 83, 4918 (2003).

[10] W. L. Wiese, J. R. Fuhr & T. M. Deters. Atomic transition probabilities of carbon, nitrogen, and oxygen: A critical data compilation. J. Phys. Chem. Ref.Data, Monograph 7. , 1, 340 (1996).

[11] Http://Www.Specair-Radiation.Net/Specair%20manual.Pdf (

[12] A. C. Q. Mithell & M. W. Zemansky Resonance radiation and excited atoms. (Cambridge University Press, Cambridge; 1961).

[13] S. Takashima, M. Hori, T. Goto, A. Kono, M. Ito et al. Vacuum ultraviolet absorption spectroscopy employing a microdiacharge hollow-cathode lamp for absolute density measurements of hydrogen atoms in reactive plasmas. Appl Phys Lett, 75, 3929 (1999).

[14] C. M. E & M. M. Absorption spectroscopy measurements of resonant and metastable atom densities in atmospheric-pressure discharges using a low-pressure lamp as a spectral-line source and comparison with a collisional-radiative model. Spectrochim. Acta, Part B, 65, 199 (2010).

[15] H. Nagai, M. Hiramatsu, M. Hori & T. Goto. Measurement of oxygen atom density employing vacuum ultraviolet absorption spectroscopy with microdischarge hollow cathode lamp. Rev. Sci. Instrum., 74, 3453 (2003).

[16] K. Sasaki, Y. Kawai & K. Kadota. Determination of fluorine atom density in reactive plasmas by vacuum ultraviolet absorption spectroscopy at 95.85 nm. Rev. Sci. Instrum., 70, 76 (1999).

[17] T. Kitajima, K. Noro, T. Nakano & T. Makabe. Influence of driving frequency on oxygen atom density in O_2 radio frequency capacitively coupled plasma. Journal of Physics D: Applied Physics, 37, 2670 (2004).

[18] Y. Ichikawa, T. Sakamoto, A. Nezu, H. Matsuura & H. Akatsuka. Actinometry Measurement of Dissociation Degrees of Nitrogen and Oxygen in N_2-O_2 Microwave Discharge Plasma. Japanese Journal of Applied Physics, 49, 16 (2010).

[19] L. G. Piper. The reactions of N(2P) with O_2 and O. Journal of Chemical Physics, 98, 8560 (1993).

[20] S. Debenedictis & G. Dilecce. Rate constants for deactivation of N_2(A) v=2-7 by O, O_2, and NO. Journal of Chemical Physics, 107, 6219 (1997).

[21] Y. Ichikawa, T. Sakamoto, A. Nezu, H. Matsuura & H. Akatsuka. Actinometry Measurement of Dissociation Degrees of Nitrogen and Oxygen in N_2-O_2 Microwave Discharge Plasma. Japanese Journal of Applied Physics, 49 (2010).

Chapter 4

Effect of neutral oxygen radicals on inactivation of spore-forming microorganisms studied with porous ceramic plate in O_2 surface wave Plasma

In this chapter, an ultra-thin porous ceramic plate was developed to study the inactivation effect of neutral radicals in plasma sterilization. The property required for this ceramic plate is blocking UV radiation but permitting neutral radicals penetrate through it. Different plasma exposure conditions for bio-indicators can be achieved with different combinations conditions of MgF_2 filter and porous ceramic plate. The properties of ceramic plate and inactivation effect of neutral oxygen radicals on spores will be studied by spore morphology and survival curve measurements with different plasma exposure conditions.

4.1 Introduction.

Our previous experimental results clearly showed that UV radiation is an important lethal factor on spores in N_2/O_2 gas mixture surface-wave plasma. But the neutral species, such as excited oxygen and nitrogen atoms, also might play a role in the inactivation of spores.[1] Although UV is very effective in kill spores at low pressure plasma, but the limitation of UV in sterilization is the penetration properties, it can penetrate the membrane or cell wall of microorganisms with the thickness in few micrometers, but it can't penetrate items with a little big thickness, therefore UV is just a surface inactivation. For some medical device with complex structures, UV alone can't comply with the requirements of sterilization t. Because the neutral radicals can diffuse freely everywhere, this characteristic can make up the deficiency of UV in sterilization.

In chapter 2 and chapter 3, the inactivation effect of oxygen and nitrogen atoms on spore-forming microorganism by the absolute atomic densities measured with VUVAS method, the result can well explain the spore etching effect in N_2 and O_2 gas mixture plasma. However, as shown in figure 4.1, the previous sterilization results after 60 sec irradiation by different N_2/O_2 gas mixture surface-wave plasmas,[2] the maximum etching happened at 90% O_2, we observed only 3-order reduction of the spores in this condition, while 80 % O_2 gas addition indicated 6-order reduction of survival spores. And for the high UV emission and high nitrogen atomic density condition which the O_2 proportion was 0, 10 % and 20%, we also get only 3 or 4-order reduction of survival spores. The effective

inactivation happened in the 30-80% O_2 gas mixture condition. Therefor the synergetic effect of radicals and UV emission is important for the sterilization process. But the effect of nitrogen and oxygen atoms in the plasma sterilization is still not clear enough.

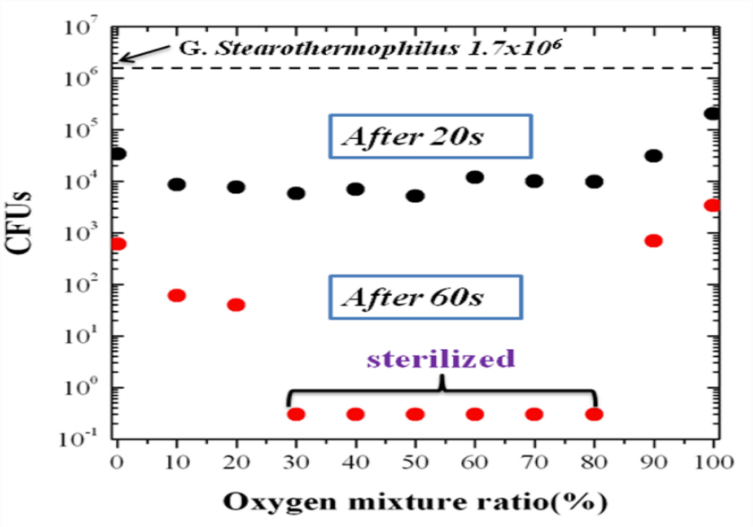

Figure 4.1 Colony forming units of *G. stearothermophilus* samples exposed to N_2/O_2 plasma 20s and 60s as a function of oxygen mixture ratio

A further study is needed to figure out the inactivation effect of radicals alone in plasma, and find the threshold radical density for inactivation. Hiroshi Hashizume et.al had studied the inactivation effects of neutral reactive-oxygen species on Penicillium digitatum spores using non-equilibrium atmospheric-pressure oxygen radical source.[3, 4] With a special X-shape atmospheric pressure plasma jet, Simon Schneider et.al had separated reactive particles (O atoms or O_3 molecules) from the plasma-generated photons in He/O_2 plasma, they found the interaction of plasma-generated VUV photons with the effluent of the plasma, the enhanced formation of O and O_3 leaded to faster inactivation of bacteria.[5] The study of Li Jia and Sakai Natsuko et.al showed that oxidative stress plays a main role in the inactivation process, neutral reactive oxygen species rather than superoxide O_2^-, are identified as dominant sources for oxidative stress[6], but most of the study were chose at atmospheric pressure, there was little study about the inactivation with neutral radical alone in low pressure plasma. At low pressure plasma discharge conditions, although the inactivation effect of neutral radicals can be considered by changing discharge conditions,

such as gas composition, and discharge power, but the interference coming from ultraviolet radiation can't exclude in this method.

As an exploratory study, the purpose of the study is to develop a new kind of filter, which can block UV and make the radicals penetrate through. As the etching effect of oxygen atoms is easy to check by scanning electron microscope, the penetration capability of neutral radicals to the new designed filter will be studied with different plasma exposure condition of spores in O_2 surface wave plasma. Subsequently, the inactivation effect of neutral species on spores in plasma can be studies with different discharge conditions.

4.2 Experimental conditions

The experimental setup consists of a stainless steel cylindrical vacuum chamber (300 mm in diameter and 300 mm in height) with a microwave launcher and 2.45 GHz microwave generator, the detail of the surface-wave plasma device was described in Chapter 2. As shown in Figure 4.2, biological indicators (*Geobacillus stearo- thermophilus*) covered with different filters are put 10 cm below the quartz window. The oxygen gas flow

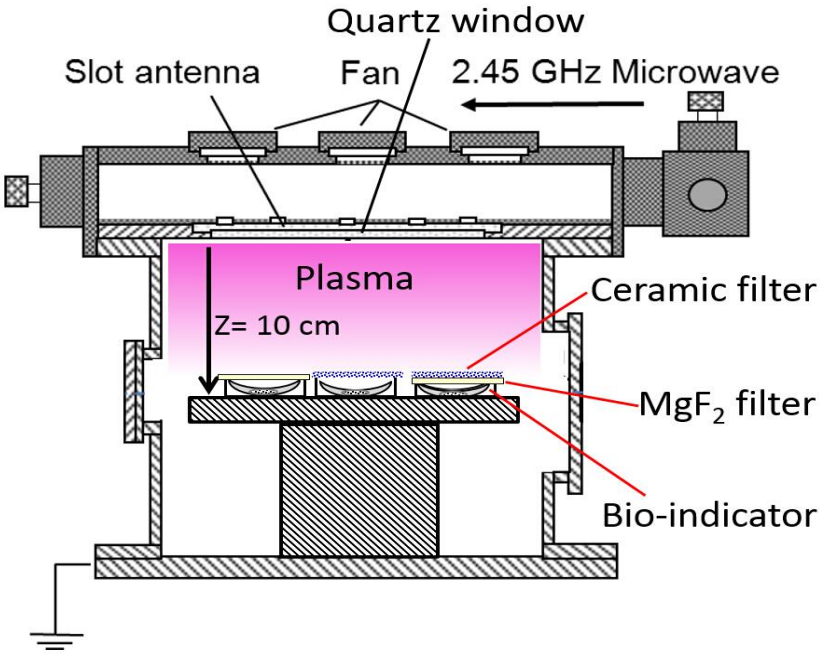

Figure 4.2 Schematic view of experimental setup

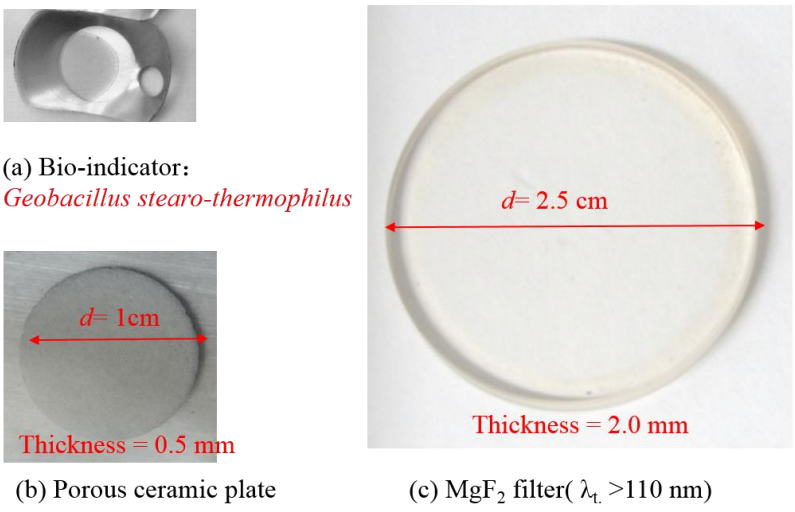

Figure 4.3 (a) Bio-indicator (*Geobacillus stearo-thermophilus* spores) (b) Porous ceramic plate and (c) MgF_2 filter used in this study. (b) Ultrathin porous ceramic plate

rate was 100 sccm, the pressure was controlled to be 13.3 Pa, the incident microwave power was 600 W, in order to control the temperature, the discharge was worked in on/off mode, 20 s on and 90 s off for each circle, and there will be a 30 min break when the total discharge time is 10 minutes. The treatment temperature was measured by a thermo-label sheets (5E-50), temperature near the bio-indicator for all the cases was maintained below 80 ℃ by on/off mode and intermittent pauses of the plasma discharges.

Porous ceramic, which has lower reflection and good stability in plasma, was used to block UV and get high radical density. MgF_2 filter can block all the species only allow emission wavelength bigger than 110 nm penetrate through. Figure 4.3 (a) showed the graphs of biological indicators (*Geobacillus stearo- thermophiles* spores) which have been bought from Raven Labs, the spores was fixed to a stainless steel discs, the number of spores fixed on disc was on the order of 10^6. MgF_2 filter shown in figure 4.3 (c) has a thickness of 2.0 mm and diameter 2.5 cm. As shown in figure 4.3 (b), the porous ceramic plate used in this study has a thickness of 0.5 mm and diameter 1 cm.

Shielding properties for UV emissions at different wavelength had been measured by Monochromator. Emission blocking ratio can be obtained by the comparing of the emission intensity measured with and without porous ceramic plate covering. The emission used for the measurement was produced by the N_2 surface-wave discharge and a UV lamp. Figure

4.4 showed the result of the emission blocking of the porous ceramic plate, More than 99% emission below 400 nm had been blocked, and the emission blocking efficiency increased with the wavelength decrease, according this result, almost all the UV with high photo energy below 200 nm will be blocked.

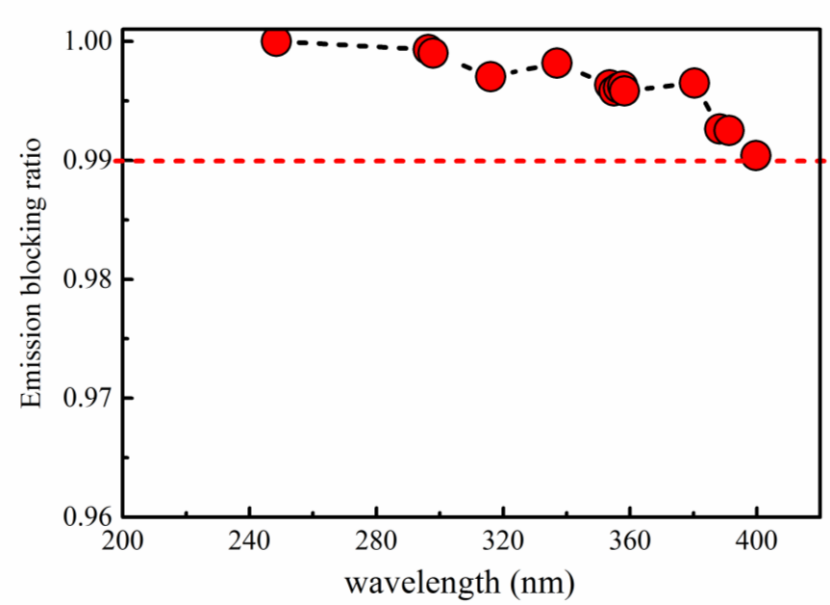

Figure 4.4 Emission blocking effect of porous ceramic plate

The schematic diagram shown in figure 4.5 illustrates intuitively the different exposure conditions of plasma inactivation factor for bio-indicators with different covering compositions. As shown in figure 4.5 (a), when bio-indicators exposes directly to the plasma, all the inactivation factor, UV, radicals and ions will come to the bio-indicators. Figure 4.5 (b) illustrate the condition when bio-indicators covered with MgF_2 window, all of the UV and radicals will be blocked, most of the UV emission (wavelength >110 nm) can contact with the bio-indicators.

When bio-indicators covered with the ultrathin porous ceramic plate, as shown in figure 4.5 (c), parts of radical should penetrate through the plate and reach to the bio-indicator, but very small amount of UV might be also penetrate through. In order to, a combination of MgF_2 filter and porous ceramic plate is used to check the inactivation effect of the very small amount of UV which can penetrate through the porous ceramic plate.

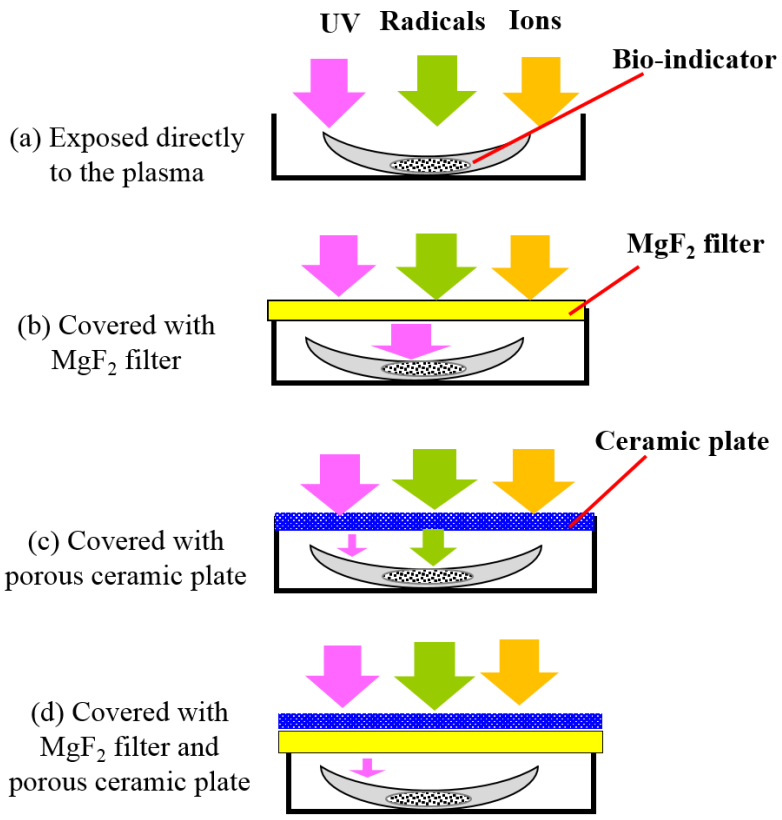

Figure 4.5 Schematic diagram of the bio-indicator exposed to different plasma factors for different cover condition

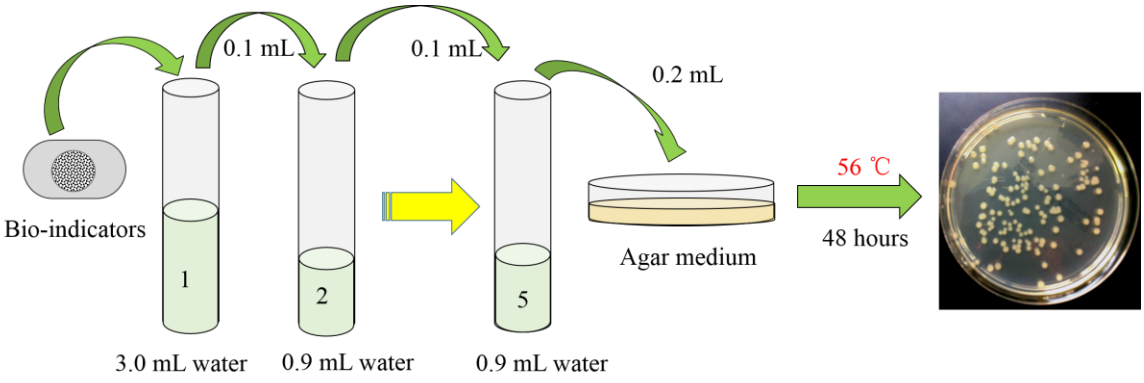

Figure 4.6 Illustration of the steps of colony-count by spread plate method.

The determination of survival curves is the most informative and most widely used way to evaluat plasma-induced effects on microorganisms. These curves are plots of the logarithm of the number of surviving microorganisms as a function of exposure time to the sterilizing agent. [7, 8] Different plasma sterilization processes can provide survival curves

with different shapes. Some researchers observe straight-line survival curves,[9, 10] but in most cases, survival curves have two or three linear segments, each representing a different inactivation phase.[11, 12] After plasma treatment, the remaining alive spores are left to inoculate for several hours before colony-forming units (CFUs) counting. The procedure of CFUs measurement was presented in figure 4.6. The treated samples were washed with 3 ml water in the test tube. Test tubes containing biological indicator carriers were stirred for 1 min at room temperature. After an appropriate serial dilutions, 0.2 ml spore suspension was inoculated onto nutrient agar media, then applied uniformly with a sterile glass rod, and after 48 hours of cultivation at 56 ℃, the CFUs each representing a surviving spore, was counted. The CFUs reduction of treated samples was compared with an untreated sample and plotted as the survival curve.

The morphological changes caused by plasma treatment are studied by a microscopic observation with scanning electron microscopy (SEM)[13] or atomic force microscopy[14, 15], in this study, SEM (HITACHI S-3000N) was used to observe the morphology change of the spores after different plasma treatment.

4.3 Result and discussions

4.3.1 The property of porous ceramic plate checked with morphology change of spores

The etching effect of oxygen atoms in N_2 and O_2 gas mixture surface-wave plasma had been verified in chapter 3. In order to confirm whether the neutral radicals can penetrat through the ultrathin ceramic plates, the morphology change of spore with different plasma treatment condition was analyzed by scanning electron microscope. Spore size changing in width and length was measured from the statistical analysis using over 60 spores' size.

As the result shown in figure 4.7 (a), when exposed directly to the plasma, the morphological change of spores was big with different plasma treatment time, and the surface of spores also changed to be rough and porous because of the etching. Spore size shown in figure 4.7 (b) decreased gradually from the initial 1.7 μm to 1.0 μm after 30 minutes treatment. But after 20 minutes treatment, the spore size changing became slowly. It might come from multilayer structure of spores.[16] When the etching went to the

nuclear area where DNA and other genetic material was protected by a hard inner membrane.

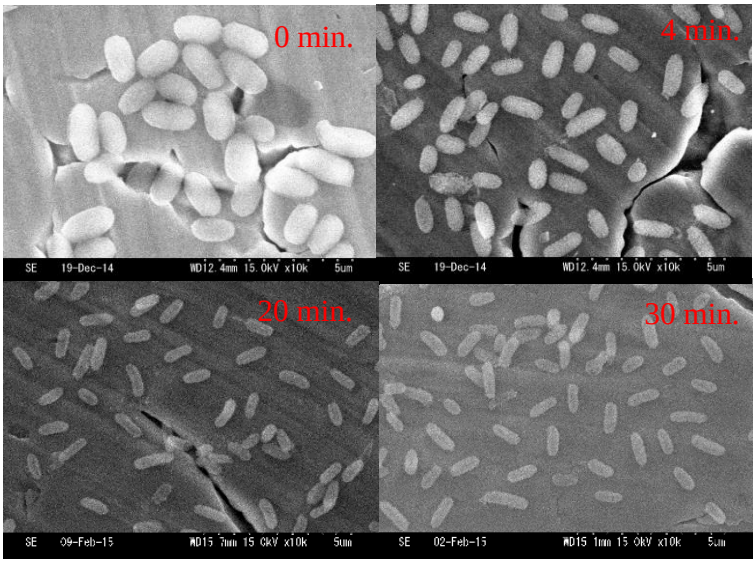

(a)

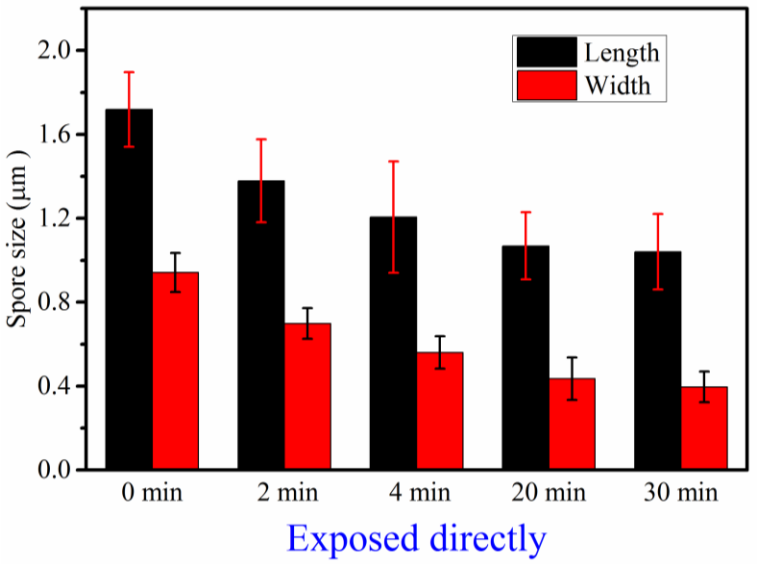

(b)

Figure 4.7 SEM photograph **(a)** and sizes (b) of *G. stearothermophilus* spores exposed directly to oxygen plasma with different treatment time

When the spores was treated with the newly developed ceramic plate in oxygen plasma, as the result shown if figure 4.8(a), even we the morphological change of spores was not

significant, but from figure 4.8(b), with the spore length and width measurement result, it clear that spore size decreased with time, it indicated the neutral oxygen atoms penetrate through the ceramic filter.

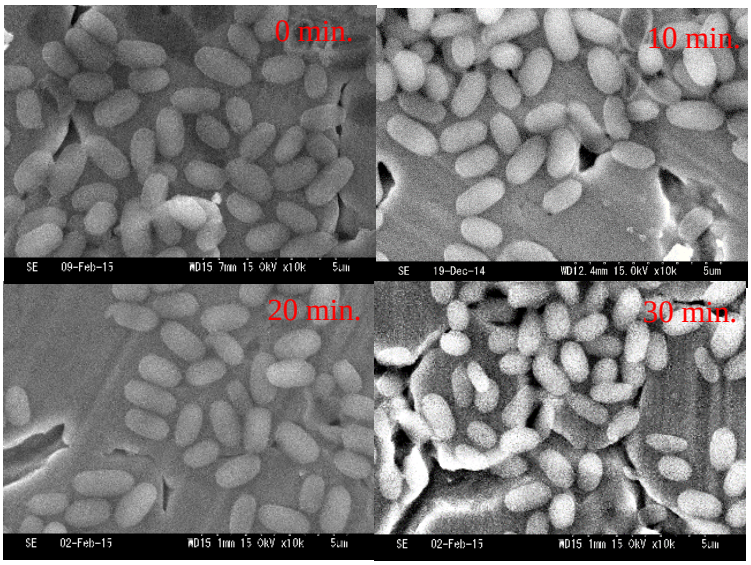

(a)

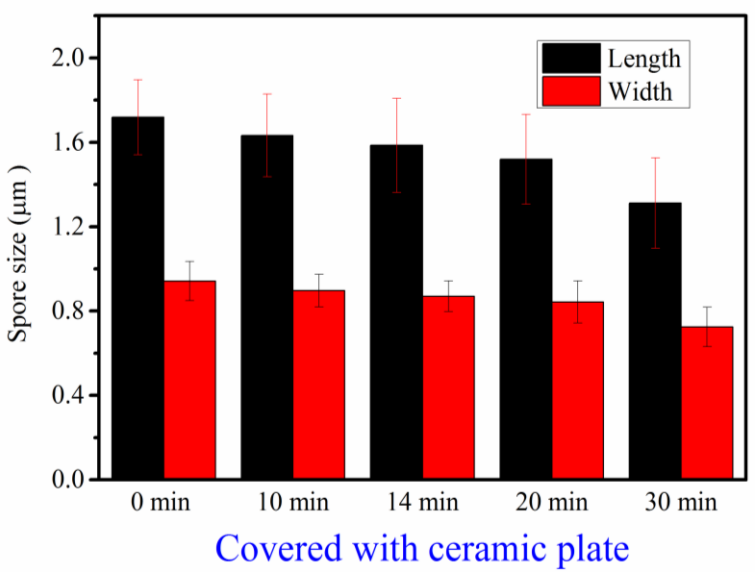

(b)

Figure 4.8 SEM photograph **(a)** and sizes (b) of *G. stearothermophilus* spores covered with ceramic plate with different treatment time in oxygen plasma

When spores were covered with both porous ceramic plate and MgF_2 filter, from the result showed in Figure 4.9, the spore almost did not have any change in morphology and also in size measurement result. This result indicated that all the spore size changing shown in figure 4.8 coming from come from the neutral oxygen atoms which penetrated through the ultrathin porous ceramic plate.

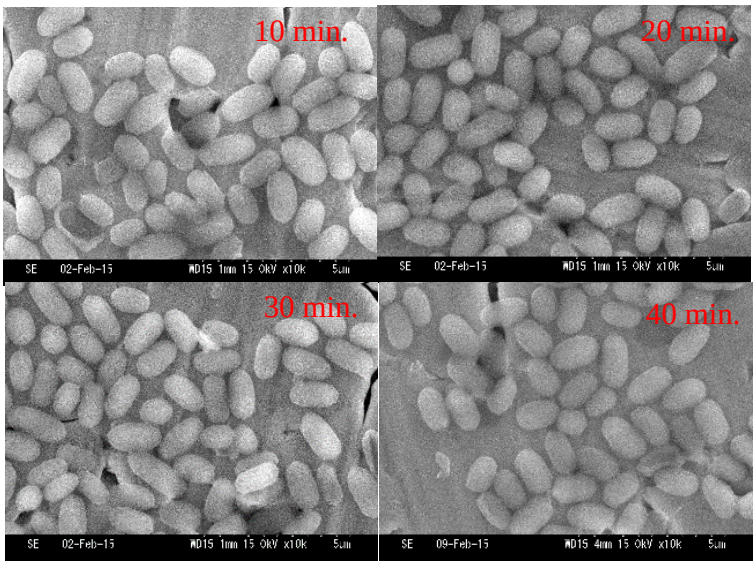

(a)

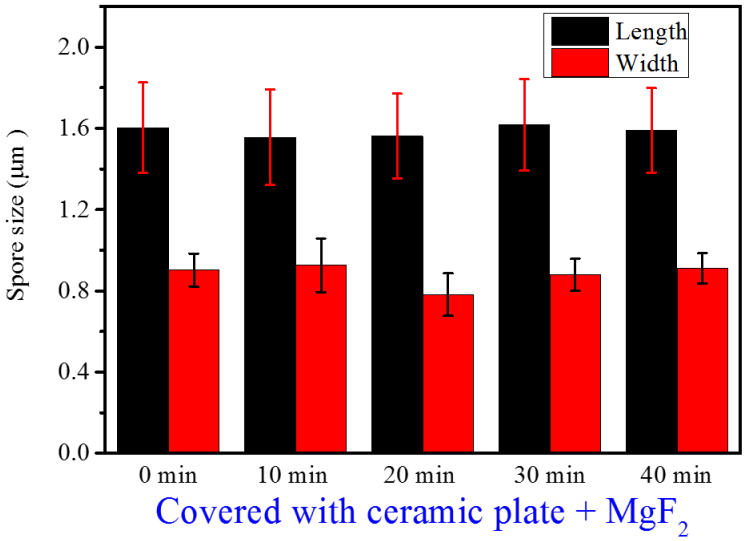

(b)

Figure 4.9 SEM photograph **(a)** and sizes (b) of *G. stearothermophilus* spores covered with both MgF_2 and ceramic plate with different treatment time in oxygen plasma

4.3.2 The property of porous ceramic plate checked with survival curves

Figure 4.10 shows the colony count results of *Geobacillus stearothermophilus* spores exposed directly to plasma, covered with MgF_2 filter and covered with ceramic plate in pure oxygen surface-wave plasma. The temperature near bio-indicators in all the cases was maintained below 80℃by on/off timer module and intermittent pauses of the oxygen plasma discharges, it had been confirmed that almost no *Geobacillus stearothermophilus* spores had been killed when the spores were only kept in 85℃ by heating for one hour. From figure 4.10, when exposed directly to the oxygen plasma, spores were killed with high efficiency, all the spores were killed in 6 minutes. When the bio-indicators were covered with MgF_2 plate, all the ions and radicals will be blocked, only emission wavelength bigger than 110 nm can reach to the spores, the inactivation decreased but not so much, it took 30 minutes to kill all the spores with a 10^6 order. This result indicates that the UV in oxygen plasma was also an important inactivation factor. As the case that the bio-indicator were covered with porous ceramic plate, the inactivation efficiency decreased seriously, there was only about 2-order reduction of the spores after 30 minutes treatment. When the bio-indicator were covered with a porous ceramic plate, ions will be blocked by plasma sheath in the surface of the ceramic and micro-holes distributed irregularly inside the ceramic plate. As shown in figure 4.8, parts of neutral oxygen atoms penetrated through the ceramic plate and produced etching on the spores, therefore, the 2-order's spore reduction might be come from the neutral oxygen atoms or the very small amount of UV which can penetrate through the ceramic plate for the small reflection of white ceramic. It was necessary to distinguish which part worked on the spores.

When both MgF_2 and porous ceramic plate covered on the spores in O_2 surface wave plasma, only the very small amount of UV which can penetrate through the ceramic plate has inactivation effect on spore. As the result shown in figure 4.11, for different treatment time, the survival curves of *G.stearothermophilus* spores in oxygen surface-wave plasma covered with ceramic plate and ceramic +MgF2 filter has a very small difference, that means the inactivation effect come from the neutral radicals can be ignored in this condition, the very small amount of UV which can penetrate through the porous ceramic plate played a major role in inactivation.

The porous ceramic plate blocked more than 99% UV, but even very small amount of UV (<1%), it can also play a significant inactivation effect and interferes our purposes to study the inactivation effect of neutral radicals in plasma. We need to develop a new kind of filter which can perfectly block UV emission from the plasma.

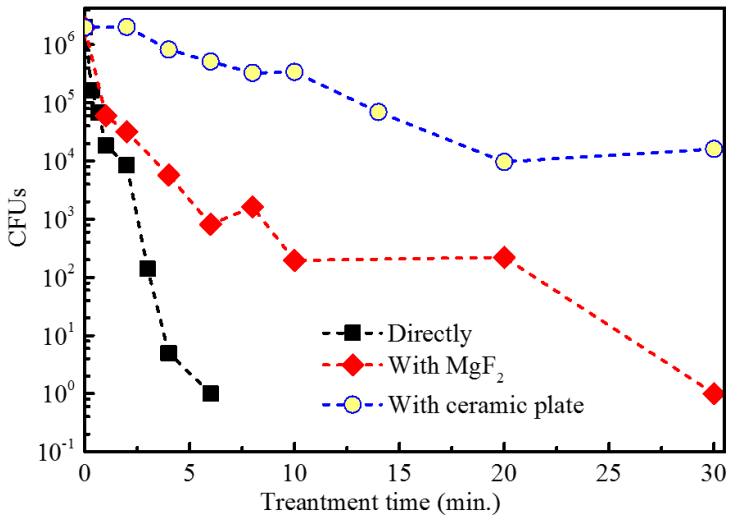

Figure 4.10 Survival curves of *G.stearothermophilus* spores in oxygen surface-wave plasma with different cover situations

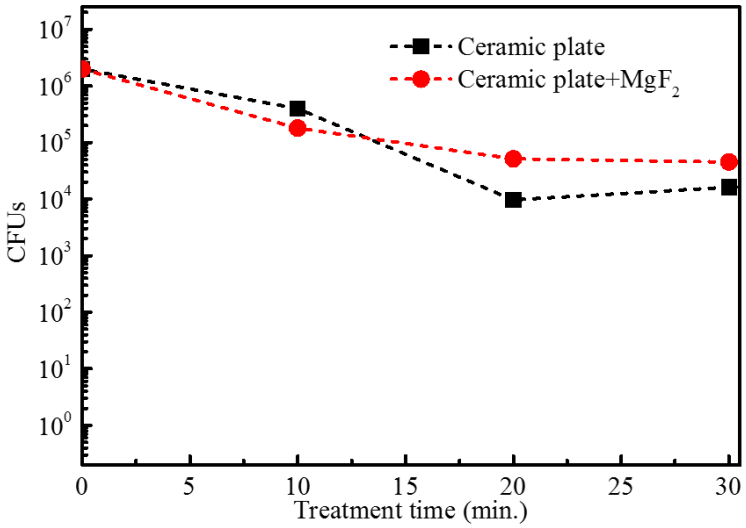

Figure 4.11 Survival curves of *G.stearothermophilus* spores in oxygen surface-wave plasma covered with ceramic plate and ceramic +MgF_2 filter

4.4 Summary

An ultra-thin porous ceramic filter was used to study the inactivation effect of neutral radicals on spores. The emission spectrometry measurement results indicated that more than 99% emission below 400 nm had been blocked by the porous ceramic plate. The morphology and spore size measurement results by scanning electron microscope demonstrate clearly that parts of neutral radicals can penetrate through the ceramic plate. The colony count results indicated that the very small amount UV(<1%) which can penetrate through the porous ceramic plate still play a main inactivation effect. A new kind of filter which can perfectly block UV emission from the plasma was needed for the study inactivation effect of neutral radicals in future.

Reference

[1] M. K. Singh, A. Ogino & M. Nagatsu. Inactivation factors of spore-forming bacteria using low-pressure microwave plasmas in an N_2 and O_2 gas mixture. New J. Phys., 11, 15 (2009).

[2] Y. Zhao, A. Ogino & M. Nagatsu. Effects of N_2–O_2 Gas Mixture Ratio on Microorganism Inactivation in Low-Pressure Surface Wave Plasma. Jpn. J. Appl. Phys., 50, 08JF05 (2011).

[3] S. Iseki, H. Hashizume, F. Jia, K. Takeda, K. Ishikawa et al. Inactivation of Penicillium digitatum Spores by a High-Density Ground-State Atomic Oxygen-Radical Source Employing an Atmospheric-Pressure Plasma. Applied Physics Express, 4 (2011).

[4] H. Hashizume, T. Ohta, K. Takeda, K. Ishikawa, M. Hori et al. Oxidation mechanism of Penicillium digitatum spores through neutral oxygen radicals. Japanese Journal of Applied Physics, 53 (2014).

[5] S. Schneider, J.-W. Lackmann, D. Ellerweg, B. Denis, F. Narberhaus et al. The Role of VUV Radiation in the Inactivation of Bacteria with an Atmospheric Pressure Plasma Jet. Plasma Process. Polym., 9, 561 (2012).

[6] J. Li, N. Sakai, M. Watanabe, E. Hotta & M. Wachi. Study on Plasma Agent Effect of a Direct-Current Atmospheric Pressure Oxygen-Plasma Jet on Inactivation of E. coli Using Bacterial Mutants. IEEE Trans. Plasma Sci., 41, 935 (2013).

[7] M. Moisan, J. Barbeau, M.-C. Crevier, J. Pelletier, N. Philip et al. Plasma sterilization. Methods and mechanisms. Pure and applied chemistry, 74, 349 (2002).

[8] M. Boudam, M. Moisan, B. Saoudi, C. Popovici, N. Gherardi et al. Bacterial spore inactivation by atmospheric-pressure plasmas in the presence or absence of UV photons as obtained with the same gas mixture. Journal of physics D: Applied physics, 39, 3494 (2006).

[9] H. W. Herrmann, I. Henins, J. Park & G. Selwyn. Decontamination of chemical and biological warfare (CBW) agents using an atmospheric pressure plasma jet (APPJ). Physics of Plasmas (1994-present), 6, 2284 (1999).

[10] M. Laroussi, I. Alexeff & W. L. Kang. Biological decontamination by nonthermal plasmas. Plasma Science, IEEE Transactions on, 28, 184 (2000).

[11] M. Moisan, J. Barbeau, S. Moreau, J. Pelletier, M. Tabrizian et al. Low-temperature sterilization using gas plasmas: a review of the experiments and an analysis of the inactivation mechanisms. International Journal of Pharmaceutics, 226, 1 (2001).

[12] K. Kelly-Wintenberg, T. Montie, C. Brickman, J. Roth, A. Carr et al. Room temperature sterilization of surfaces and fabrics with a one atmosphere uniform glow discharge plasma. Journal of Industrial Microbiology and Biotechnology, 20, 69 (1998).

[13] M. Laroussi, D. Mendis & M. Rosenberg. Plasma interaction with microbes. New J. Phys., 5, 41 (2003).

[14] S. P. Kuo, O. Tarasenko, S. Nourkbash, A. Bakhtina & K. Levon. Plasma effects on bacterial spores in a wet environment. New J. Phys., 8, 41 (2006).

[15] R. Pompl, F. Jamitzky, T. Shimizu, B. Steffes, W. Bunk et al. The effect of low-temperature plasma on bacteria as observed by repeated AFM imaging. New J. Phys., 11, 115023 (2009).

[16] L. M. Prescott, J. P. Harley & D. A. Klein Microbiology, Edn. 5. (McGraw-Hill, 2002).

Chapter 5

Conclusions

In this thesis, the effect of neutral oxygen and nitrogen atoms on the inactivation of spore forming microorganisms in low pressure N_2/O_2 mixture surface-wave plasma had been studied.

In order to measure the oxygen atomic density in surface-wave plasma, we proposed a self-absorption-calibrated VUVAS method, based upon the resonance escape factor theory and numerical analysis of the emission profiles with *Specair*. With a compact microwave plasma light source, absolute oxygen atomic densities were simultaneously and consistently determined by a self-absorption-calibrated VUVAS method with probes at 130.22 and 130.49 nm. With the self-absorption-calibrated absorption curves, we obtained very similar oxygen atomic densities at two different light probes. The oxygen atomic density varied from about 1.32×10^{12} to 3.98×10^{12} cm^{-3} with a changing N_2/O_2 gas mixture ratio, peaking at an N_2/O_2 ratio of 1:9. The variation of absolute oxygen atomic density with respect to N_2/O_2 gas mixture ratio is analogous to previous spore etching results measured under the same discharge conditions, and also to the variation of the emission intensity of oxygen atoms at 844.6 nm. It can be inferred that the spore etching effect in N_2/O_2 gas mixture SWP primarily comes from the oxygen atoms. We also found that a minimum oxygen density is needed for effective etching to begin. As etching plays an important role in plasma inactivation, the synergistic effect of etching with other plasma factors will be helpful to improve plasma sterilization properties in the future.

The self-absorption calibration method present in this thesis can significantly decrease the light source performance required for VUVAS measurements, and will be useful for the VUVAS measurement in other plasma sources as a plasma diagnostic tool.

Using a light source condition with self-absorption of nitrogen resonance line near 120 nm at negligible level, the nitrogen atomic densities were measured with different N_2 and O_2 gas mixtures in surface-wave plasma. we inferred from these atomic density results that nitrogen atomic density in N_2 and O_2 mixture surface-wave plasma has small contributions on the spore etching and spore inactivation.

In order to study the inactivation effect of neutral oxygen species in low pressure plasma, an ultra-thin porous ceramic plate was developed to block UV and make the neutral species penetrate through selectively. More than 99% emission below 400 nm had been blocked by the porous ceramic plate. And the morphology change of spores demonstrate clearly that parts of neutral radicals can penetrate through the porous ceramic plate. The survival curves indicated that the very small amount UV (<1%) which can penetrate through the porous ceramic plate still play a main inactivation effect.

Although much work has been done, but the inactivation effect with neutral radicals alone is still unclear now, for a further study, we need to develop a new kind of filter which can perfectly block UV emission and allow most of neutral radicals penetrate through in future. The reflection properties of the materials to make filter is important to get perfect UV blocking. The inactivation effect of neutral oxygen species and nitrogen species in low pressure surface-wave plasma should be studied in next step.

Acknowledgements

I want to thank everyone who help me to complete this thesis from the bottom of my heart.

I would like to express my warmest thanks to my supervisor Prof. Masaaki Nagatsu for his patient, invaluable guidance on my research. Thanks so much for the opportunity he gave me to join this group and perform research in his laboratory. I am grateful for financial support of Prof. Nagatsu and his help in the application of scholarship. I am also study a lot from his diligence conscientious in work.

Thanks Prof. Koichi Sasaki in Hokkaido University for his useful comments on the VUVAS experiment. I wish to extend my appreciation to Mr. Waichi Tomoda, IJRC, Shizuoka University for his help during operating SEM.

I am grateful to all the members in our laboratory for their help. Thanks to my work partners, Okada Naoya, Reitou Tei and Syuhei Hamajima for theri help in many experiments, I am also appreciate them for the help in Japanese translation for the scholarship application. Thanks so much for the help and valuable suggestions of Mr. Raman, Mr. Mihai, Mrs. Shubing Yang, and other members in our laboratory.

Especially, I would like to thank Dr. Chen Yue come from Kyoto University for the help on the calculation program of theoretical absorption curve. He was very professional on program languages and had patiently taught me to use the compiler software and modify the program,

The present work has been supported in part by a Grant-in-Aid for Scientific Research (Grant No. 2110010) from the Japan Society for the Promotion of Science (JSPS). I would like to acknowledge the scholarship provide by Amano Institute of Technology and the scholarship provide by Japan Student Service Organization which supported my life in Hamamatsu.

I must thank my family in China and especially my husband, their understanding, tolerance, and support is very important for my study in Japan. Thanks every friend in Japan and China, because of your great concern and help, I have a very happy life in Hamamatsu.

Many thanks to all the friends who gave me help, but I can’t mention above, I cherish all the time with you for the past few years I studied in Japan.

List of publications

1. **Xiaoli Yang**, Xijiang Chang, Reitou Tei, Koichi Sasaki, and Masaaki Nagatsu. Oxygen atomic density measured with a self-absorption calibrated vacuum ultraviolet absorption spectroscopy and its effect on spore etching in N_2/O_2 surface-wave plasma. *Japanese Journal of Applied Physics*. 54, 070308 (2015).
2. **Xiaoli Yang** 1, Koichi Sasaki, and Masaaki Nagatsu. Self-absorption-calibrated vacuum ultraviolet absorption spectroscopy for absolute oxygen atomic density measurement. *Plasma Sources Science and Technology*. (accepted)
3. **Xiaoli Yang**, Xijiang Chang, Reitou Tei, and Masaaki Nagatsu, Nitrogen atoms density measured with vacuum ultraviolet absorption spectroscopy and its effect on spore inactivation at low pressure surface-wave plasma, Journal of Physics D: Applied Physics (Prepared).

Conferences

Domestic conferences

1) Xiaoli Yang, Syuhei Hamajima, Reitou Tei, Masaaki Nagatsu, " Effect of Radicals on Inactivation of Spore-forming Microorganisms Studied with Porous Ceramic Plate in N2/O2 Surface-wave Plasma",（口頭発表）, 2015 年第 62 回応用物理学会春季学術講演会, 東海大学　湘南キャンパス, (2015.3.11 -14).

2) Xiaoli Yang, Tei Reitou, and Masaaki Nagatsu, "Effects of Excited Oxygen and Nitrogen Atoms in N_2/O_2 Surface-wave Plasma on Inactivation of Spore-forming Microorganisms",（ポスター発表: 20PB-119）, Plasma Conference 2014、朱鷺メッセ (2014.11.18-21).

3) 鄭　霊東、楊　小麗、永津　雅章, "小型マイクロ波プラズマ光源を用いた励起窒素原子密度測定用真空紫外域吸収分光システムの開発", （ポスター発表）、Plasma Conference 2014、朱鷺メッセ (2014.11.18-21).

4) Xiaoli Yang, Tei Reitou, Koichi Sasaki and Masaaki Nagatsu, "Absolute O Atom Density Measured in N_2/O_2 Surface-wave Plasma Using a VUVAS Method with a Calibration of Self-absorption of Light Source", (ポスター発表:17a-S10-4), 第 75 回応用物理学会秋季学術講演会、北海道大学札幌キャンパス (2014.9.17-20).

5) 鄭 霊東, Xiaoli Yang, 永津雅章, "小型マイクロ波プラズマ光源を用いた表面波励起酸素・窒素プラズマの真空紫外吸収分光計測",（口頭）, 平成 26 年度電気・電子・情報関係学会東海支部連合大会, 中京大学名古屋キャンパス (2014.9.8-9)

6) Xiaoli Yang, Xijiang Chang, Tei Reitou, Koichi Sasaki, and Masaaki Nagatsu, "Effect of Reactive Atomic Species in N_2/O_2 Surface-wave Plasma on Inactivation of Spore-

forming Microorganisms", (ポスター発表: 04aE21P), プラズマ・核融合学会第 30 回年会、東京工業大学 大岡山キャンパス (2013.12.3-6).

7) Xiaoli Yang, Sonia Muradia, Okada Naoya and Masaaki Nagatsu,"Inactivation of Geobacillus Stearothermophilus Spore Wrapped by Tyvek Sheet Using Bubble Discharge Plasma in Water", (ポスター発表), 2013 年第 74 回応用物理学会秋季学術講演会, 同志社大, 京田辺キャンパス, (2013.9.17-20).

8) Xiaoli Yang, Toshiki Mitsui, Masaaki Nagatsu, "Study on the effect of catalyst on the low temperature plasma sterilization", (poster: P2-23), 30th symposium on plasma processing (SPP-30), Hamamatsu, アクトシティ浜松・研修交流センター (2013.1.21-23)

International conferences

1) Xiaoli Yang, Reitou Tei, and Masaaki Nagatsu," Measurement of Oxygen Atomic Density with Dual-wavelength Self-absorption-calibrated VUVAS Method", (Poster: PS-51), 2015 International Symposium toward the Future of Advanced Researches in Shizuoka University, Hamamatsu, Japan (2015.1.27-28)

2) Xiaoli Yang, Reitou Tei , Xijiang Chang, Koichi Sasaki, and Masaaki Nagatsu," Roles of Oxygen and Nitrogen Atoms in N_2/O_2 Plasmas on Inactivation of Spore-forming Microorganisms",(Poster: 19-P03-11) , 5th International Conference on Plasma Medicine (ICPM5), Nara Prefectural New Public Hall, Nara, Japan (2014. 5.18-23).

3) Xiaoli Yang, Xijiang Chang, Reitou Tei, and Masaaki Nagatsu, "Effect of Nitrogen Atoms in N_2/O_2 Surface-wave Plasma on the Inactivation of Spore-forming Microorganisms" , (poster:5P-AM-S12-P39), 8th International Conference on Reactive Plasmas/31st Symposium on Plasma Processing, Fukuoka Convention Center, Fukuoka, Japan (2014. 2.4-7).